STUDIES OF LUMINESCENCE IN CADMIUM SULPHIDE

by

HOWARD LEIGH MALM

B.Sc., University of Alberta, 1963
M.Sc., University of Alberta, 1964

A DISSERTATION SUBMITTED IN PARTIAL FULFILMENT

OF THE REQUIREMENTS FOR THE DEGREE OF

DOCTOR OF PHILOSOPHY

in the Department

of

Physics

SIMON FRASER UNIVERSITY

AUGUST 1971

APPROVAL

Name: Howard Leigh Malm

Degree: Doctor of Philosophy

Title of Thesis: Studies of Luminescence in Cadmium Sulphide

Examining Committee:

Chairman: K.E. Rieckhoff

R.R. Haering
Senior Supervisor

R.F. Frindt
Examining Committee

K. Colbow
Examining Committee

J.C. Irwin
Examining Committee

F. Morehead
External Examiner
Thomas J. Watson Research Center
P.O. Box 218
Yorktown Heights, New York

Date Approved: Aug 2/71.

ABSTRACT

Below 30°K the photoluminescent spectrum near the band edge of CdS can have some 30 or more sharp lines together with a series of broad bands. Investigation of the photoluminescence from CdS using a monochromator and a spectrometer together has extended the understanding of luminescent processes in the II-VI semiconductors.

Our excitation experiments show that an electron-phonon interaction is a common feature for all the luminescent transitions in CdS. This interaction can be understood in terms of a Franck-Condon model. Calculations for the value of the electron-phonon interaction parameter S for a bound carrier were extended to include the free exciton, the bound exciton, and the bound to bound transition. Experiments showed that $\hat{S}$ for excitons varied inversely with the exciton size in agreement with theory. Calculations which showed that $\overline{S}$ for the bound to bound transitions varied with the donor-acceptor separation were verified by experiment.

Our study of the luminescence has enabled the measurement of excited state energies of a neutral donor, of an exciton bound to a neutral donor, and of an exciton bound to a neutral acceptor. A radiative Auger decay process was discovered for the exciton bound to a neutral donor. It is also shown that

the ionization energies of donors and acceptors can be accurately measured using a combination of experimental techniques described in the thesis.

Calculations on the energy and spectral line shape for bound to bound luminescence showed that saturation effects and also an electron-hole correlation effect were important. Both effects were demonstrated by experiment.

TABLE OF CONTENTS

LIST OF TABLES

LIST OF FIGURES

LIST OF SYMBOLS

A	top most valence band; exciton from a hole in this band
$A(h\nu)$	absorption spectrum
a	Bohr radius
a_D	Bohr radius of a donor in the hydrogenic approximation
a_e	electron Bohr radius for the exciton
a_h	hole Bohr radius for the exciton
a_o	total exciton Bohr radius
B	valence band; exciton from a hole in this band
C	valence band; exciton from a hole in this band
c	the hexagonal axis in CdS
c	longitudinal sound velocity
$D_{ac}(\omega)$	coupling function for acoustic phonons and electrons
$D(\omega)$	coupling function for LO phonons and electrons
$\bar{E}$	electric vector of the light
E_A	binding energy of a hole to an acceptor
E_D	binding energy of an electron to a donor
$E(R)$	bound to bound emission energy as a function of the donor-acceptor separation
E_a	adiabatic potential
E_d	deformation potential
E_g	band gap energy of CdS at $\bar{k} = 0$
E_p	energy of an acoustical phonon

e	the electronic charge = 4.802×10^{-10} electrostatic units
g_p	generation rate for p th level
H	Hamiltonian for an electron in a deformable lattice
H_e	electronic Hamiltonian
H_{eL}	electron-lattice Hamiltonian
H_L	lattice Hamiltonian
h	Planck's constant = 6.624×10^{-27} eg. sec
$\hbar$	Planck's constant divided by 2π
$I_{ac}(\bar{r})$	electron-acoustical phonon interaction coefficient
$I(\bar{r})$	electron-LO phonon interaction coefficient
I_1	a sharp line in absorption or luminescence resulting from an A exciton bound to a neutral acceptor
I_2	an A exciton bound to a neutral donor
I_3	an A exciton bound to an ionized donor
$I_{1B'}$, I_{1B}	a B exciton bound to a neutral acceptor
I_{2B}	a B exciton bound to a neutral donor
I, $I_\perp$, $I_\parallel$	total intensity, intensity perpendicular and parallel to the c axis
k, $\bar{k}$	wave vector
kT	Boltzmann energy
LO	longitudinal optical phonon
M	ion mass per unit cell
m	vibrational level of the ground state
m'	number of acoustical phonons emitted or absorbed

m_e	effective mass of the electron
$m_{e\perp}$	effective mass of the electron perpendicular to the c axis
$m_{e\parallel}$	effective mass of the electron parallel to the c axis
m_h	effective mass of the hole
$m_{h\perp}$	effective mass of the hole perpendicular to the c axis
$m_{h\parallel}$	effective mass of the hole parallel to the c axis
N	number of unit cells in the crystal
N_A, N_D	concentrations of acceptors and donors
N_p	population of p th state
n	density of free electrons
n	principal quantum number
n_A, n_D	concentrations of neutral acceptors and donors
$\bar{P}$	exciton polarization
$P(h\nu)$	probability that the excited state decays to the observed luminescent state
p	vibrational level of the excited state
p_o	p state with the z component of angular momentum equal to zero
$p_{\pm 1}$	p state with the z component of angular momentum equal to plus or minus one
Q	a configurational coordinate
q	normal mode of the lattice
R	separation between a donor and an acceptor
$R(h\nu)$	reflectivity spectrum
R_1, R_2	ratios measuring the electron-hole correlation effect

r, R	distance
S, $\hat{S}$, $\bar{S}$	strength parameter for the electron-phonon interaction for a single localized charge, for an exciton, and for a donor-acceptor pair
S'	trapping cross-section
s	s state in the hydrogenic "atom"
s_L	s state exciton with a longitudinal polarization
s_T	s state exciton with a transverse polarization
T	temperature
TO	transverse optical phonon
t	LO phonon relaxation rate
V	crystal volume
V_o	volume of the unit cell
v	electron velocity
W	transition probability for a bound to bound transition
W_o	transition probability for a bound to bound transition at zero donor acceptor separation
W_{pm}	transition probability between the p th level in the excited state and the m th level in the ground state
α	ratio of the electron Bohr radius to the hole Bohr radius
α_p	relative probabilities of LO phonon relaxation to phonon plus radiative relaxation
Γ	irreducible group representation
Γ_q	radiative relaxation rate for the q th level
γ	ratio of donor-acceptor separation to the donor electron radius

Δ, Δ_{ac}	change in the equilibrium configurational coordinate between the ground and excited states due to the electron-phonon interaction for LO phonons, for acoustic phonons
ΔE_2	energies of excited states of the I_2 complex
ε_a	adiabatic transition energy
ε_o	minimum allowed transition energy
$\varepsilon_{gm}, \varepsilon_{ep}$	energy eigenvalues for the ground and excited states
κ_o	optical dielectric constant
κ_s	static dielectric constant
λ_{LUM}	wavelength of the luminescence
λ_{max}	wavelength of the maximum intensity of the bound to bound luminescence
ρ	density
φ	electronic part of the wavefunction
φ_e, φ_g	electronic wavefunctions for the excited and ground states
φ_D, φ_A	electronic wavefunctions for an electron bound to a donor and for a hole bound to an acceptor
χ	lattice part of the wavefunction
Ψ	wavefunction
ω	angular frequency
ω_o	frequency of LO phonon
+	a hole
-	an electron
$\oplus$	a singly charged donor impurity
$\ominus$	a singly charged acceptor impurity

ACKNOWLEDGEMENTS

I wish to express my gratitude to Rudi Haering for his enthusiastic and invaluable assistance in both the experimental and theoretical aspects of the work leading up to this thesis. I also wish to thank the other members of the Department of Physics from whom I have had courses and with whom I have had useful discussions. The excellent facilities of the laboratories for doing experimental research are acknowledged.

Acknowledgement is made to Atomic Energy of Canada Limited for partial salary during my educational leave of absence, and to the National Research Council of Canada for providing the research facilities for this work.

1. THESIS INTRODUCTION

The optical properties of cadmium sulphide crystals, particularly the luminescence, have been the subject of extensive experimental and theoretical investigation. The experimental techniques described in this thesis have improved the understanding of the electron-phonon interaction in a polar material, in the evaluation of the role of excitons in luminescence, and in the precise measurement of donor and acceptor binding energies.

The photoluminescence of CdS at low temperatures is known to consist of both sharp lines and broad bands. The intense sharp lines result from free and bound excitons; this identification was first made by Thomas and Hopfield (1959, 1962) and Hopfield and Thomas (1961) and subsequently by many other workers. One of the most common broad bands, the "green emission", was shown by Thomas, Hopfield and Colbow (1964) and Colbow (1966) to result from the radiative recombination of a hole bound to an acceptor with either an electron bound to a donor (low temperatures) or a free electron (temperatures less than 150°K). However, the electronic transitions responsible for many of the weaker lines and broad bands are still under investigation (see, for instance, Henry and Nassau (1970), Gutsche and Goede (1970)). Some of the difficulties have

arisen because the ionization energies for the donors and acceptors are not known accurately.

Techniques described in this thesis have proven useful in understanding the origin of many of the weaker luminescent transitions which are observed in CdS at low temperatures. In addition, results which have enabled an accurate determination of donor and acceptor ionization energies are presented. Evidence is also given which indicates the existence of a radiative Auger process for the bound exciton.

The luminescence in CdS demonstrates a coupling between the localized charges of the luminescent centers and the phonons of the lattice. This was first recognized by Hopfield (1959) for the bound electron-bound hole transition. A strong coupling between excitons and the longitudinal-optical phonons was demonstrated in the photoconductivity spectra of Park and Langer (1964), and in the optical excitation of luminescence reported first by Conradi and Haering (1968), and later by Park and Schneider (1968), and Gross et al. (1970).

Results in this thesis show that this electron-phonon coupling is a common feature of almost all luminescence in CdS. This coupling, which is expected for a polar lattice, can best be understood in terms of a Franck-Condon model. The coupling strength is determined by a coupling parameter S whose magnitude depends on the size of the luminescent center in accordance with the theory of Toyozawa (1967). Toyozawa's theory

is extended to allow calculation of S for free excitons, bound excitons, and bound to bound transitions. The theory is in quantitative agreement with experiment in all cases where the electronic wavefunctions are sufficiently well-known to permit an actual calculation.

The broad-band green emission wavelength is known, from the work of Thomas and his colleagues, to depend on the donor-acceptor separation. However, recent theories which attempt to explain the position, width and shape (Hagston 1970, Gutsche and Goede 1970) of this broad band luminescence have been only partially successful. A detailed analysis requires knowledge of all processes which can affect the luminescence.

Results are presented which show that two previously unreported effects must be considered. It is shown that there exists an electron-hole correlation effect due to excitons which enhances the bound to bound emission for donor-acceptor separations of the order of the exciton radius. The Franck-Condon effect for the bound to bound transitions mentioned earlier also causes a dependence of the luminescence on the spectrum of the exciting light. The well-known broadening due to emission of acoustical phonons is also considered. The results then, suggest that the shape and position of the broad band luminescence depends on many parameters.

2. LUMINESCENCE IN CdS - A BRIEF REVIEW

2.1 Introduction

A brief review of the photoluminescence of single crystal CdS is given below to provide a background for the present work. Since the literature on the luminescent properties of CdS is extensive and sometimes repetitive, only the more important references are included. Review articles by Reynolds, Litton and Collins (1965a,b) and Shionoya (1970), a book edited by Aven and Prener (1967), and a book by Ray (1969) are an excellent source of information of II-VI semiconductors, with emphasis on the properties of CdS.

The progress in understanding the luminescence from CdS has largely been tied to the ability to produce single crystals of high quality and of high chemical purity. The difficulty in synthesis imposed by the additional degree of freedom in a two component semiconductor and the difficulty of obtaining highly pure components for growth of single crystals has been a considerable problem (Lorenz 1967). The preparation of CdS crystals with known donor and acceptor impurities at low concentrations has only recently been reported by Nassau, Henry and Shiever (1970).

Study of the luminescence of CdS near the band edge requires the use of low temperatures (usually 4°K and 77°K) to make weakly bound states of holes and electrons observable.

The luminescence consists of a number of sharp lines from 2.43 eV to the band edge at 2.58 eV, and a number of broad lines below 2.43 eV.

2.2 Luminescence due to Excitons

The exciton, first introduced by Frenkel (1931), is in CdS an electron and hole bound by their coulombic attraction with a Bohr radius of about 30 Å. This is the so-called Wannier exciton (Wannier 1937).

Excitons in CdS were first reported by Gross, Razbirin and Iakobson (1957) and by Gross and Razbirin (1957). The most definitive studies of excitons in CdS were done by Thomas and Hopfield (1959), Hopfield and Thomas (1960), and by Hopfield (1960). The effect of magnetic fields on excitons was studied by Hopfield and Thomas (1961) and Wheeler and Dimmock (1962).

In CdS the conduction band is s like and almost isotropic, while the valence band is p like and split into 3 bands due to the spin-orbit interaction and the crystal field interaction which is non-zero in the wurtzite structure (Birman 1959a,b). The energy band deduced by Thomas and Hopfield (1959) is shown in Fig. 1.

Excitons formed of an electron in the conduction band and of a hole in the A valence band are known as A excitons and are

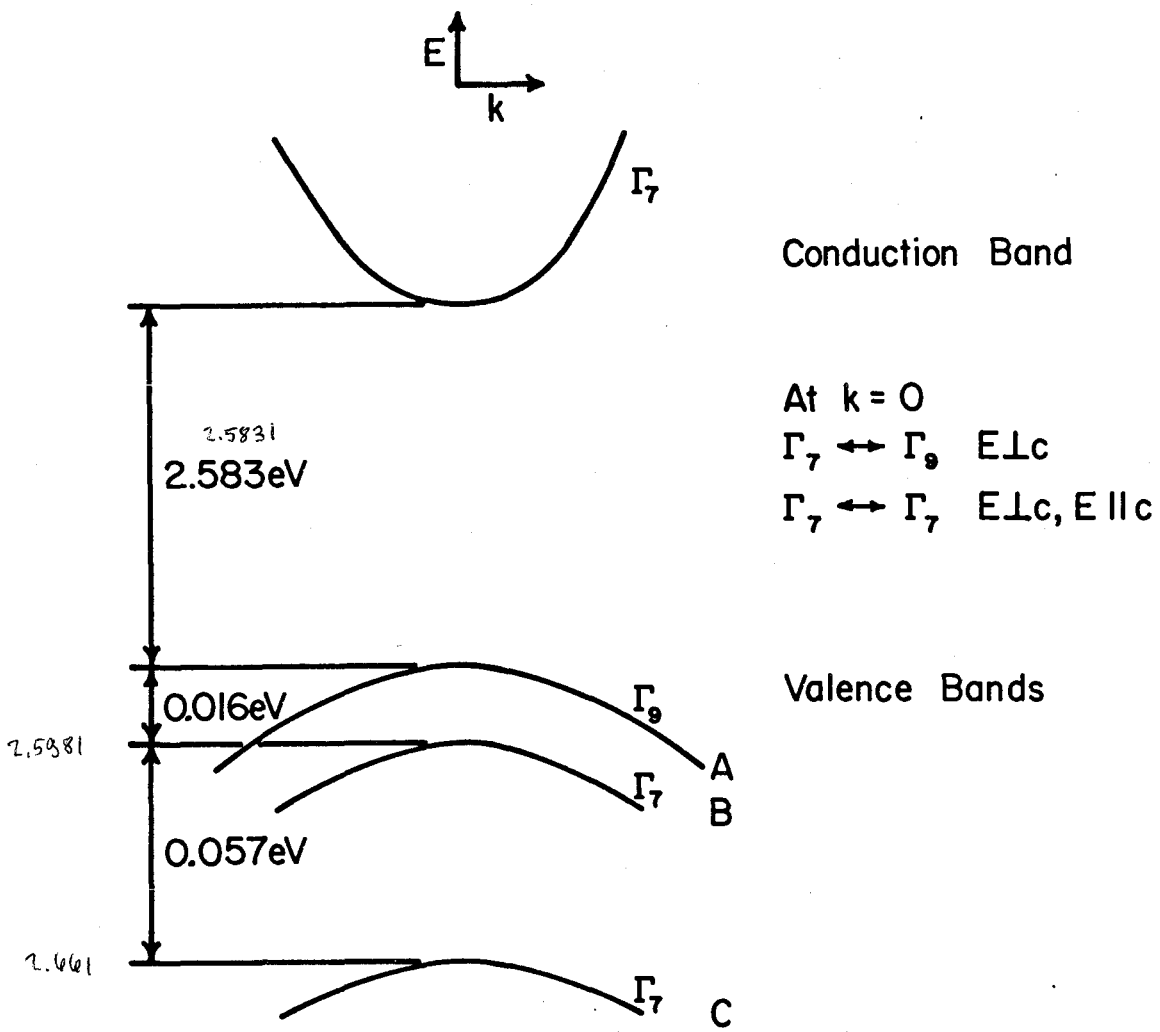

Fig. 1 Energy bands for CdS centered at k = 0 from Thomas and Hopfield (1959). A, B, and C refer to the three hole bands and Γ_7 and Γ_9 refer to the band symmetry.

most active in absorption (emission) for light polarized with $\bar{E} \perp c$ where $\bar{E}$ is the electric vector of the incident (emitted) light and c is the hexagonal axis of the CdS crystal. Excitons of holes from the B and C bands are active in both polarizations. Table I shows the wavelength and energy of the various exciton states together with binding energies.

In group notation used by Hopfield and Thomas (1961), the $\bar{k} = 0$ A exciton states with a principal quantum number n = 1 formed from an electron in the Γ_7 conduction band and a hole in the Γ_9 valence band are Γ_5 (allowed) and Γ_6 (forbidden). The $A(\Gamma_5)$ exciton with electron and hole spins antiparallel, is observed for $\bar{E} \perp c$ as a transverse exciton (exciton polarization $\bar{P} \perp c$) and for $\bar{E} \parallel c$ as a weaker Γ_5 longitudinal exciton. The Γ_6 exciton with electron and hole spins parallel is observed because $\bar{k} \neq 0$ for photons.

Luminescence from excitons is observed for the $A(\Gamma_{5T})$ and $A(\Gamma_6)$ excitons and at one and two longitudinal-optical phonon energies below these states. [Gross, Permogorov, and Razbirin, (1966a,b) and Bleil (1966)]. The phonon replicas are broadened according to a Maxwellian distribution due to the kinetic energy of the excitons before radiative emission.

Fig. 2 shows a typical photo-luminescence spectrum from a lightly doped crystal of CdS at 5.3°K. Most of the lumines-

Excitons in CdS

Table I

Line	Position Å	eV*	Absorption or Luminescence	Polarization	Binding Energy	Reference
$A(1s\ \Gamma_6)$	4857.1	2.55185	a,ℓ	$\bar{E}\|c$		Nassau et al. (1970a)
					ΔE = 1.30 meV	Hopfield and Thomas (1961)
$A(1s_T\ \Gamma_5)$	4854.8	2.55306	a,ℓ	$\bar{E}_\perp c$	29.8 meV	" "
$A(1s_L\ \Gamma_5)$	4852.9	2.55406	a	$\bar{E}\|c$		" "
B(n=1)	4826.1	2.56824	a,ℓ	both	29.5	
$A(n=2,\ p_o)$	4814.2	2.57459	a	$\bar{E}\|c$	7.5	" "
$A(n=2,\ s_L)$	4812.9	2.57526	a,ℓ	both	6.9	" "
$A(n=2,\ p_{\pm1})$						
A(n=3)	4805.5	2.57925	a		2.8	" "
A(n=4)	4803.3	2.58043	a		1.7	" "
B(n=2)	4784.9	2.59036	a	both		" "
C	4710	2.632	a	both	26	Thomas and Hopfield (1959)

* Evaluated using $\frac{hc}{e}$ = 1.23946 x 10^{-4} cm eV. (CRC Handbook of Physics and Chemistry, 1966 edition). The refractive index for air at 15°C, 76 cm of Hg was used.

Hopfield and Thomas apparently used an index of 1 and slightly different values for the fundamental constants.

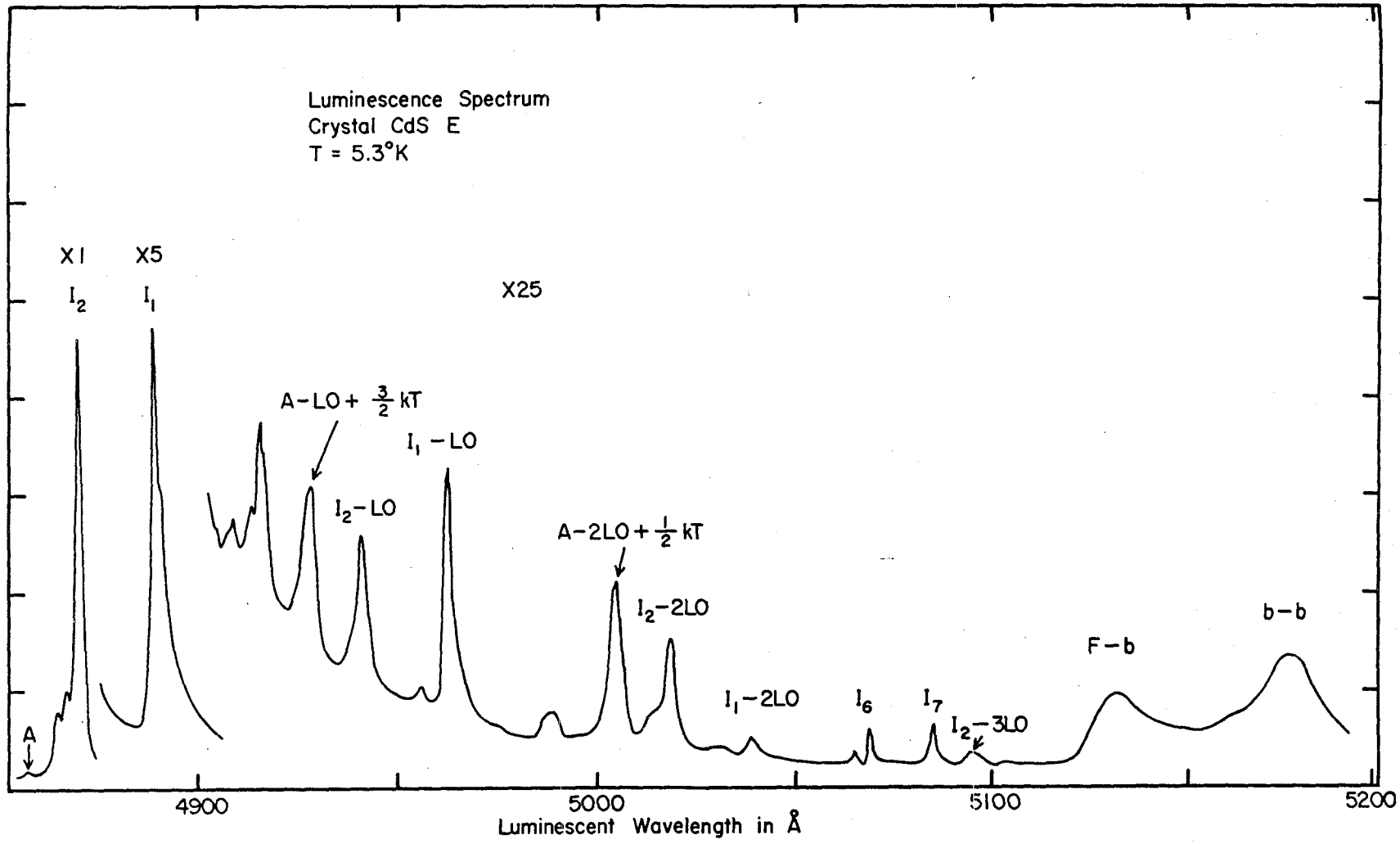

Fig. 2 Luminescence from a lightly doped CdS crystal at 5.3°K. The crystal was illuminated with a high pressure Hg lamp using a 4360 Å bandpass interference filter.

cent intensity is from excitons bound to impurities in complexes crudely analogous to H_2 and H_2^+. The recombination of an electron and hole gives a photon, returning the center to its ground state.

Lines labelled I_1 refer to an A exciton bound to a neutral acceptor and may be represented schematically as Θ^+_+- where Θ refers to the fixed acceptor impurity; + and - refer to a hole and to an electron respectively. Lines labelled I_2 refer to an A exciton bound to a neutral donor and are represented as $\oplus^-_-+$. I_3 refers to an A exciton bound to an ionized donor and is represented as $\oplus^-+$.

Thomas and Hopfield (1962) first identified the above lines by analysing their Zeeman splitting using magnetic fields to 30 Kg. Later work by Nassau, Henry and Shiever (1970), and by Henry, Nassau and Shiever (1970) has enabled chemical identification of many of the donor and acceptor impurities in CdS. The precise emission wavelength of the above lines depends on the impurity.

In CdS where the effective hole mass is about 4 times the effective electron mass, Hopfield (1964) showed that an exciton is not bound to an ionized acceptor. Indeed no such line has been seen in absorption or luminescence.

The previous results for polarization of photons from excitons are generally valid for weakly bound states such as

bound excitons. The lines I_1, I_2, and I_3 are active only for $E \perp c$ since the holes are from the A band.

In absorption, Thomas and Hopfield (1962) also observed lines active for both polarizations and identified these lines as follows. I_{2B} is from a B exciton bound to a neutral donor. I_{1B} and $I_{1B'}$ are from a B exciton bound to a neutral acceptor. The distinction between I_{1B} and $I_{1B'}$ is due to the spin of the two holes being parallel ($I_{1B'}$) and antiparallel (I_{1B}).

Line positions and chemical impurities are listed in Table II. Binding energies of excitons to the various impurities are also given.

Several sharp lines appear at energies of one or two LO phonon energies below I_1 and I_2. These are generally called LO phonon replicas. A few other sharp lines are probably from deep impurity centers and have been labelled I_6 and I_7 by Reynolds and Litton (1963).

2.3 Broad Band Luminescence

Luminescence in CdS was first reported by Kröger (1940) who irradiated CdS at 93°K by the 3650 Å line of Hg. He observed a series of green luminescent bands starting at 5130 Å and at intervals of 314 cm^{-1} lower in energy. Klick (1951)

Table II Bound Excitons in CdS
Luminescence and Absorption

Line	Position Å	Position ev	Chemical Impurity*	Binding Energy of A Exciton	Polarization	Reference
I_{1a}	4888.5	2.53546	Li a	17.6 meV	$\vec{E}_{\perp}c$	i
I_{1b}	4888.2	2.53562	Na a	17.4	"	i
I_2	4870.6	2.54479	F d	8.25	"	iii, ii
	4869.9	2.54515	In d	7.89		iii
	4869.2	2.54548	Cl d	7.58		iii
	4868.9	2.54565	I d	7.39		iii
	4867.1	2.54661	[Li d]+	6.5		iv, v
I_3	4870.3	2.54495	F id	8.09		iii
	4866.6	2.54686	Cl id	6.20		iii
	4865.8	2.54729	I id	5.75		iii
	4861.7	2.54943	[Li id]+	3.63		iv, v
I_6	5068.5	2.4454	?		$\vec{E}\|c$	vi
	5069.2	2.4451	?		$\vec{E}\|c$	vi
I_7	5084.8	2.43758	?		both	vi
Absorption Only				Binding Energy of B Exciton		
I_{1B}	4863.7	2.54839	Li or Na	19.8 meV	$\vec{E}\|c$	v
	4863.2	2.54865	Li or Na		$\vec{E}_{\perp}c$	v
$I_{1B'}$	4860.8	2.54991	Li or Na	18.3	$\vec{E}\|c$	v
I_{2B}	4837.7	2.56209	[Li d]+	6.2	both	v

* a - neutral acceptor; d - neutral donor; id - ionized donor.

\+ tentative assignment.

Table II (Cont'd.)

i	Henry, Nassau and Shiever (1970)
ii	Thomas, Dingle and Cuthbert (1967)
iii	Nassau, Henry and Shiever (1970)
iv	Henry (1971)
v	Thomas and Hopfield (1962)
vi	Reynolds and Litton (1963)

observed the same luminescence at 77°K but noted a decrease in energy of 0.03 meV of each member of the series in going to 4°K. The spacing of each member of the series was recognized by Kröger and Meyer (1954) to be that of the longitudinal optical (LO) phonon in CdS. Hopfield (1959) showed that the intensity of these LO phonon replicas required one trapped carrier to provide sufficient coupling to the lattice. The origin of the decrease in energy in going to lower temperatures was suggested by Thomas and Hopfield (1959) and later shown by Pedrotti and Reynolds (1960) to be due to a bound state of the electron existing near the bound hole. Later, Thomas, Hopfield and Colbow (1964) and Colbow (1966) confirmed these results in studies of the time resolved luminescence.

Fig. 3a) shows the green luminescent spectra at two temperatures while Fig. 3b) shows the energy level scheme. At low temperatures both the electron and hole are trapped on donor and acceptor impurities respectively and the emission is at E_1 (bound to bound emission). As the temperature increases the electron becomes free and the emission is at E_2 (free to bound emission). At still higher temperatures the hole becomes free from the acceptor trap and the green luminescence is quenched (Maeda 1965).

The dependence of the emission energy E(R) from a donor-acceptor pair separated by a distance R is given by

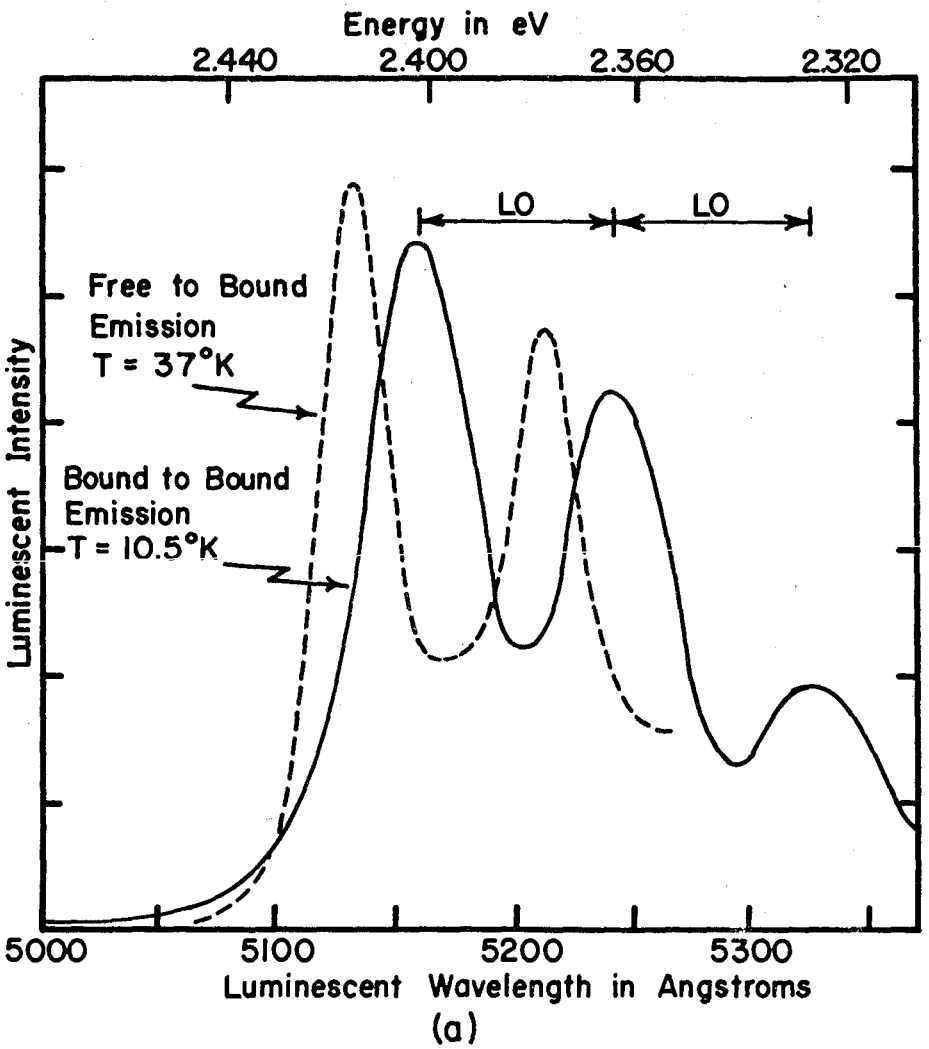

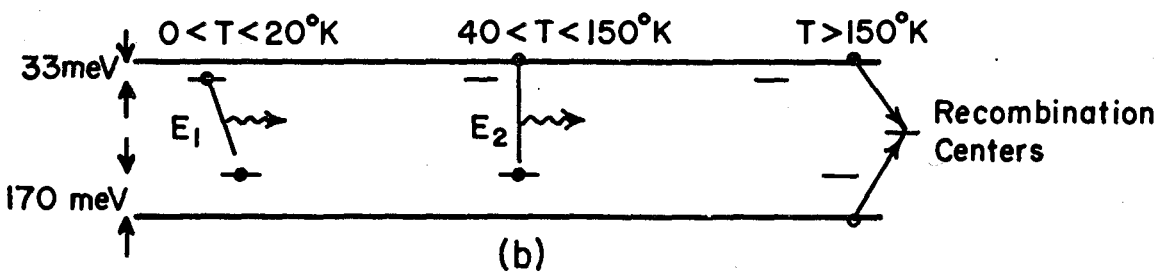

Fig. 3a The luminescence at 10.5°K is due to bound to bound transitions while the luminescence at 37°K is due to a free electron radiatively recombining with a bound hole.

b Principal recombination processes in a compensated crystal for 3 temperature ranges.

$$E(R) = E_g - (E_A + E_D) + \frac{e^2}{\kappa_s R}$$

where E_g is the band gap energy, E_A and E_D are the binding energies of isolated acceptors and donors, and κ_s is the static dielectric constant. The transition probability W is given in the Heitler-London approximation by the overlap of the wave-functions. If the acceptor is much deeper than the donor, then

$$W = W_o \, e^{-\frac{2r}{a_D}}$$

where W_o is a constant and a_D is the Bohr radius of the donor.

Thomas et al. (1964) showed that the above expressions correctly described the broad band luminescence in both GaP and CdS. Sharp lines due to donors and acceptors being at discrete separations were observed by them in GaP and recently by Henry et al. (1969) and Reynolds et al. (1969) in CdS.

Many crystals, however, do not exhibit all the features expected in the free to bound and bound to bound models. Kingston (1968) has observed a dependence of luminescent energy on annealing conditions and Gutsche and Goede (1970) have raised some objections to the free to bound model.

As will be shown later, the precise position and shape of the bound to bound luminescent band is complicated by mechanisms for feeding the bound to bound luminescent band which

have not been considered by other workers.

2.4 Measurements of Other Parameters for CdS

Other parameters characterizing CdS are listed in Table III. For a more complete list the II-VI Semiconducting Compounds Data Tables compiled by Neuberger (1969) may be consulted.

2.5 Excitation Spectra

In this technique a property of a crystal is studied as a function of energy of the incident radiation. The variation of electrical conductivity as a function of incident wavelength (photoconductivity) has been studied in most semiconductors and has an extensive literature [see Bube (1960), Pell (1971)].

The study of the luminescent intensity as a function of incident energy has a shorter history. Luminescent excitation spectra have been made for various deep centers in the alkali-halides [Fitchen (1966), Stiles and Fitchen (1966)], and for a few deep centers in the II-VI semiconductors [Gross, Razbirin, and Shekhmamet'ev (1962) in CdS, and by Deitz et al. (1962) in ZnTe]. Luminescent excitation spectra using resolutions from 10 - 30 Å have also been reported by Gross and Shekhmamet'ev (1962, 1963) for HgI_2, PbI_2 and the copper halides.

TABLE III Measured Parameters of CdS

		Reference
Effective mass in terms of the free electron mass	$m_{e\perp} = 0.171$ $m_{e\parallel} = 0.153$	Baer and Dexter (1964)
	$m_{e\perp} = .190 \mp .002$ $m_{e\parallel} = .180 \mp .010$	Henry and Nassau (1970a)
	$m_{h\perp} = 0.7 \mp 0.1$ $m_{h\parallel} = 5.0$	Thomas and Hopfield (1959)
Dielectric constant		
- static κ_s (77^oK)	$\kappa_{\parallel} = 9.48$ $\kappa_{\perp} = 8.48$	Berlincourt et al. (1963)
Refractive index ($\kappa_o = n^2$)	$n = 2.29 = (5.24)^{\frac{1}{2}}$	Czyzak et al. (1957)
Phonon energies (Raman Scattering)	$LO(\Gamma_1)$ 305 cm^{-1} $LO(\Gamma_5)$ 305 cm^{-1} $TO(\Gamma_1)$ 235 cm^{-1} $TO(\Gamma_5)$ 228 cm^{-1}	Tell, Damen and Porto (1965)
Density ρ	4.82 $\frac{g}{cm^3}$	
Deformation potential E_d	1.7 eV	Rowe et al. (1967)

In CdS Gross, Razbirin and Shekhmamet'ev (1962) found that the luminescent excitation spectra of the free to bound band at 77°K was similar to the photoconductivity spectra and depended somewhat on surface treatment and annealing history.

Excitation of luminescence from bound excitons in CdS using better resolution was first reported by Conradi and Haering (1968, 1969) and by Park and Schneider (1968). These studies revealed that the I_2 complex (exciton on a neutral donor) could be created at energies of p LO above the I_2 line (Conradi and Haering 1968) or above the A exciton (Park and Schneider 1968). LO is the energy of the longitudinal optical phonon and p is an integer from 1 to 6. More recently Gross et al. (1970) have reported similar excitation spectra for free excitons.

2.6 Franck-Condon Effects in Semiconductors

A linear interaction between an electronic excitation and the lattice vibrations was first considered by Huang and Rhys (1950) and later by Lax (1952) and O'Rourke (1953). As will be explained later, this model made use of the adiabatic approximation of the wavefunction of the excitation and the Franck-Condon approximation. The absorption bands of impurities in semiconductors, particularly in the alkali-halides, were interpreted using a Franck-Condon model, using the strength of the interaction as an adjustable parameter (Fitchen 1968). Keil (1965) extended the model to consider interaction with both linear and quadratic modes.

Recently, Toyozawa (1967) proposed a means of calculating the strength of the interaction between an electronic excitation localized on an impurity and the lattice vibrations. This was extended formally by Toyozawa (1970) to include the interaction between the exciton and the lattice.

3. THEORY

3.1 The theory is divided into five parts. The first part describes how a localized electronic excitation in a deformable lattice may be described in terms of the Franck-Condon principle. The second section discusses the analysis of excitation spectra. In the third section saturation effects in the bound to bound luminescence are discussed while in the fourth section the influence of excitons on the bound to bound luminescence is considered in terms of an electron-hole correlation effect. The last section contains a brief discussion of the excited states of a bound exciton.

3.2 Franck-Condon Effects

A localized electronic excitation such as a hole bound to an acceptor, an electron to a donor, or an exciton causes a distortion in the lattice of a polar material. The optical absorption line shape or luminescent emission line shape depends then on the interaction of the electronic state with the vibrational modes of the crystal. The strongest electron-phonon interaction occurs between the longitudinal optical modes and the electrons. In the optical modes the positive and negative ions are displaced in opposite directions.

In long wavelength acoustic modes the neighbouring ions move in phase, and in a non-piezoelectric crystal there is no strong electrostatic coupling to acoustical phonons. Then, a

localized electronic excitation may couple to acoustic phonons by virtue of the deformation potential. In a wurtzite crystal such as CdS the piezoelectric electron-phonon interaction can also be important. Qualitatively, one expects that the stronger the binding to the impurity, the stronger is the interaction with acoustic modes.

The interaction between the charged carriers and the longitudinal-optical phonons in II-VI semiconductors is sufficiently strong to exclude a perturbation treatment. The luminescent transitions in CdS show sidebands with up to 6 longitudinal optical (LO) phonons whose relative intensity varies by less than an order of magnitude. (Conradi and Haering 1968). A non-perturbation treatment of the electron-LO phonon interaction is essential. In the following section the interaction is treated in the Franck-Condon and adiabatic approximations following Huang and Rhys (1950), Lax (1952) and Keil (1965). The theory for the strength of the electron-phonon coupling for a localized excitation is due to Toyozawa (1967, 1970) and is extended here to include free excitons, bound excitons and the bound hole-bound electron system.

The Hamiltonian of the electron-phonon system $H + H_L$ is the sum of the electronic energy in a deformable lattice H and the lattice vibrational energy H_L. In the adiabatic approximation the wavefunction for the electronic state Ψ may be written as (Keil 1965)

$$\Psi_{a\alpha} = \varphi_a(\bar{r},q)\ \chi_{a\alpha}(q) \qquad 3.201$$

where φ_a refers to the electronic part of the wavefunction in state a and $\chi_{a\alpha}$ refers to the dependence on the normal coordinates of the lattice.

Substituting in the Schroedinger equation

$$(H + H_L)\ \varphi_a(\bar{r},q)\ \chi_{a\alpha}(q) = \varepsilon_{a\alpha}\ \varphi_e(\bar{r},q)\ \chi_{a\alpha}(q). \qquad 3.202$$

Separating the equation gives

$$H\varphi_a(\bar{r},q) = E_a(q)\ \varphi_a(\bar{r},q) \qquad 3.203$$

where $E_a(q)$ is the adiabatic potential for the nuclei. The other equation is

$$[(H_L + E_a(q)]\ \chi_{a\alpha}(q) = \varepsilon_{a\alpha}\ \chi_{a\alpha}(q). \qquad 3.204$$

For the ground state the adiabatic potential may be expanded in a Taylor series about the equilibrium lattice positions. In terms of normal modes, the ground state potential is

$$E_1(q) = \frac{1}{2} \sum_i \omega_{il}^2\ q_i^2 \qquad 3.205$$

where q_i and ω_{il} are the normal coordinate and frequency of the i th mode. In terms of normal mode coordinates equation 3.204 becomes

$$\sum_i \left[-\frac{\hbar^2}{2} \frac{\partial^2}{\partial q_i^2} + \frac{1}{2} \omega_{il}^2 q_i^2 \right] \chi_{l\alpha i(\bar{q}_l)} \; \varepsilon_{l\alpha} \chi_{l\alpha(\bar{q}_l)}. \qquad 3.206$$

For each mode i, the solution is $\chi_{l\alpha i}(q)$, a harmonic oscillator wavefunction.

The potential of the excited state E_2 can, to a fairly good approximation (Keil 1965), be expanded in the normal coordinates of the ground state

$$E_2(q) = \varepsilon_a + \sum_i \gamma_i q_i + \frac{1}{2} \sum_i \omega_{i2}^2 q_i^2 . \qquad 3.207$$

By completing the square

$$E_2(q) = \varepsilon_o + \frac{1}{2} \sum_i \omega_{i2}^2 (q_i - \Delta_i)^2 \qquad 3.208$$

where

$$\Delta_i = - \frac{\gamma_i}{\omega_{i2}^2} \qquad 3.209$$

and

$$\varepsilon_o = \varepsilon_a - \frac{1}{2}\Sigma_i \omega_{i2}^2 \Delta_i^2. \qquad 3.210$$

The potential for the excited state is displaced vertically by ε_o and horizontally by Δ_i from the potential for the ground state.

For purposes of illustration the lattice coordinates are represented by a single configurational coordinate Q[†]. Assuming the frequency is the same for the ground and excited states, the energy eigenvalues for the ground state are

$$\varepsilon_{gm} = \hbar\,(m+\tfrac{1}{2})\;\omega_o$$

and for the excited state are

$$\varepsilon_{ep} = \hbar\,(p+\tfrac{1}{2})\;\omega_o$$

where ω_o is the frequency of the LO phonon. The energy diagram in terms of a single configurational coordinate is shown in Fig. 4.

The probability of an optical transition is proportional

[†]A single coordinate model is a reasonable approximation for the LO phonons since the LO phonon band is narrow and since the electron-LO phonon interaction strongly weights small g values.

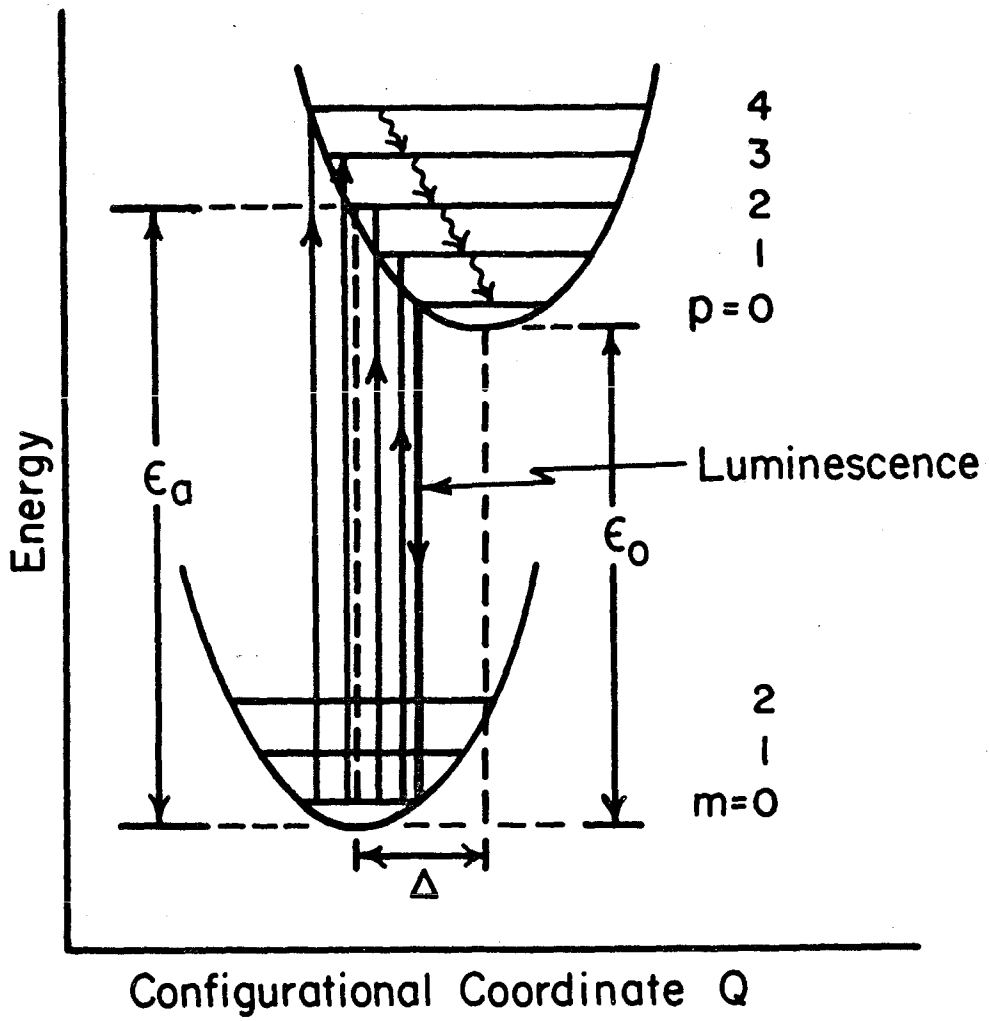

Fig. 4 Adiabatic potentials in a one dimensional configurational coordinate model for a localized excitation. In our case, the spacing of vibrational levels in these parabolic potentials is the longitudinal optical (LO) phonon energy. Vertical arrows represent photon absorption or emission.

to the square of the dipole matrix element $\langle \Psi_{ep} | \bar{r} | \Psi_{gm} \rangle$. Using expression 3.201 this can be factored into

$$\langle \varphi_e | r | \varphi_g \rangle \langle \chi_{ep} | \chi_{gm} \rangle \qquad 3.211$$

in the Franck-Condon approximation. The optical absorption (or emission) spectrum is then a series of sharp lines at energy intervals of $\hbar\omega_o$ with relative intensities given by $|\langle \chi_{ep} | \chi_{gm} \rangle|^2$, the vibrational overlap integral squared between the ground and excited states. For two harmonic oscillators displaced by Δ the relative transition probability W_{pm} is given by

$$W_{pm} = |\langle \chi_{ep} | \chi_{gm} \rangle|^2 = |\langle \chi_p(Q+\Delta) | \chi_m(Q) \rangle|^2$$

$$= e^{-S} S^{p-m} \left(\frac{m!}{p!}\right) L_m^{p-m}(S) \qquad 3.212a$$

$$S = \frac{\omega_o}{2\hbar} \Delta^2$$

where L_m^{p-m} is an associated Laguerre polynomial. For $T = 0$ when only the lowest vibrational state $m = 0$ is occupied, expression 3.212 becomes $W_{po} = e^{-S} \frac{S^p}{p!}$. The absorption spectrum consists of a series of lines starting at ε_o and spaced by $\hbar\omega_o$ with intensities proportional to

$$e^{-s}\frac{s^p}{p!} \qquad 3.212b$$

From the above, Malm and Haering (1971a) recognized that it was necessary to invoke the Franck-Condon principle in the interpretation of results of resonant Raman scattering in CdS reported by Leite and Porto (1966); Leite, Scott and Damen (1969); Klein and Porto (1969); Scott, Damen, Silfvast, Leite and Cheesman (1970); Scott, Leite and Damen (1969). These workers observed up to nine "overtone" Raman lines which differed in frequency from the incident light frequency by an integral number of LO phonon frequencies. The relative intensities varied by less than one order of magnitude. This again suggests that the interaction is sufficiently strong to exclude a perturbation treatment. In the Franck-Condon model the incident energy is resonant with one of the excited state energy levels. For the case where the p = 0 level is populated by the incident photons, light is Raman scattered at frequencies of ε_o - mLO with relative intensities given by $e^{-s}\frac{S^m}{m!}$. Fig. 5 shows a number of examples for various values of S. The most probable number of phonons emitted is about equal to S. In general, the interaction parameter S is large for strongly polar materials.

Generalizing the single mode analysis given above to a multidimensional coordinate system, the contribution to S comes from a number of frequencies (Toyozawa 1967).

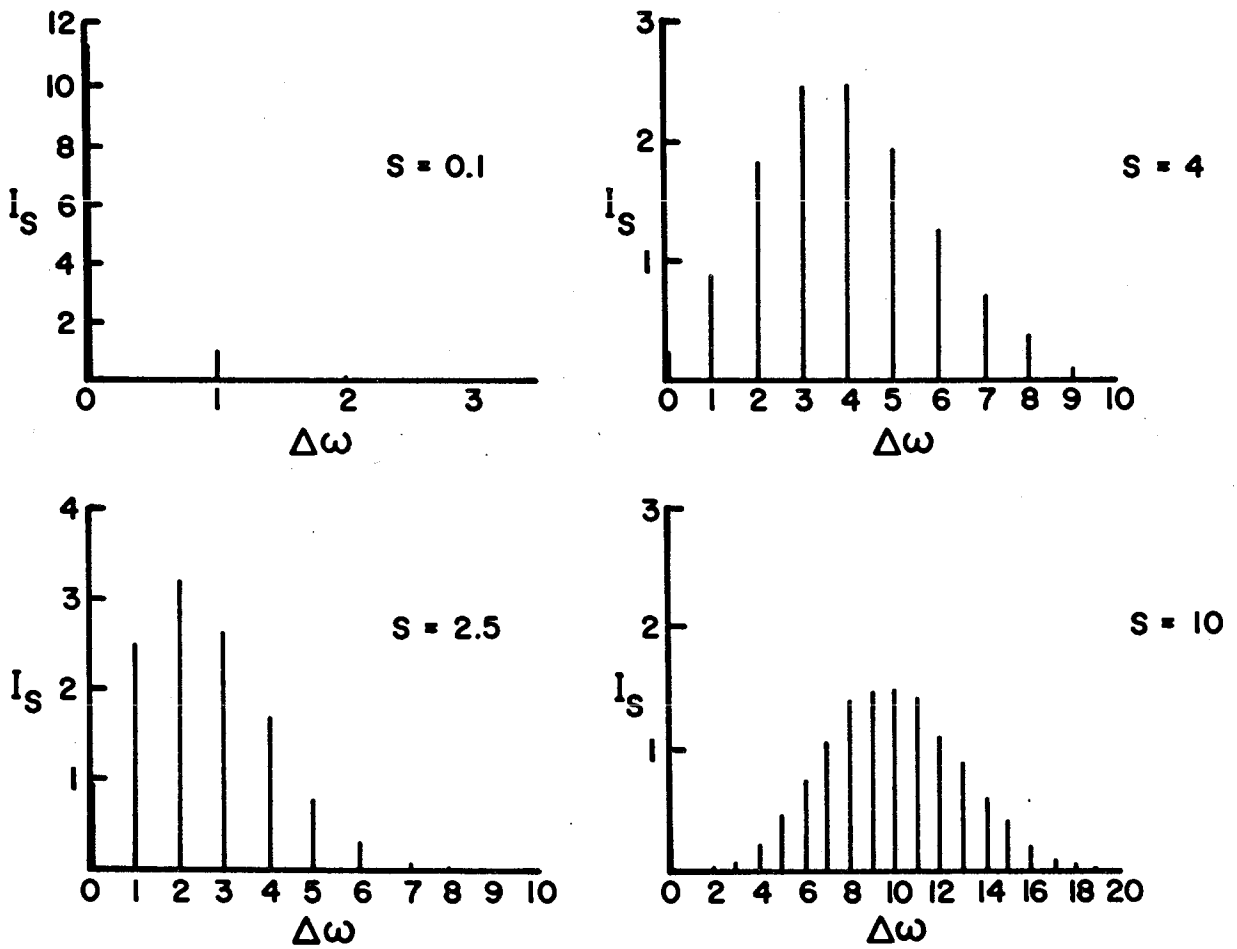

Fig. 5 Intensities of LO phonon replicas for various values of S.

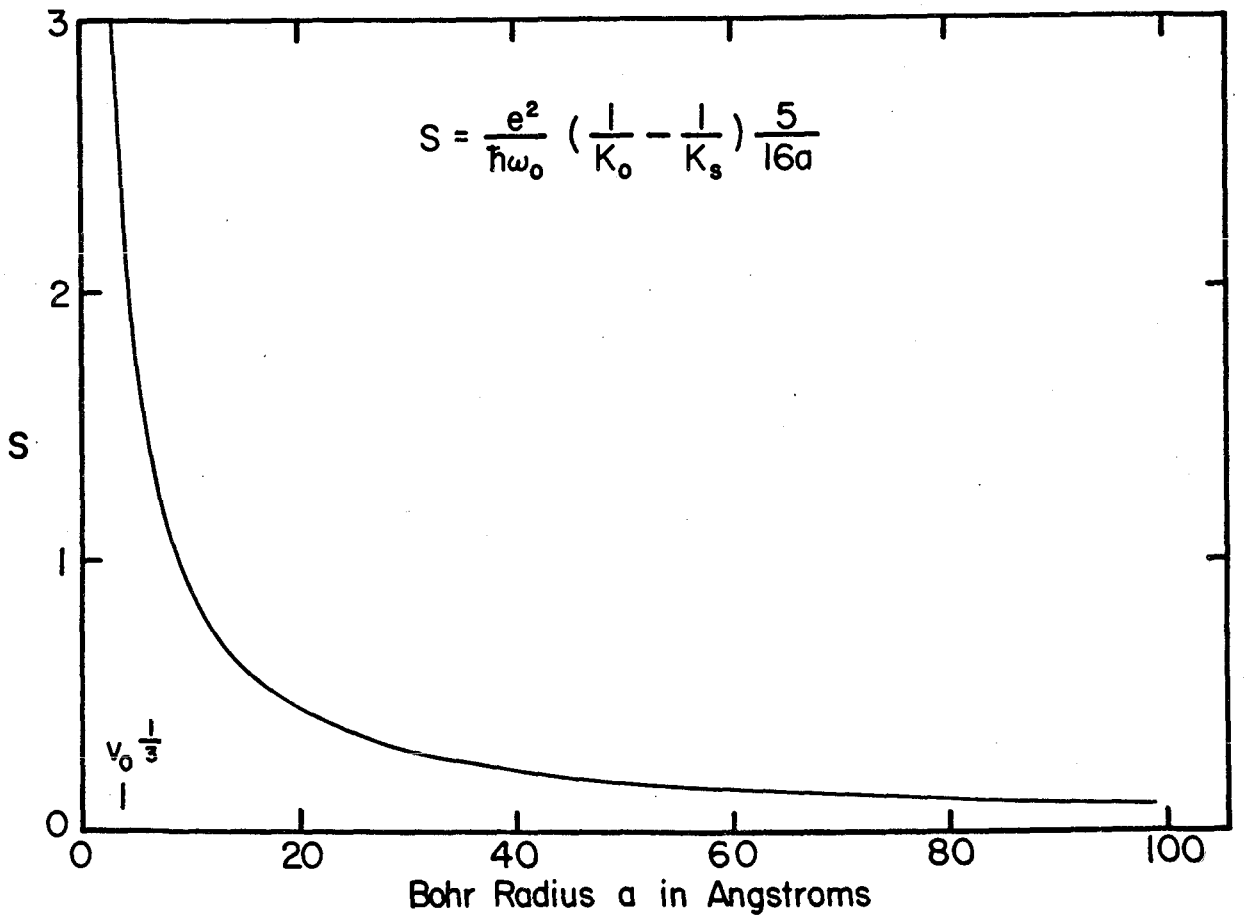

Fig. 6 Plot of the parameter S for CdS as a function of the Bohr radius of a localized excitation according to Toyozawa (1967).

to $V_o^{\frac{1}{3}}$, where V_o is the volume of the unit cell, the larger is S. For strongly localized charges such as F centers in the alkali-halides S ~ 20, whereas in II-VI semiconductors S ~ 1-2.

In Fig. 6 expression 3.221 is plotted for CdS. The longitudinal optical phonon energy was taken as 37.7 meV, while $\kappa_o = 5.24$ was taken from Czyzak et al. (1957), and $\kappa_s = 8.9$ evaluated from $\sqrt{\kappa_{11}\kappa_{33}}$ at 77°K from the data of Berlincourt et al. (1963). The coupling parameter given here would be appropriate for radiative transitions involving a bound hole (electron) and a free electron (hole).

The interaction coefficient for acoustical phonons is expressed in terms of the deformation potential E_d,

$$I_{ac}(\bar{r}) = \left(\frac{E_d^2}{NM}\right)^{\frac{1}{2}} k\, e^{i\bar{k}\cdot\bar{r}} \quad \dagger \qquad 3.222$$

M is the mass per unit cell and N is the number of unit cells in the crystal. Assuming the hydrogenic wavefunction in equation 3.219 gives

$$\Delta_{ac} = \frac{1}{\omega^2}\left(\frac{E_d^2}{NM}\right)^{\frac{1}{2}} \left[\left(\frac{ka}{2}\right)^2 + 1\right]^{-2} \cdot \qquad 3.223$$

---

†The subscript "ac" is used to refer to acoustical phonon interactions. No subscript is used for the electron-LO phonon parameters.

The electron-phonon interaction coefficient $I_i(\bar{r})$ for LO phonons of frequency ω_o is taken from Frohlich (1954).

$$I_i(\bar{r}) = \left[\frac{4\pi\omega_o{}^2 e^2}{V}\left(\frac{1}{\kappa_o} - \frac{1}{\kappa_s}\right)\right]^{\frac{1}{2}} \frac{e^{i\bar{k}\cdot\bar{r}}}{k} \qquad 3.218$$

where κ_s and κ_o are the static and optical dielectric constants, k is the phonon wavevector and V is the crystal volume.

For the case in which an electron (hole) localized to an impurity recombines with a free hole (electron) one finds, assuming a hydrogenic wavefunction for the bound carrier,

$$\varphi_e = \left(\frac{1}{\pi a^3}\right)^{\frac{1}{2}} e^{-\frac{r}{a}}, \qquad 3.219$$

that $$\Delta = \left[\frac{1}{k\omega_o}\ \frac{4\pi e^2}{V}\ \left(\frac{1}{\kappa_o} - \frac{1}{\kappa_s}\right)\right]^{\frac{1}{2}} \left[\left(\frac{ka}{2}\right)^2 + 1\right]^{-2} \qquad 3.220$$

Assuming no dispersion for the optical phonons, equations 3.214 and 3.215 give

$$S \approx \frac{e^2}{\hbar\omega_o}\left(\frac{1}{\kappa_o} - \frac{1}{\kappa_s}\right)\frac{5}{16a} \qquad 3.221$$

$$V_o^{\frac{1}{3}} < a \ .$$

The smaller the Bohr orbit of the bound carrier in relation

$$S = \int D(\omega)\, d\omega \qquad 3.214$$

$$D(\omega) = \sum_i \frac{\omega_i \Delta_i^2}{2\hbar}\, \delta(\omega-\omega_i) \qquad 3.215$$

where $D(\omega)$ is the coupling function. The zero phonon line is sharp with intensity given by e^{-S} while the one phonon line shape is given by $e^{-S}\, D(\omega)$. The two phonon line shape is given by the convolution $\frac{1}{2}\, e^{-S} \int D(\omega-\omega')\, D(\omega')\, d\omega'$ and higher orders by further convolutions.

Evaluation of S requires knowledge of the electronic wavefunctions in the ground and excited states. H, the electronic energy in a deformable lattice, may be expanded in terms of the normal coordinates q_i. Keeping the linear term only

$$H = H_e + H_{eL} \approx H_e + \sum_i I_i(\bar{r})\, q_i. \qquad 3.216$$

H_e is the electronic energy while H_{eL} is the electron-lattice interaction. Evaluating $\langle \varphi_g | H_{eL} | \varphi_g \rangle$ and $\langle \varphi_e | H_{eL} | \varphi_e \rangle$ where φ_e and φ_g are the wavefunctions in the excited state and the ground state, enables one to evaluate γ_i in equation 3.209. Then,

$$\Delta_i = -\frac{\gamma_i}{\omega_i^2} = \frac{1}{\omega_i^2} \int \left[|\varphi_g|^2 - |\varphi_e|^2 \right] I_i(\bar{r})\, d\bar{r}\ . \qquad 3.217$$

Using $\omega = ck$ where c is the sound velocity of the longitudinal branch gives

$$D_{ac}(\omega) = \frac{E_d^2 \omega}{\rho \hbar 4\pi^2 C^5 \left[\frac{\omega a}{2c}^2 + 1\right]^4} \quad . \qquad 3.224$$

$$V_o^{\frac{1}{3}} < a$$

Curves proportional to expression 3.224 are shown in Fig. 7 for centers of various Bohr radii. The maximum of $D_{ac}(\omega)$ comes at a frequency given by

$$\omega = \frac{2c}{\sqrt{7}\, a} \quad , \qquad 3.225$$

Calculation of the strength parameter S_{ac} using equation 3.224 gives (Toyozawa 1967)

$$S_{ac} = \frac{E_d^2}{\hbar \rho c^3} \quad \frac{1}{6\pi^2 a^2} \quad . \qquad 3.226$$

As noted earlier an electron-acoustical phonon interaction through the piezoelectric effect is also possible in CdS. The piezoelectric effect is anisotropic, making detailed calculations very difficult. However, it is possible that for certain bound states which are also anisotropic (e.g. the bound hole) the piezoelectric coupling has a relatively small effect.

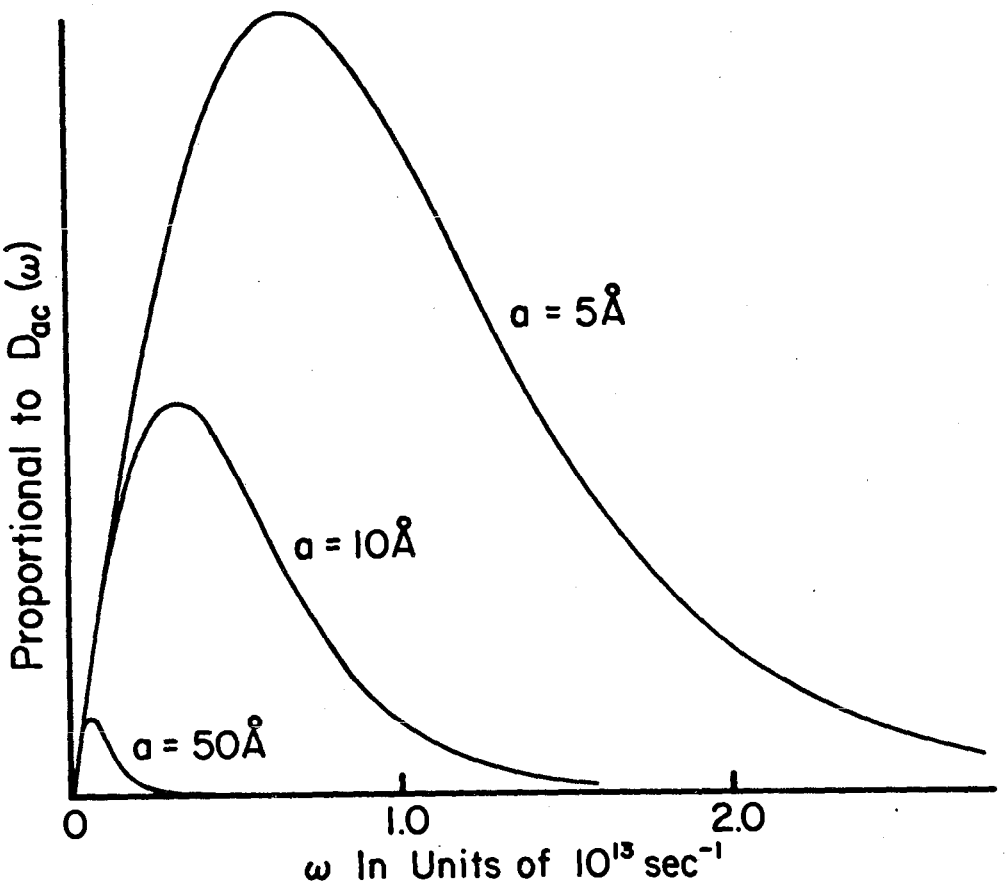

Fig. 7 Plot of $D_{ac}(\omega)$ using the deformation potential interaction for centers with Bohr radii 5 Å, 10 Å, and 50 Å. A longitudinal sound velocity (room temp.) of 4.4×10^5 cm/sec was used.

Since $S_{ac} \alpha \frac{1}{a^2}$, then for deep localized centers (such as deep acceptor or isoelectronic traps), the strong interaction with acoustical phonons tends to wash out the LO phonon structure, resulting in a broad featureless band of luminescence or absorption. For instance, the luminescence of CdS doped with the isoelectronic impurity Te (Aten et al. 1965, Cuthbert and Thomas 1968) has the maximum of its luminescence corresponding to the emission of 8 LO phonons; however, strong acoustical phonon interaction has smoothed out the structure.

In expression 3.221, S was evaluated for one of the carriers being localized to an impurity. The corresponding calculation of S for a transition involving an exciton presents a slightly more complex problem. Ignoring the effect of exciton recoil energy (Toyozawa 1970) one obtains

$$\hat{D}(\omega) = \sum_i \frac{\omega_i}{2\hbar} |\Delta_i^e - \Delta_i^h|^2 \delta(\omega - \omega_i) \qquad 3.227$$

where Δ_i^e and Δ_i^h are calculated using equation 3.217 for the electron and hole.

Toyozawa (1970) introduced a factor to allow for the kinetic energy of the exciton as a result of the recoil momentum from the emission of a phonon with wave vector $\bar{k}$. Our results for exciton-LO phonon effects in CdS indicate that

the effects of recoil energy are small so that the exciton may be treated as a localized excitation. We treat the exciton center of mass as fixed and write

$$|\Psi_{ex}|^2 = \left(\frac{1}{\pi a_o^3}\right) \exp\left(-\frac{2r}{a_o}\right) \delta(\bar{R}-\bar{R}_o) \qquad 3.228$$

where $\bar{r} = \bar{r}_e - \bar{r}_h$ and $\bar{R} = \frac{m_e\bar{r}_e + m_h\bar{r}_h}{m_e + m_h}$. The exciton Bohr radius a_o is given by $a_o = a_e + a_h$. The quantities a_e and a_h are the Bohr radii of the electron and hole. Integrating over $\bar{r}_e$ to give the wavefunction for the hole gives

$$|\Psi_h|^2 = \left(\frac{1}{\pi a_h^3}\right) \exp\left(-\frac{2r_h}{a_h}\right) \qquad 3.229a$$

and for the electron $|\Psi_e|^2 = \left(\frac{1}{\pi a_e^3}\right) \exp\left(-\frac{2r_e}{a_e}\right)$. 3.229b

Evaluation of $\hat{D}(\omega)$ for the exciton in equation 3.227 results in the following expression for $\hat{S}$, the strength parameter for an exciton.

$$\hat{S} = \frac{5}{16}\frac{e^2}{\hbar\omega_o}\left(\frac{1}{\kappa_o} - \frac{1}{\kappa_s}\right)\left[\frac{1}{a_h} + \frac{1}{a_e} - \frac{16}{5}\frac{\alpha^2 + 3\alpha + 1)}{a_e(\alpha + 1)^3}\right] \qquad 3.230$$

where $\alpha = \frac{a_e}{a_h}$. As before $a_e > V_o^{\frac{1}{3}}$ and $a_h > V_o^{\frac{1}{3}}$. In the

hydrogenic model $\alpha = \left(\frac{m_e}{m_h}\right)^{-1}$ where m_e and m_h are the effective masses of the electron and the hole respectively.

Factoring out a_h,

$$\hat{S} = \frac{5}{16} \frac{e^2}{\hbar\omega_o} \left(\frac{1}{\kappa_o} - \frac{1}{\kappa_s}\right) \frac{1}{a_h} \left[\frac{(\alpha - 1)^2 \left(1 + \frac{14}{5}\alpha + \alpha^2\right)}{\alpha(1 + \alpha^3)}\right] \geq 0 . \qquad 3.231$$

For $a_h = a_e$, $\hat{S} = 0$ as expected. When expression 3.221 is written for the particle with the smaller Bohr orbit, in this case the hole, one obtains

$$\frac{\hat{S}}{S} = \frac{(\alpha-1)^2 \left(1 + \frac{14}{5}\alpha + \alpha^2\right)}{\alpha (1 + \alpha)^3} . \qquad 3.232$$

This expression is plotted in Fig. 8 using the convention that $\alpha \geq 1$. This curve shows how $\hat{S}$ varies as a function of the electron and hole radii in the exciton. For $\alpha >> 1$, then $\hat{S}$ approaches S, the result for a localized hole (or electron). Thus the strength of the interaction between excitons and LO phonons in semiconductors depends on the ratio of the effective masses of the electrons and holes.

The exciton may be bound to a neutral acceptor, which is written schematically as $\Theta_+^{+\ -}$ where + and - represent the hole and the electron respectively, or the exciton may be bound to a neutral donor written schematically as $\oplus^{-}_{-}$ +. Then the

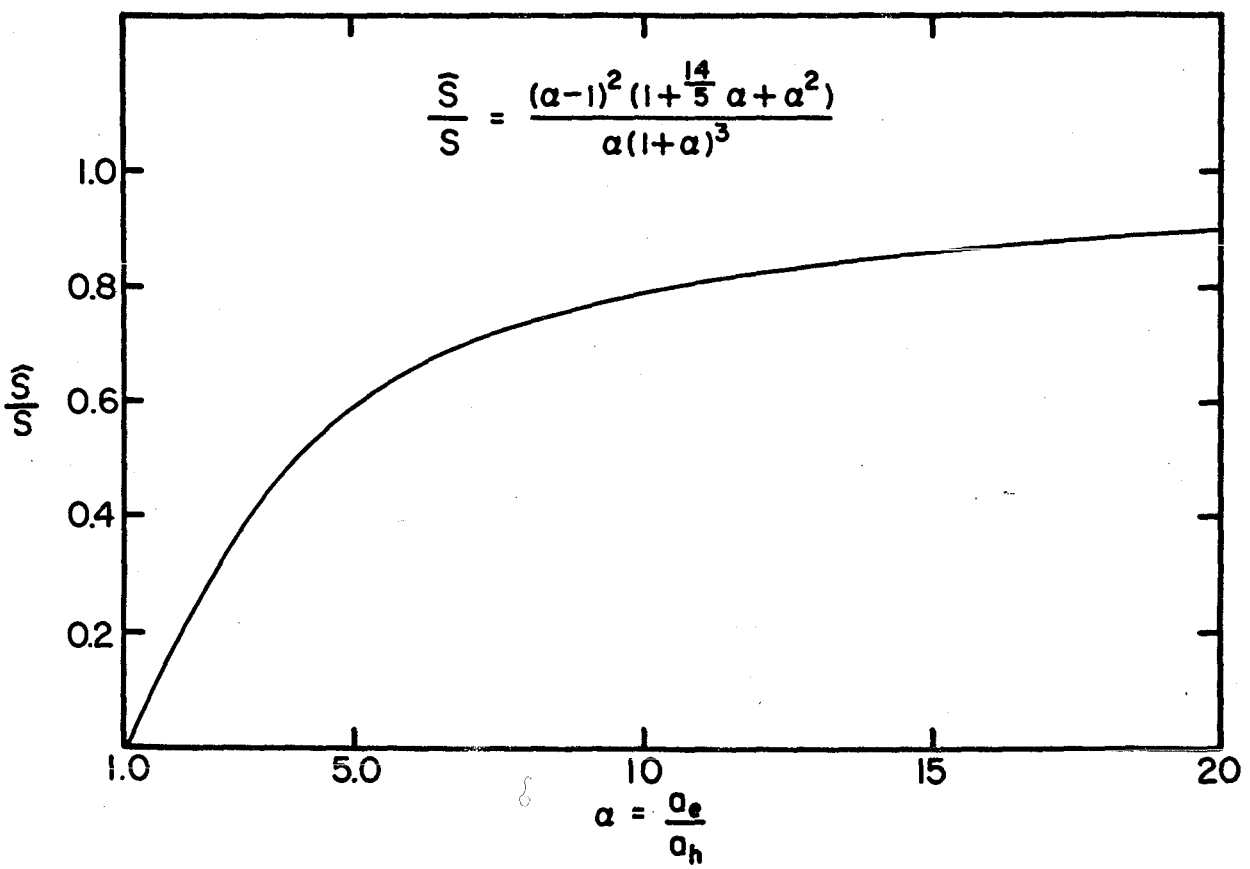

Fig. 8 Plot of the ratio $\hat{S}$ for an exciton divided by S for a localized hole as a function of the ratio of the Bohr radii of the electron and the hole with the convention $\alpha > 1$.

expression for D for the exciton bound to a neutral donor may be written

$$D(\omega) = \sum_i \frac{\omega_i}{2\hbar} |\Delta_i^{e_1} + \Delta^{e_2} - \Delta_i^{h} - \Delta_i^{e_2'}|^2 \delta(\omega - \omega_i) \qquad 3.233$$

where

$$\Delta_i^{e_1} + \Delta_i^{e_2} - \Delta_i^{h} - \Delta_i^{e_2'} = \frac{1}{\omega_o^2}\int\left[|\varphi_{e_1}|^2 + |\varphi_{e_2}|^2 - |\varphi_h|^2 - |\varphi'_{e_2}|^2\right] I(\bar{r})\, d\bar{r} \; . \qquad 3.234$$

φ_{e1} is the wavefunction for electron 1 } on the
φ_{e2} is the wavefunction for electron 2 } bound exciton
φ_h is the wavefunction for the hole } complex

φ'_{e_2} is the wavefunction for the electron remaining on the donor after the recombination of electron 1 and the hole.

As discussed by Henry and Nassau (1970a) and Malm and Haering (1971b) luminescence has been observed for cases where φ'_{e_2} corresponds to the 1s, 2s, 2p, 3s, etc., states. Expression 3.233 then allows for a difference in the initial and final electron configuration of the residual electron. Explicit forms of the wavefunctions for the exciton bound to a neutral donor or a neutral acceptor are required in order to evaluate $\hat{D}$ in equation 3.233. These wavefunctions are presently unknown. If it is assumed that the exciton states are

unaltered by the impurity, equation 3.230 may be used for the case $\varphi_{e2} = \varphi'_{e2}$.

The coupling strength can also be evaluated for the bound to bound transition. The bound to bound luminescence consists of the radiative recombination of an electron bound to a donor and a hole bound to an acceptor. Consider a donor at $\bar{r} = 0$ and an acceptor at $\bar{r} = \bar{R}$. In this case

$$\Delta_{DA} = \frac{1}{\omega_o^2}\int\left[|\varphi_D|^2 - |\varphi_A|^2\right] I(\bar{r})\,d\bar{r} \quad . \qquad 3.235$$

Hydrogenic donor and acceptor wavefunctions are assumed.

$$\varphi_D = \left(\frac{1}{\pi a_e^3}\right)^{\frac{1}{2}} \exp\left(-\frac{r}{a_e}\right) \qquad 3.236a$$

$$A = \left(\frac{1}{\pi a_h^3}\right)^{\frac{1}{2}} \exp\left(-\frac{r'}{a_h}\right) \qquad 3.236b$$

with $\bar{r}' = \bar{r} - \bar{R}$.

Evaluating Δ_{DA} and $D(\omega)$ for this case gives the following result for $\bar{S}$, the strength parameter appropriate for a donor and acceptor separated by R.

$$\bar{S} = \frac{e^2}{\hbar\omega_o}\left(\frac{1}{\kappa_o} - \frac{1}{\kappa_s}\right)\left[\frac{5}{16a_h} + \frac{5}{16a_e} + T\right] \qquad 3.237$$

where

$$T = -\frac{2}{a_h \alpha\gamma} \frac{1}{(\alpha^2 - 1)^2} \left[(\alpha^2 - 1)^2 - \frac{(3\alpha^2 - 1)}{(\alpha^2 - 1)} e^{-\alpha\gamma} \right.$$

$$\left. - \frac{\alpha\gamma e^{-\alpha\gamma}}{2} - \frac{\alpha^4(\alpha^2 - 3)}{(\alpha^2 - 1)} e^{-\gamma} - \frac{\alpha^4\gamma}{2} e^{-\gamma} \right].$$

and $\alpha = \frac{a_e}{a_h}$, $\gamma = \frac{2R}{a_e}$.

Again using expression 3.221 for S evaluated for the particle with the smaller Bohr orbit (the hole), one obtains

$$\frac{\overline{S}}{S} = 1 + \frac{1}{\alpha} + \frac{16}{5} a_h T . \qquad 3.238$$

In this convention $\alpha \geq 1$. The above result has been plotted as a function of $\gamma = \frac{2R}{a_e}$ for several different values of α in Fig. 9. For a zero donor-acceptor separation, the coupling strength $\overline{S}$ is equal to the free exciton result of equation 3.231. The coupling strength $\overline{S}$ varies most strongly with R when the electron and hole masses are equal, for in this case $\overline{S}$ for the bound to bound transitions varies from 0 at R = 0 to 2S as $R \to \infty$. For mass ratios $\alpha > 1$, the variation with donor-acceptor separation is pronounced.

Evaluation of the coupling strength $\hat{S}$ and $\overline{S}$ for the exci-

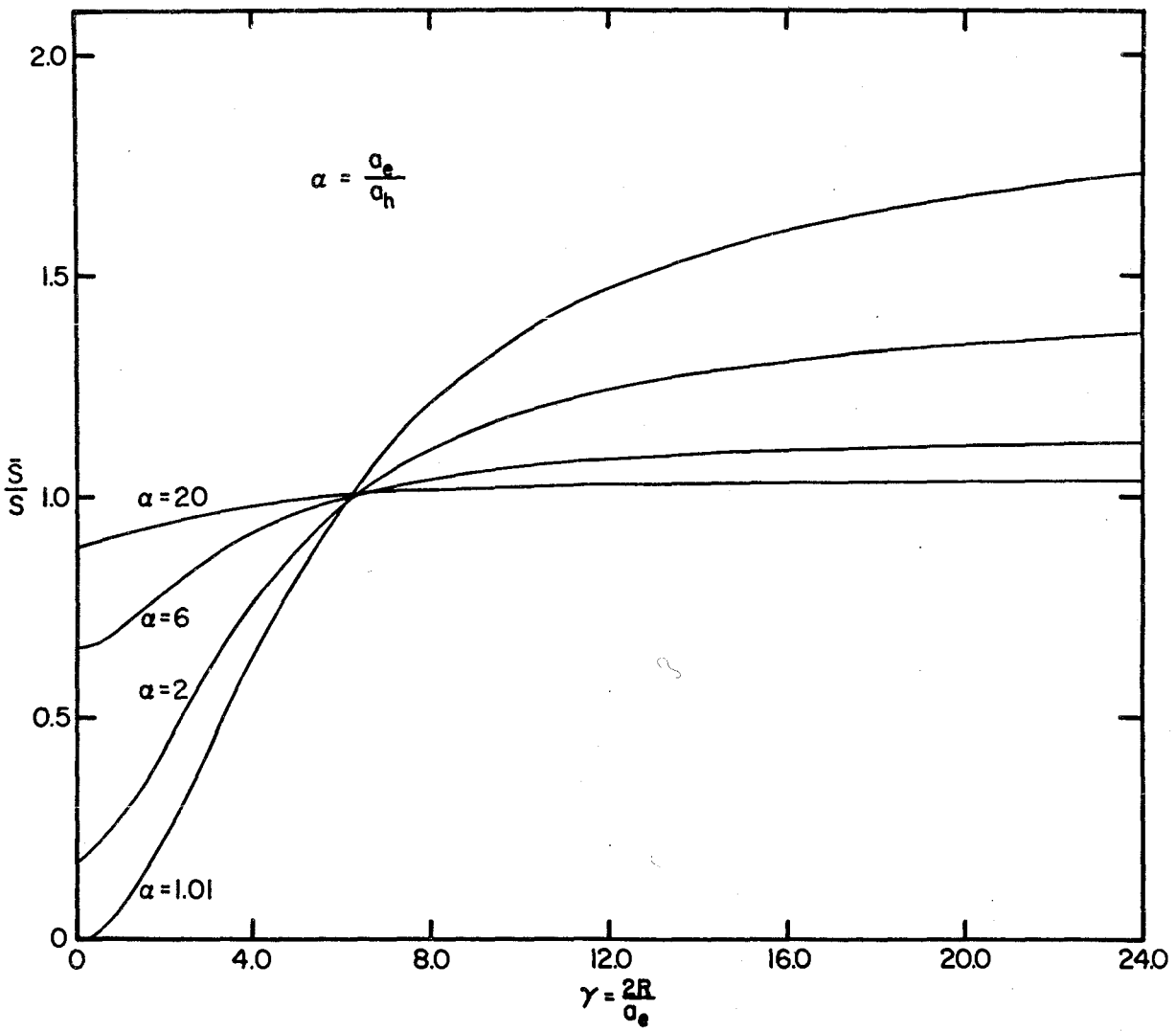

Fig. 9 Plot of the strength parameter $\bar{S}$ for a bound to bound transition normalized to S for a localized hole as a function of the donor-acceptor separation R in units of a_e the Bohr radius of the bound electron.

ton and bound to bound transitions requires knowledge of the radii of the electron and the hole. Using the results of Henry and Nassau (1970a) for the electron effective mass, which is $m_{e\perp} = 0.19\ m$ and $m_{e\parallel} = 0.18m$ in terms of the electron mass m, and the dielectric constants reported by Berlincourt et al. (1963), which are $\kappa_{11} = 8.48$ and $\kappa_{33} = 9.48$ (77°K), gives $a_{e\perp} = 23.5\ n^2$ Å and $a_{e\parallel} = 28\ n^2$ Å. The principal quantum number is n. Thus the electron is approximately isotropic. However, the hole effective mass measured by Hopfield and Thomas (1961) is highly anisotropic. Their values of $m_{h\perp} = 0.7m$ and $m_{e\parallel} = 5m$ give $a_{h\perp} = 6.4n^2$ Å and $a_{h\parallel} = 1\ n^2$Å. This value of $a_{h\parallel}$ is less than $V_o^{\frac{1}{3}}$. The correct value of a_h as seen by the long wavelength phonons is open to question and detailed calculations will be necessary to properly account for the effect of the mass anisotropy. If effective values of a_e and a_h are assumed, $\hat{S}$ and $\bar{S}$ may be evaluated from equations 3.231 and 3.237. These equations may also be used to predict general trends. For example, excitons with principal quantum number $n > 1$, according to the above, have a value for $\hat{S}$ equal to n^{-2} times the value for the $n = 1$ exciton.

3.3 Analysis of Excitation Spectra

The theory presented in the foregoing section is a theory applicable to absorption processes. The validity of the application of this theory to excitation spectra requires some

comment since an excitation spectrum E(hν) is the product of the absorption spectrum A(hν) and the probability P(hν) that the excited state decays to the observed luminescent state. The observed resonant effects in excitation spectra may, in general, arise from A(hν), or from P(hν) or from a combination of both of these terms.

The interpretation of our data is based on the assumption that the RELATIVE intensities of the LO phonon resonances are associated with A(hν). For each luminescent transition in a crystal, P(hν) is determined by the relative importance of energy loss of the photoexcited complex by the emission of LO phonons compared to energy loss by other relaxation phenomena (emission of acoustic phonons, impurity trapping of excitons, etc.). In general P(hν) is a complicated function depending on the type and concentration of impurities in the crystal.

The following considerations are intended to make our interpretation plausible although they do not constitute a general proof. Consider a level structure similar to that shown in Fig. 4 which is optically pumped to the p th level while the luminescence associated with p = 0 level is monitored. Assuming that the dominant relaxation of the n th level is to the (n - 1) th level via the emission of an LO phonon, the appropriate rate equations are (Fischer et al. 1971)

$$\frac{dN_p}{dt} = g_p - tN_p - \Gamma_p N_p \quad , \qquad 3.301$$

$$\frac{dN_q}{dt} = tN_{q+1} - tN_q - \Gamma_q N_q \quad , \qquad 3.302$$

$$0 < q < p$$

$$\frac{dN_o}{dt} = tN_1 - \Gamma_o N_o \qquad 3.303$$

where t denotes the LO phonon relaxation rate (assumed to be independent of q), Γ_q denotes the radiative relaxation rate from the q th level, and g_p denotes the generation rate for the p th level. The quantity g_p is proportional to the absorption A(hν) and contains the resonant LO structure associated with A(hν), i.e. $g_p = \alpha \frac{e^{-s} s^p}{p!}$. The value of Γ_q is proportional to $|\langle \chi_{eq} | \chi_{gm} \rangle|^2$ and also may be affected by the presence of resonant energy levels such as bound excitons, etc.

In the steady state where the time derivatives equal zero, one finds that the relative probabilities of optical transitions from the excited to the ground state are

$$1, \alpha_{p-1}, \alpha_{p-2}, \ldots\ldots, \frac{\alpha_o \alpha_1 \ldots\ldots \alpha_{p-1}}{1 - \alpha_o} \qquad 3.304$$

for the p th, (p - 1) th ....., p = 0 levels respectively.

$$\alpha_q = \frac{t}{t+\Gamma_q}$$

For $\alpha_q \to 1$ (i.e. $\Gamma_q << t$) the most probable optical transition is from the p = 0 level of the excited state. The presence or absence of luminescent transitions of energy $\varepsilon_o + p\hbar\omega_o$ (p>0) in this model gives a measure of the relative magnitudes of t and Γ_i.

For the case when $\Gamma_q << t$ (q≠0), which corresponds to the rate of emission of LO phonons by the photoexcited complex being much larger than the radiative recombination rate, then $N_o \approx \frac{g_p}{\Gamma_o}$. Hence the luminescent intensity which is proportional to N_o mirrors the absorption A(hν) and the relative intensities of the resonances are given by $\frac{e^{-s}s^p}{p!}$. However, the line widths of excitation spectra may in general differ from the absorption lines due to the resonant nature of P(hν). A detailed discussion requires a consideration of competing relaxation phenomena due to acoustic phonons and exciton trapping by impurities. Differences in P(hν) between crystals are discussed in a later section on non-resonant processes.

One may ask why the pronounced resonant effects observed in some excitation spectra are not seen with equal facility in the absorption spectrum. This is thought to be due to the

competition of other absorption processes which are eliminated in the excitation spectrum because a single luminescent process is monitored in the latter case.

3.4 Saturation Effects in Bound to Bound Luminescence

In the following we use the term bound to bound for the low energy series (LES) and free to bound for the high energy series (HES). At low temperatures the energy of emission E from a bound hole and bound electron is given by

$$E = E_g - (E_A + E_D) + \frac{e^2}{\kappa_s R} - mLO \pm m'E_p \qquad 3.401$$

where E_g is the direct band gap of CdS,

E_A is the acceptor binding energy,

E_D is the donor binding energy, and

$\frac{e^2}{\kappa_s R}$ is the Coulomb energy between the electron and hole separated by a distance R in a dielectric medium of dielectric constant κ.

LO is the energy of the longitudinal optical (LO) phonon.

m is the number of LO phonons emitted simultaneously with the photon emission. LO phonon absorption is negligible at low temperatures.

$m'E_p$ refers to absorption and emission of acoustical phonons.

The recombination rate for a bound electron and bound hole

is deduced from the overlap of the wavefunctions. In CdS where the acceptor radius (<10Å) is much less than the donor radius (30Å), the rate W is given by

$$W \alpha |\psi_D|^2$$

or

$$W = W_o e^{-\frac{2R}{a_D}}$$

assuming a hydrogenic donor where a_D is the donor radius, obtained from

$$E_D = \frac{e^2}{2\kappa_s a_D}.$$

E_D is the donor binding energy.

Assuming a random distribution of donors and acceptors,† one can write down an expression for the shape of the bound to bound emission, not including phonon absorption or emission.

$$N(E) = \int_o^\infty n_A(O)\, n_D(R)\, W_o e^{-\frac{2R}{a_D}} 4\pi R^2 \delta(E - E(R))\, dR \qquad 3.402$$

$n_D(R)$ and $n_A(O)$ are the concentrations of neutral donors and acceptors separated by a distance R which have respectively bound electrons and bound holes.

† Effects due to clustering of donors and acceptors may be important in certain situations. However, these effects are not included in our model.

$$E - E(R) = E - \left[E_g - (E_D + E_A) + \frac{e^2}{\kappa_s R} \right] .$$

If all the acceptors and donors were neutral so $n_A = N_A$, the acceptor concentration, and $n_D = N_D$, the donor concentration, then

$$N(E) = 4\pi N_A N_D \frac{\kappa_s}{e^2} W_o e^{-\frac{2R_o}{a_D}} R_o^4; \quad R_o = \frac{e^2}{\kappa_s (E - E_g + E_A + E_D)} . \qquad 3.403$$

This treats the donor-acceptor pair as being isolated. Morgan et al. (1969) has added a nearest neighbour factor to equation 3.403. This factor is important only at high doping concentrations and is not included here.

Under the assumption that all the donors and acceptors are neutral the bound to bound emission described by equation 3.403 has a maximum at $E = E_g - E_A$ (at $R = 2a_D$). This is observed for the bound to bound luminescence of GaP under flash excitation [Thomas et al. (1964)]. However, in CdS the maximum of the bound to bound luminescence occurs at an energy less than $E_g - E_A$. This is a consequence of the much larger radiative recombination rate in CdS ($W_o = 4 \times 10^8$ sec^{-1}) compared to GaP ($W_o = 5 \times 10^5$ sec^{-1}).

One can readily understand that in CdS donors and accep-

tors of small separations are mostly ionized. Consideration of carrier trapping rates in the following simplified model shows why this is so. In CdS, the acceptor trapping cross-section >> donor cross-section. Suppose that an acceptor has trapped a hole; the proportion of neutral acceptors then depends on the incident intensity. Neglecting other forms of recombination, the rate equation describing the density of neutral donors (n_D) nearby is given by

$$\frac{dn_D}{dt} = n(N_D - n_D)\ S'v - n_D\ W_o \exp(-\frac{2R}{a_D}) \qquad 3.404$$

where n is the density of free electrons in the region, S' is a trapping cross-section and v is the electron velocity. The first term represents the donor trapping rate while the second term is the bound to bound recombination rate. Under steady state conditions

$$\frac{dn_D}{dt} = 0. \text{ Solving; } n_D = N_D \left[1 + \frac{W_o \exp(-\frac{2R}{a_D})}{nS'v}\right]^{-1} \cdot \qquad 3.405$$

For small donor-acceptor separations $W_o \exp(-\frac{2R}{a_D}) >> nS'v$ and $n_D \simeq N_D\ W_o^{-1} \exp(\frac{2R}{a_D}) nS'v$, while in the opposite extreme $n_D \simeq N_D$. Then for small separations where the donors are mostly ionized, expression 3.402 upon integration becomes

$$N(E) = n_A N_D nS'v\, 4\pi \frac{\kappa_s}{e^2} R_o^4 \qquad R_o < R_c \quad .$$

Dependence on the electron-hole creation rate is in n and n_A. R_c is the separation at which $W_o \exp(-\frac{2R}{a_D}) \sim nS'v$.

For some CdS crystals the shape of the bound to bound emission band follows the R_o^4 dependence fairly closely for small donor-acceptor separations up to some characteristic R_C where the bound to bound recombination rate is comparable to the electron trapping rate.

The difference between CdS and GaP is in the values of W_o. For GaP $W_o \simeq 5 \times 10^5$ sec^{-1} while for CdS $W_o \simeq 4 \pm 2 \times 10^8$ sec^{-1} [Colbow (1966)]. Hence the inequality $W_o \exp -(\frac{2R}{a_D}) > nS'v$ holds for pairs of larger R in CdS than in GaP under similar incident intensities.

3.5 Correlation Effects in the Bound to Bound Luminescence

As a result of exciton formation, there is (for a hole situated at or near an acceptor site) an increased probability of finding an electron a distance a_o away, where a_o is the exciton radius. This additional effect in the bound to bound luminescence is proportional to the probability density of finding an electron a distance from a hole. In the hydrogenic approximation this is given by $A(\frac{R}{a_o})^2 \exp(-\frac{2R}{a_o})$ where A is a parameter which measures the effect of electron hole correlation due to excitons. With this additional effect equation 3.402 now becomes

$$N(E) = \int_o^\infty \left[1 + A\left(\frac{R}{a_o}\right)^2 \exp\left(-\frac{2R}{a_D}\right)\right] n_A(O) N_D(R) \exp\left(-\frac{2R}{a_D}\right) 4\pi R^2 \delta(E - E(R)\,dR)$$

$$= N_1(E) + A\,N_2(E) \qquad 3.501$$

where $N_1(E)$ gives the line shape without electron-hole correlation effects and $N_2(E)$ is the new contribution. The relative importance of this exciton effect can be expressed by

$$\frac{A\,N_2(E)}{N_1(E)}. \qquad 3.502$$

Differentiation shows that this has a maximum at $R_o = a_o$, the exciton Bohr radius. For excitons with principal quantum number n = 2, the maximum of this expression is expected at $4a_o$.

The overall effect of the electron-hole correlation effect is to shift the position of maximum intensity of the bound to bound luminescence to a higher energy than with the capture of uncorrelated electrons and holes by ionized donors and acceptors.

3.6 Excited States of Bound Excitons

An exciton may be bound to a neutral or charged impurity in a manner analogous to the bound state of the hydrogen mole-

cule. In a theoretical paper (Hopfield 1964) showed that in CdS where $\frac{m_h}{m_e} > 1.4$ the exciton could be bound to a neutral donor and an ionized donor, but not an ionized acceptor. This is in agreement with the luminescent lines which were identified by Thomas and Hopfield (1962). The electron is not bound to a neutral acceptor since the kinetic energy in localizing it in a bound state is too large.

However, a detailed calculation of the wavefunction of the bound exciton complex has not yet been done. Although the hydrogen molecule may be used as a guideline, the mass ratio $\frac{m_h}{m_e}$ in CdS is about 4, which is much less than in a hydrogen atom. In addition, the magnitude of the central cell correction which describes the difference in electron affinity between the impurity atom and the host lattice is not known. Both of these factors give difficulties in evaluating the ground state wavefunction and hence the excited state energies.

4. OPTICAL EXCITATION - TECHNIQUE AND APPARATUS

4.1 Optical System

In studies of photoluminescence of a material, it is usual to illuminate the material with a broad band of above band-gap radiation. A high resolution spectrometer is used to analyze the luminescent radiation.

When a monochromator is used to define the incident photon energy band, two types of experiment become possible.

MODE I: The incident wavelength from the monochromator is selected to coincide with a resonant absorption line of the crystal. A Spectrum of the luminescence at lower energies by the spectrometer then shows luminescent transitions associated with the excited line. This technique enables one to rapidly sort out a complicated spectrum by grouping lines which belong to the same complex.

MODE II: The spectrometer is used to select a luminescent wavelength for study. Then the monochromator is used to vary the incident photon energy and a recording of intensity of the luminescent transition selected by the spectrometer vs. incident wavelength gives a luminescent excitation spectrum. Conradi and Haering (1969) used this mode in recording excitation spectra of bound excitons in CdS. A recording of current through the sample (at constant voltage) vs. incident wavelength gives a photoconductivity excitation spectrum.

The use of a monochromator to define the incident wavelength reduces the incident intensity considerably so that careful design of the optical system is required. There is a trade-off between observed intensity and resolution.

For our experiments the lamp was focussed onto the incident slit of a Spex Industries Model 1700 monochromator which had

a linear dispersion in second order of 5 Å/mm. The lamp was arranged to fully illuminate the grating (F-6.8). With 1mm slits, the power at the exit slit was 0.05 mW at 4800 Å using a 100 W high pressure Hg lamp and 0.01 mW using a 100 W tungsten lamp.

The intensity from the Hg lamp was fairly constant in the range 4450 Å to 4900 Å. The tungsten lamp was used to extend this range to longer wavelengths. A correction technique used by Conradi (1968) for variations in incident intensity was found to be unnecessary for good lamps (lamps with little flicker).

The incident light was focussed onto the crystal using a high quality camera lens having a focal length of 55 mm. Since the intensity of the bound exciton lines varies with incident intensity I as $I^{1.4}$ [Maeda (1965)], a small focal length is advantageous. The average angle of incidence on the crystal was about 60°.

The luminescent light from the crystal was gathered by a second camera lens (F-1.4) or a F-3.5 lens and focussed onto the slit of a Spex Industries Model 1702 spectrometer so as to fully illuminate the grating. The light was chopped at 80 Hz and detected with a high sensitivity photomultiplier (S-20 response) connected to a lock-in amplifier. An x-y recording was made of luminescent intensity vs. wavelength. Fig. 10

A

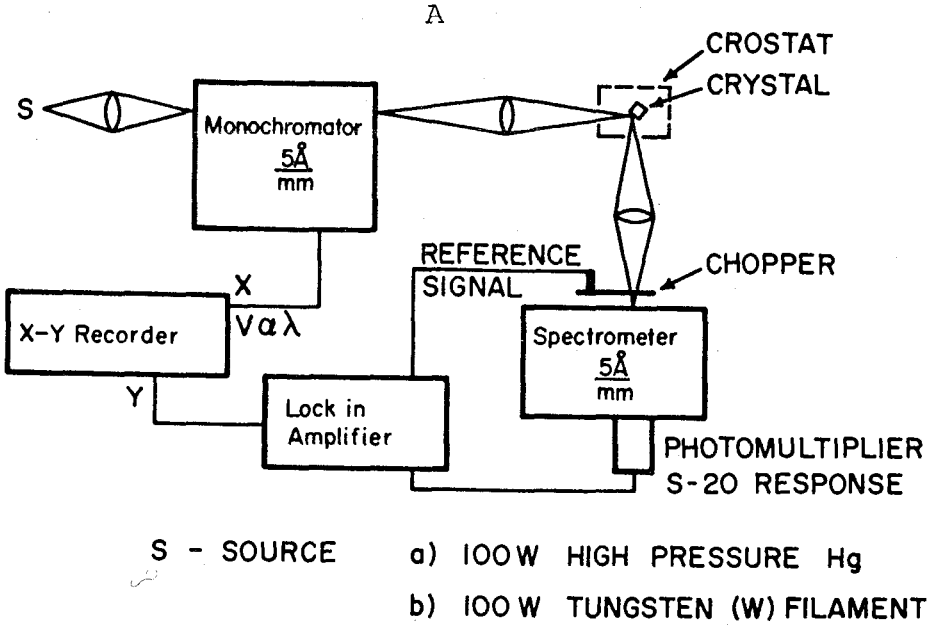

S - SOURCE a) 100 W HIGH PRESSURE Hg
b) 100 W TUNGSTEN (W) FILAMENT

B

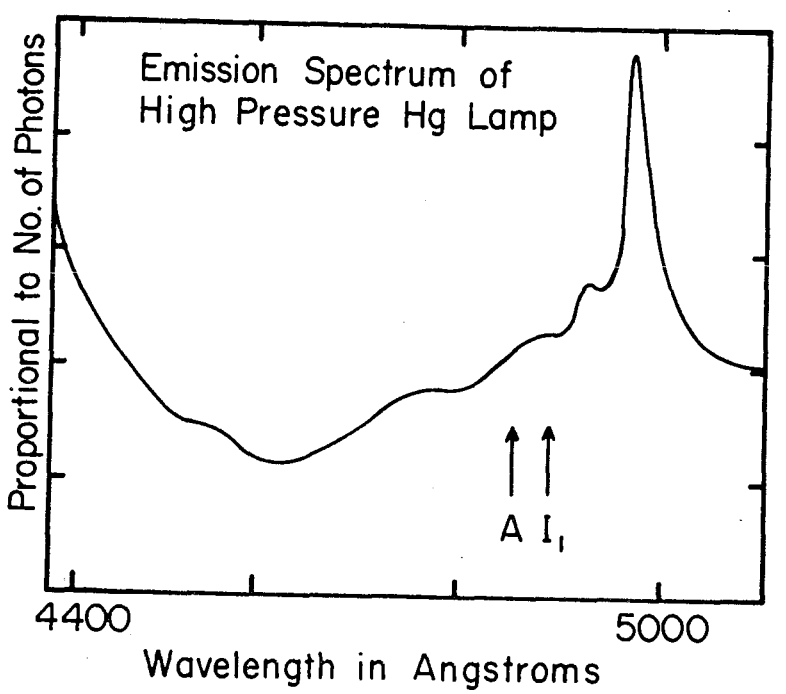

Fig. 10A Schematic of the experimental apparatus for optical excitation of the luminescence.

B Spectrum of the incident light expressed in terms of number of incident photons. Position of the A exciton and I_1 luminescence are shown.

shows a schematic of the experiment and the spectrum of the Hg lamp source.

4.2 Cryostat

The crystal was mounted onto a copper block with a dab of nail polish in a variable temperature cryostat (manufactured by Andonian Associates Inc.). The crystal ambient was flowing cold He gas during an experiment. Temperature was measured using a Au + 0.03 at % Fe vs. Au-Ag thermocouple*. Temperatures from 2°K to 100°K were used in the experiments.

Care was taken to orient the crystal to minimize the reflected light intensity on the slit of the spectrometer.

4.3 Crystal Preparation

CdS crystals were purchased from Eagle-Picher or were grown by a vapor transport method†. Following the method of Handelman and Thomas (1965) some crystals were converted from an n type to a compensated type (high resistivity) by a vacuum anneal of 4 to 24 hrs at 600°C. Compensated crystals were converted to n type by an anneal at 600°C with an excess of Cd present.

Crystals that were n type always showed the I_2 luminescence (exciton bound to a neutral donor) at low temperatures

*Kindly donated by Prof. D.J. Huntley, Simon Fraser University

†Two crystals were obtained from K. Yuen, Simon Fraser University

while compensated crystals (number of donors ≈ number of acceptors) showed a bound to bound luminescence together with weaker I_1 (exciton bound to a neutral acceptor) and I_2 lines. Handelman and Thomas (1965) were the first to establish that the acceptor responsible for I_1 was also responsible for the bound to bound luminescence.

However, certain n type crystals were not compensated and did not show the bound to bound luminescence after a 600°C vacuum anneal. After these crystals were annealed in the presence of $NaNO_3$ at 600°C for 24 hrs, the green bound to bound and I_1 luminescence appeared. This suggests that Na is an acceptor in CdS (Henry, Nassau and Shiever 1970). Consequently, crystals that are originally deficient in Na (or Li) cannot be compensated by a simple vacuum anneal.

Doping concentrations were estimated by measuring the room temperature conductivity of the n-type crystal and using the expression $\sigma = ne\mu$ to evaluate the donor concentration n. The electronic charge is e and the electron mobility μ was taken to be 300 cm^2/volt sec (Maeda 1965). Crystals were converted to n type by the Cd anneal described above. Donor concentrations quoted have an estimated precision of 30%.

Crystals were either cleaved or etched in HCl. Only cleaved crystals were used in experiments investigating polarization effects as etching made $\frac{I_\perp}{I_\parallel} \rightarrow 1$ for all lines. The usual etch was for 1 minute in concentrated HCl followed by a

thorough wash in distilled water. The etching rate is 36 μ per min. (Woodbury and Hall 1967) so shorter etches were sometimes used. An etch suggested by Conradi (1968) ($KMnO_4$ in conc. H_2SO_4) was found to be good for compensated crystals, but introduced a luminescent band centered at 4940 Å in n type crystals. Prolonged exposure to air (a few hours) reduced the luminescent efficiency of all crystals and also produced the luminescent band at 4940 Å in n type crystals. Therefore all crystals were maintained in a He atmosphere after mounting. The c axis of the crystal (the hexagonal axis) was in the plane of a freshly cleaved or etched surface.

5. OPTICAL EXCITATION - RESULTS AND DISCUSSION

5.1 Most of the luminescent transitions in CdS were studied by use of the Mode I and Mode II techniques discussed earlier and by observation of the luminescence as a function of temperature. This chapter is divided into six sections dealing with the identification of the luminescent transitions, evaluation of the acceptor energy, Franck-Condon effects in absorption and luminescence, non-radiative and radiative relaxation rates, and observation of electron-hole correlation effects in the bound to bound luminescence.

5.2 Excited States of Neutral Donors and Bound Excitons in CdS

5.2.1 Identification of Spectrum Lines

In compensated CdS crystals doped to levels $>10^{16} cm^{-3}$ the luminescence is similar to that shown in Fig. 11. Most of the luminescence comes from the green bound to bound band and its phonon replicas, while the free and bound exciton lines are relatively weak. However, in a crystal doped at lower concentrations ($\sim 10^{15}$ cm^{-3}), the bound to bound emission intensity drops considerably and the luminescence from free and bound excitons increases. This is a consequence of the radiative transition rate for the separated donor-acceptor pair varying as $e^{-\frac{2R}{a_D}}$. Increasing the mean value of R by decreasing the doping concentration decreases the relative probability of bound to bound luminescent transitions compared to bound exciton transitions. Fig. 12 shows the luminescence from such a CdS crystal illuminated through a 4360 Å monopass interference filter by an Hg lamp. Some 30 or more lines can be observed.

The strongest emission line is I_2 which is associated with an exciton bound to a neutral donor. Although this crystal was not intentionally doped, the donor is likely Cl, since the observed wavelength (4869.1 Å) agrees with that from another crystal which was intentionally doped with Cl, and also agrees with the results of Henry and Nassau (1970a). Longitudinal optical (LO) phonon replicas of the I_2 line can be seen at 4942.9 Å and 5018.7 Å (and 5017.8 Å). A second strong emission line is a doublet, I_{1a} and I_{1b} due to Li and Na acceptors respectively (Henry, Nassau and Shiever 1970). LO phonon

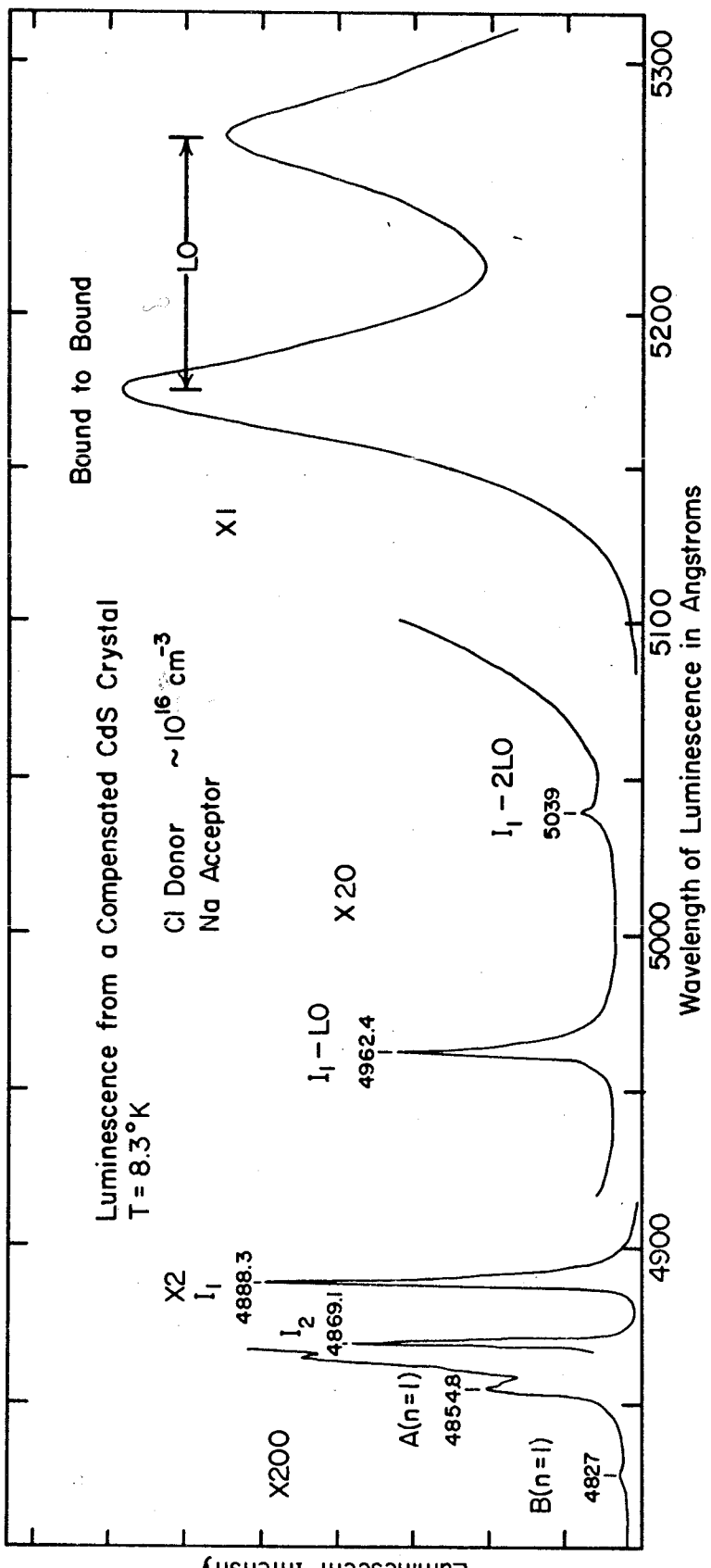

Fig. 11 Luminescence spectrum of a compensated crystal of CdS under irradiation with photons of energy larger than E_g the band gap. No correction was made for the S-20 response of the photomultiplier.

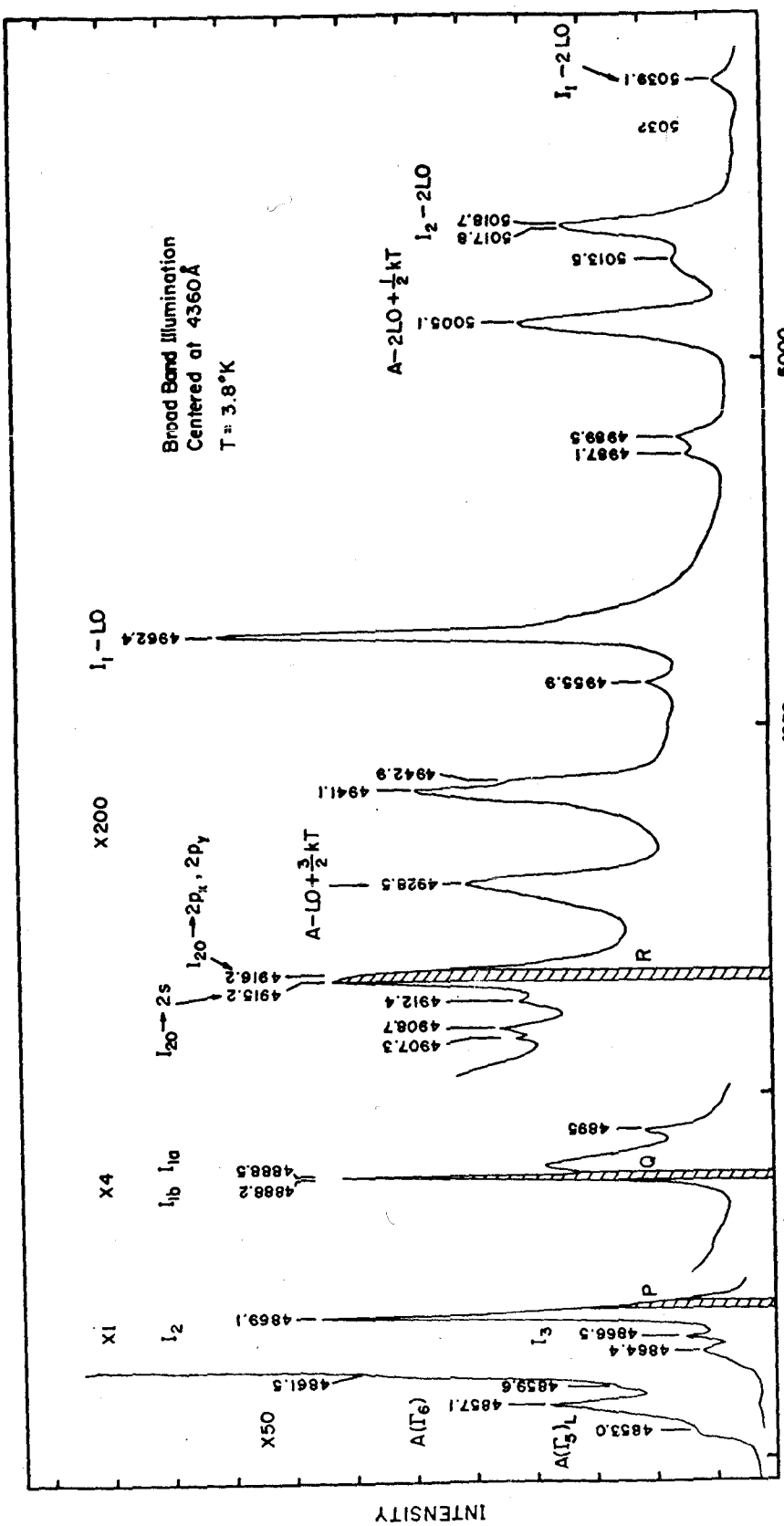

Fig. 12 Luminescence of a lightly doped crystal under irradiation with photons of energy > E_g. The shaded portions, P, Q, and R refer to luminescent transitions monitored in excitation experiments.

replicas of this line appear at 4962.4 Å and 5039.1 Å. The $A(\Gamma_6)$ exciton comes at 4857.1 Å with phonon replicas at 4928.5 Å and 5005 Å. Gross et al. (1966) first showed that these replicas are broadened as a consequence of the kinetic energy of free excitons at the moment of radiative decay. The I_3 line at 4866.5 Å, due to an exciton bound to an ionized donor (Henry and Nassau 1970a), is much less intense than I_2 in this crystal.

Lines at 4915.2 Å and 4916.2 Å are labelled according to Henry and Nassau (1970a) as $I_{20} \rightarrow 2p_x$, $2p_y$. I_{20} refers to the ground state of the I_2 complex while 2s and 2 p_x, $2p_y$ refer to the excited states of the donor after emission of a photon from the I_2 complex. Henry and Nassau (1970a) deduced from energy differences that the lines at 4912.4 Å, 4908.7 Å and 4907.3 Å were associated with excited states of the I_2 complex. Not shown in Fig. 12 are the broad bands centered at 5130 Å and 5162 Å which are due to free to bound and bound to bound transitions respectively (Colbow 1966).

A considerable simplification in the photoluminescent spectrum is possible when a spectrum is taken in Mode I. In Fig. 13 the crystal was illuminated at the energy of I_2 and a spectrum of the luminescence at lower energies was recorded. Note particularly that the intensity of lines associated with the I_1 complex or free A excitons has dropped relative to I_2 replicas by a factor of 15 to 20. The absence of a spectrum line at 5005 Å (A - 2LO + $\frac{1}{2}$ kT) in Fig. 13 indicates that the

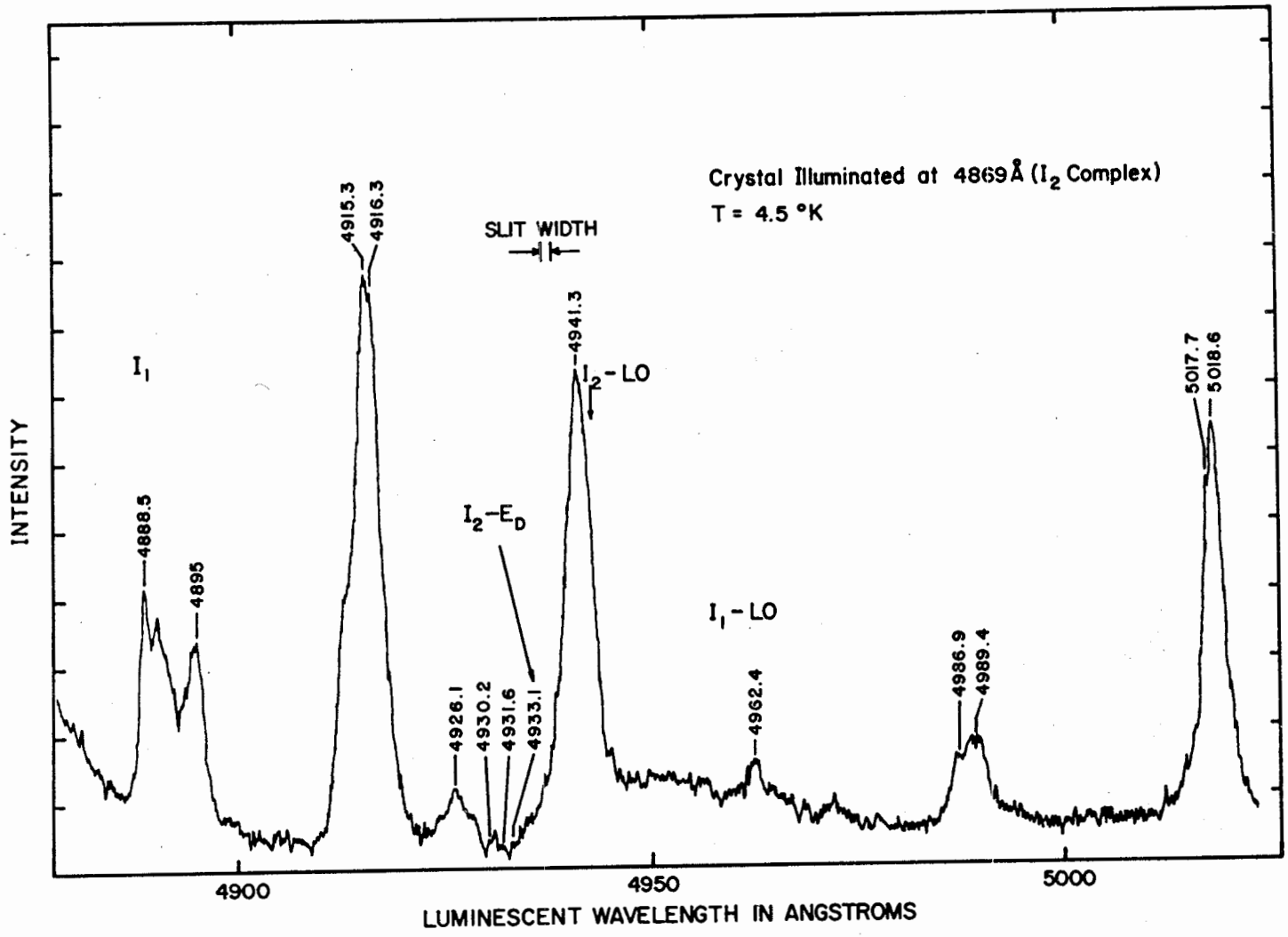

Fig. 13 Spectrum of the luminescence observed when the crystal was illuminated at 4869 Å, the I_2 transition. Note that luminescent lines due to other exciton complexes are suppressed, thereby aiding identification of all lines. Energy levels of the neutral donor were obtained from this spectrum.

crystal temperature is too low to allow the A excitons to become unbound from the I_2 complex.

With this simplification in the spectrum one can now observe luminescent transitions from the I_2 complex where an electron and hole recombine to emit a photon while the remaining electron is left in states of the neutral donor with principal quantum numbers n = 3 (4926.1 Å), n = 4 (4930.2 Å) and n = 5 (4931.6 Å) as well as in the n = 2 state discussed earlier. In addition there is a broad band corresponding to the donor electron being ejected into the conduction band - a radiative Auger process. The peak at 4941.3 Å is likely a combination of this Auger process and the one LO phonon replica of I_2.

This spectrum also demonstrates that the lines at 4986.9 Å and 4989.4 Å are excited by the I_2 complex. Consideration of energy differences using an LO phonon energy of 37.7 meV shows that they are LO phonon replicas of the 4912.4 Å line and the 4915.2 Å line ($I_{20} \rightarrow 2s$).

The strength of the electron-phonon interaction parameter S for emission from an exciton bound to a donor may be estimated from the ratio of the intensities of the zero and one phonon replicas. From Fig. 12, the transition $I_{20} \rightarrow 1s$ (4869.1 Å) has $S \sim 0.01$ while from Fig. 13 the transition $I_{20} \rightarrow 2s$ has $S \sim 0.11$. This difference is easily understood from expression 3.324. In the hydrogenic approximation the probability function for an electron bound in an s state is

$$|\varphi_{e_2}'|^2 = \left(\frac{1}{\pi n^3 a_D^3}\right) \exp\left(-\frac{2r}{na_D}\right)$$

where n is the principal quantum number. For the $I_{20} \rightarrow 1s$ transition n = 1, while for the $I_{20} \rightarrow 2s$ transition n = 2. The larger value of $D(\omega)$ in equation 3.233 for n = 2 is a consequence of the larger spatial extent of the bound electron in the 2s state compared to the 1s state. This results in a larger S for the $I_{20} \rightarrow 2s$ transition.

A spectrum taken in Mode I for the I_1 transition at 4888.5 Å is shown in Fig. 14. As expected, LO phonon replicas may be observed. In addition, less intense replicas of I_1 appear at 4955.9 Å and 5032.3 Å and may be due to a binding of the LO phonon to the exciton as discussed by Reynolds, Litton and Collins (1971) and Toyozawa and Hermanson (1968). Lines which appear between 5065 Å and 5086 Å are thought to be the I_6 and I_7 lines which originate from other deep impurities.

When the crystal is illuminated at an energy appropriate to the free A exciton, the luminescence spectrum at lower energies shown in Fig. 15 resembles the complicated spectrum observed under broad band illumination. However, illumination at the A exciton energy instead of broad band illumination increases the relative intensity of the LO phonon replicas of the A exciton. With illumination at the exciton energy only free excitons are formed, while broad band illumination creates

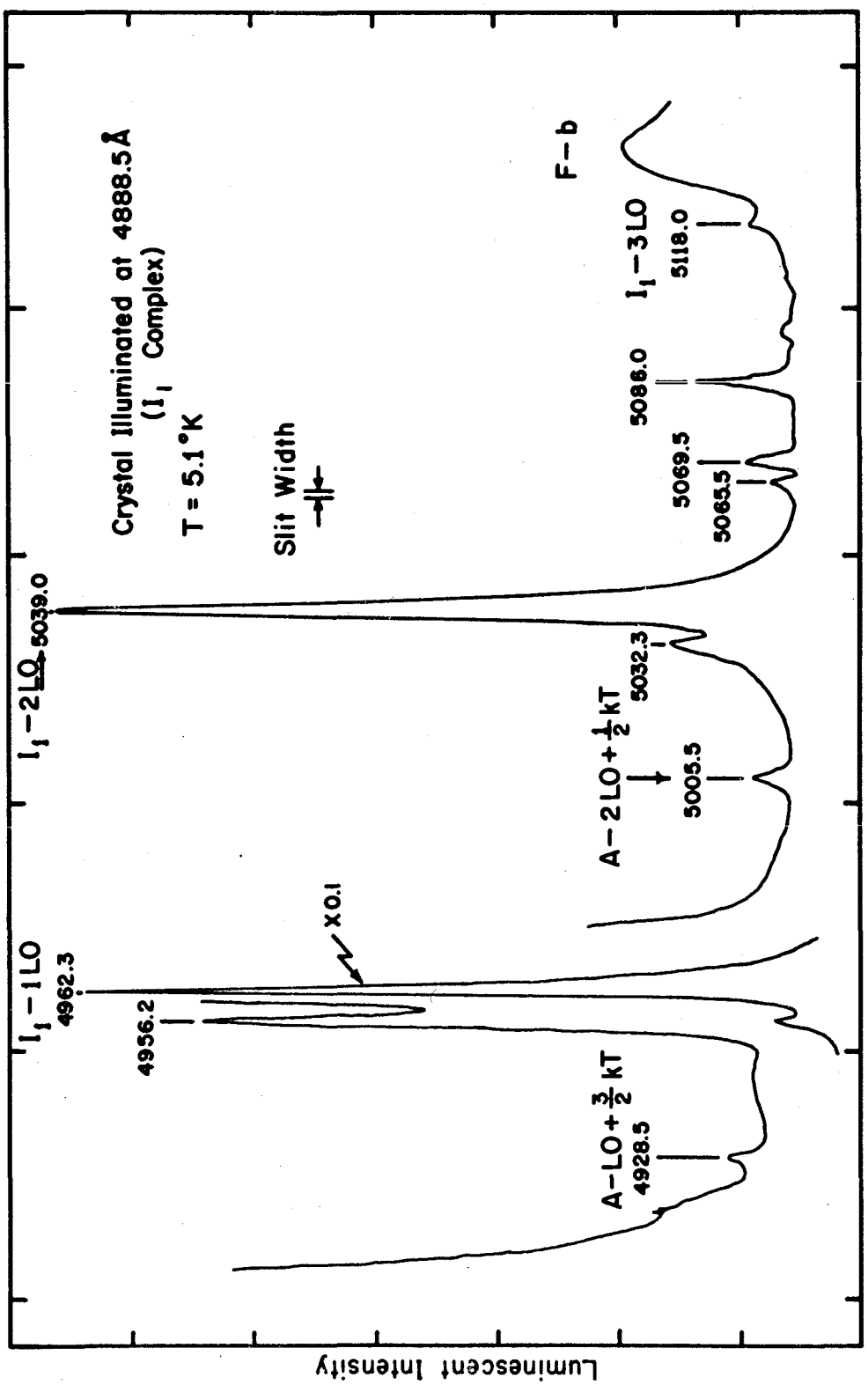

Fig. 14 Luminescence with the crystal illuminated at 4888.5 Å, the I_1 transition. Lines at 4956.2 Å and 5032.3 Å beside the LO phonon replicas are thought to be due to a bound state of the LO phonon.

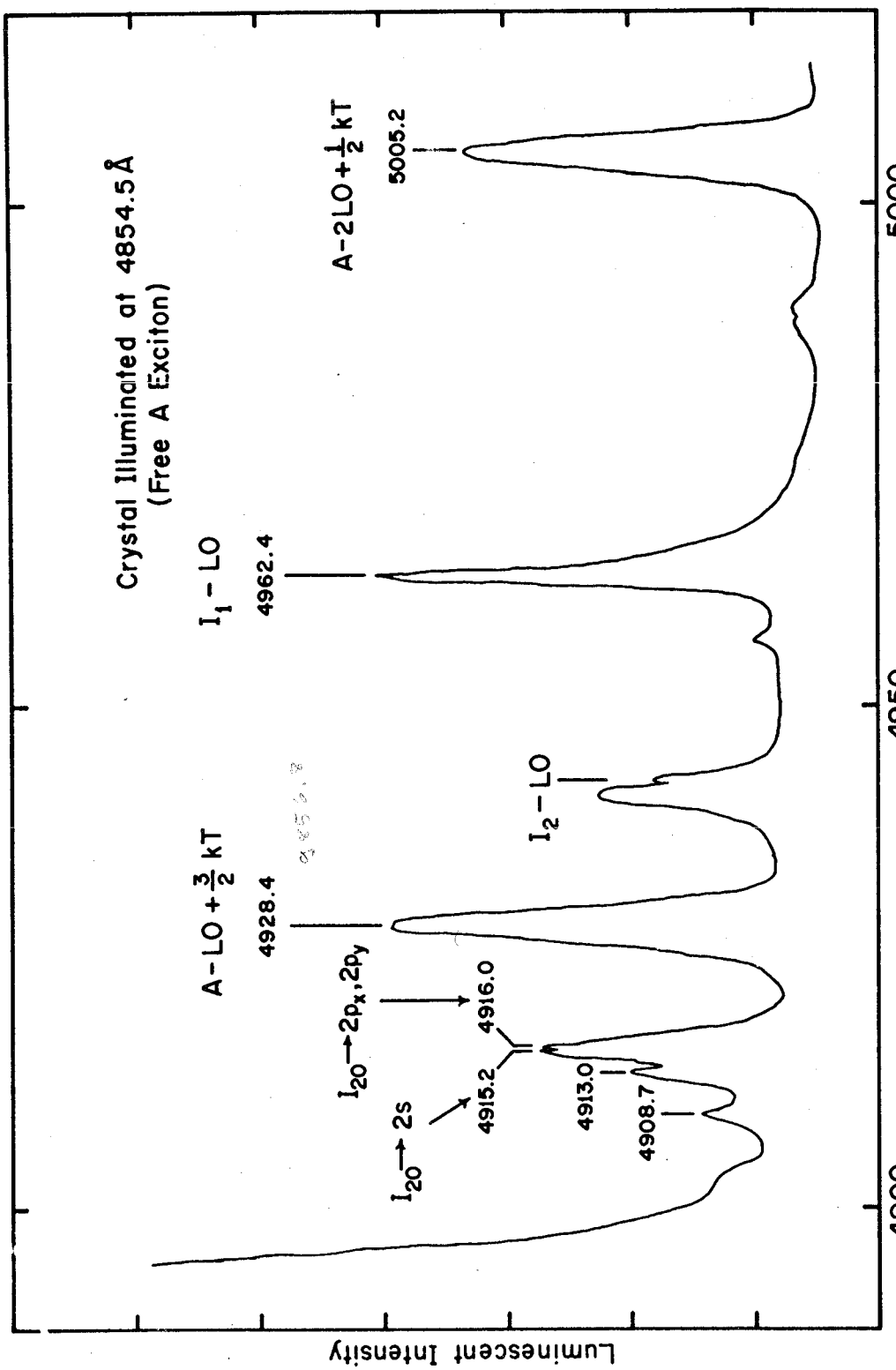

Fig. 15 Luminescence with the crystal illuminated at 4854.5 Å, the free A exciton. The presence of I_2 and I_1 replicas is a consequence of the movement of free excitons in the crystal. T = 6.1°K.

excitons resonantly (via a Franck-Condon process) or creates free electrons and holes, some of which may subsequently combine into excitons. Separate experiments have shown that the resonant processes make only a small contribution to creating excitons in this crystal. Comparison of the relative intensities of the A-LO and I_1-LO lines in Figs. 15 and 12 shows that a substantial proportion of the free electrons and holes created by illumination at 4360 Å form excitons.

One of the uses of luminescence excitation spectra (Mode II) is in the investigation of excited states of bound exciton complexes. In Fig. 16a the luminescent intensity at 4871 Å (the shaded portion P in Fig. 12), the acoustic phonon wing of I_2, was monitored as a function of exciting photon energy. The band width of the exciting radiation from the monochromator was 0.15 Å (full width at half maximum intensity). The peaks in the excitation spectrum of I_2 are due to the bound exciton complex being created in excited states. The free $A(\Gamma_6)$ exciton has a well resolved peak while the broader $A(\Gamma_5)_T$ exciton does not show up as a distinct line.

To enable a clearer observation of low energy excited states of I_2, the luminescent intensity of the $I_{20} \rightarrow 2p_x$, $2p_y$ and $I_{20} \rightarrow 2s$ transitions (shaded portion R in Fig. 12) was monitored. In Fig. 16b these results are shown. An energy scale with a zero at the energy of I_2 (4869.1 Å) is given to show the energy levels of these excited states.

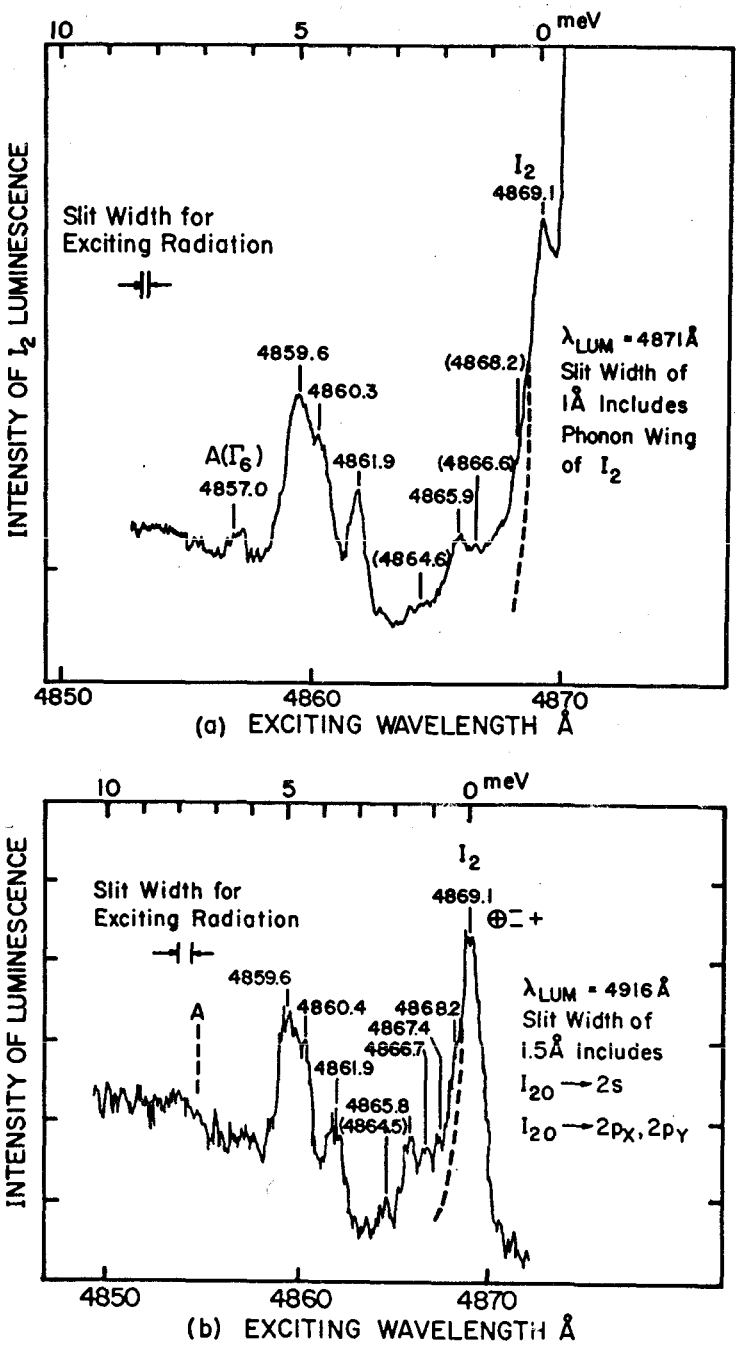

Fig. 16 In part a) the luminescent intensity of the phonon wing of I_2 at a wavelength λ_{LUM} = 4871 Å was monitored as a function of the incident photon energy; T ~ 5°K. In part b) λ_{LUM} = 4916 Å, a transition which is fed by the I_2 complex, was monitored; T = 4.5°K. The peaks in these excitation spectra are due to excited states of the bound exciton-neutral donor complex. Brackets indicate tentative wavelength assignments. Other experiments have shown that the line at 4864.4 Å is not associated with the I_2 complex.

A series of excitation experiments for the lines at 4907.3 Å, 4908.7 Å and 4912.4 Å showed that these luminescent lines originate from the radiative decay of the I_2 complex in one of its excited states to a neutral donor in a 2p state. For instance, at a temperature below 6°K, the luminescent line at 4908.7 Å is not excited at an incident wavelength of 4869.1 Å, the I_2 transition, but is excited at wavelengths of 4861.9 Å and 4860.4 Å, two of the excited states of I_2. Careful analysis of a series of excitation spectra has enabled us to establish the most probable decay paths for the excited states to the unexcited state of the exciton bound to a neutral donor. This information is displayed by the slanted lines in the energy level diagram of Fig. 17.

Excited states of I_1, an exciton bound to a neutral acceptor ($\oplus$ $\ddagger$ -), were observed by monitoring band Q in Fig. 12. Two excited state energy levels were observed corresponding to one of the holes originating from the B band. The results, shown in Table IV, agree generally with the findings of Thomas and Hopfield (1962) although some significant differences are observed between crystals.

An excited state of I_2, namely I_{2B}, where the hole is from the B band has also been observed at 15.3 meV above the energy of I_2 (2.54555eV). This state was also originally reported by Thomas and Hopfield (1962).

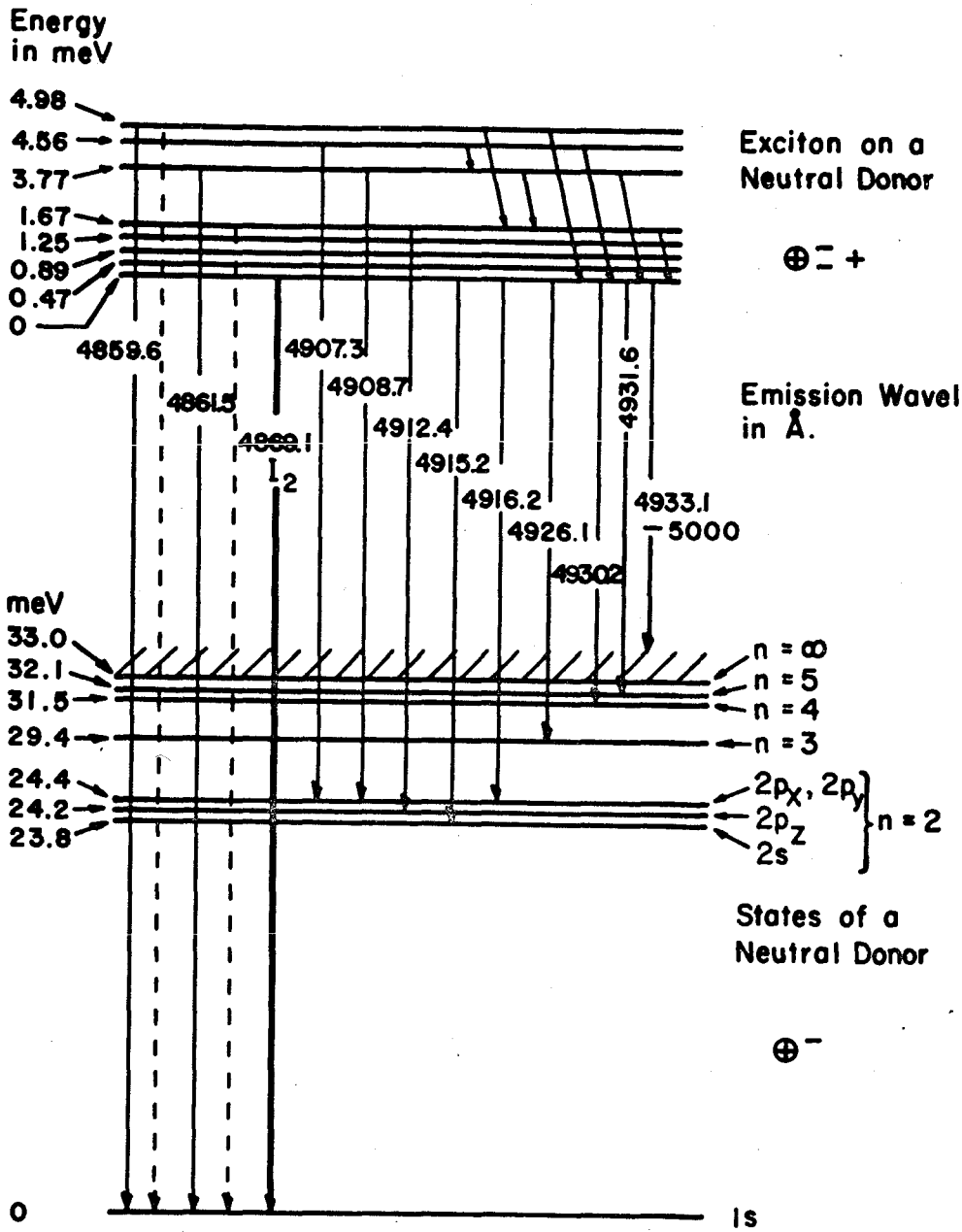

Fig. 17 Energy level diagram showing excited states of the neutral donor and excited states of the exciton on the neutral donor. Wavelengths of zero phonon luminescent transitions are shown. The dotted lines represent transitions which were not observed in the present experiments but were observed by Henry and Nassau (1970). Slanted lines represent observed routes for the decay of excited states to the unexcited state of this complex.

TABLE IV

Energy Levels of Excited States of Bound Exciton Complexes

Exciton Bound to a Neutral Donor		Exciton Bound to a Neutral Acceptor	
Present Results	Henry and Nassau (1970a)	Present Results	Thomas and Hopfield (1962)
meV	meV	meV	meV
0		0	
0.47		12.8 ± 0.1	12.9 (I_{1B})
0.89 ± 0.05		(12.2 ± 0.1)[a]	ΔE=1.5 meV
1.25			
1.67	1.66 ± 0.02	14.2	14.4 ($I_{1B'}$)
3.77	3.77	(14.0)[a]	
4.56	4.49		
4.98			

(a) a more heavily doped, compensated crystal. ΔE = 1.8 meV

In addition to investigating excited states, the excitation spectra of Mode II have generally confirmed identification of lines made from Mode I spectra. Mode II spectra have been particularly useful for certain difficult regions of the luminescent spectrum. For example, excitation spectra have shown that a line at 5013.5 Å (see Fig. 12) is not excited at I_1 or I_2 but is excited at 4864.4 Å, a luminescent transition in Fig. 12. The energy interval is 2 LO phonons.

5.2.2 Exciton Bound to a Neutral Donor (I_2 Complex)

The information derived from the two Modes is displayed in an energy level diagram shown in Fig. 17. The vertical arrows show the wavelengths of the luminescent transitions which are associated with an exciton bound to a neutral donor. The energy levels of the neutral donor were obtained from Mode I spectra (e.g., Fig. 13) while the energy levels of the exciton bound to a neutral donor were obtained from Mode II spectra. The first four energy levels of the bound exciton were not observed explicitly in luminescence due to resolution limitations and so are not shown as luminescent transitions in Fig. 17. The slanted arrows represent the most probable transitions between the states of the I_2 complex deduced from excitation spectra of each of the lines between 4907.3 Å and 4916.2 Å. Undoubtedly, selection rules are important in predicting the allowed transitions.

In Table IV the present results are shown to agree with the three excited states deduced by Henry and Nassau (1970a) The zero of energy is the unexcited I_2 complex. The first four or five energy levels have approximately equal energy intervals ($\sim$0.43 meV). The observed excited states do not yet have any theoretical explanation. However, two observations are in order. The relative separations of the energy levels above 1.67 meV are not unlike those found for the electronic states of molecular H_2 (Herzberg 1965). However, a simple analogy cannot be made because the excited state energies are less than the binding energy for the exciton, while in H_2 the excited state energies are greater than the binding energy of the two hydrogen atoms. This difficulty may possibly be resolved by making a second observation from the work by Henry, Nassau and Shiever (1970), where they measure the binding energy of an exciton to a neutral donor ($\ominus$ + +) and the binding energy of an exciton to an ionized donor ($\oplus$ + +). They find that a consideration of the electronegativity difference between the donor atom and the host lattice is important in determining binding energies. This suggests to us that an inclusion of both a central cell correction and electronegativity factor will be important in a calculation of excited state energy levels.

5.2.3 Neutral Donor

The experimental values of the energy levels of a neutral donor are shown together with the results of Henry and Nassau

(1970a) in Table V. The ionization limit was determined by the energy separation between the leading edge of the broad band emission, labelled $I_2 - E_D$ in Fig. 13, and the I_2 emission. Using $E_D = 33.0 \pm 0.2$ meV for Cl in CdS, the hydrogenic energy levels of the neutral donor were calculated, with no central cell or anisotropy correction or correction due to acoustic phonons. These factors are most important for small principal quantum numbers. As can be seen from Table V, the calculated values agree fairly well with the observed values. The donor energy measured in our experiments is consistent with the results calculated by Henry and Nassau (1970a) of 32.7 ± 0.4 meV for Cl in CdS and with the Hall studies of Piper and Halstead (1961) which gave a binding energy of 32 ± 2 meV for donors in CdS.

The broad band luminescence beginning at $I_2 - E_D$ in Fig. 13 and extending to lower energies is probably due to a radiative transition where an electron and hole recombine and the second electron is ejected into the conduction band taking with it some kinetic energy. The shape of this radiative Auger transition is clear from Fig. 13; however, there is not yet any theory for the radiative Auger transition from a bound exciton complex.

The existence of this radiative Auger process has important consequences in the explanation of the photoconductivity spectra of CdS. Many low temperature photoconductivity spectra

TABLE V - Energy levels of a Cl donor in CdS

Principal Quantum No.	Present Results	Henry and Nassau (1970)	Hydrogenic Model (no corrections)
	meV	meV	meV
1	0	0	0
$2p_x$, $2p_y$	24.4 ± 0.05	24.36 ± 0.02	
$2p_z$	24.2	24.19	24.7
2s	23.8	23.88	
3	29.4 ± 0.1		29.3
4	31.5		31.0
5	32.2		32.1
∞	33.0 ± 0.2	32.7 ± 0.4	33.0 (from experiment)

of CdS have maxima at the wavelengths corresponding to excitons and bound excitons [see, for example, Park and Reynolds 1963].

The Auger process is one mechanism by which the electron (or hole) from the exciton is released into the conduction (valence) band thereby contributing to the photoconductivity. In principle, the exciton need only be in the vicinity of the impurity for the Auger process to give a free electron or hole.

5.2.4 Exciton Bound to a Neutral Acceptor (I_1 Complex)

Excitation spectra of the luminescence from the I_1 complex have shown the two excited states given in Table IV. These correspond to the absorption lines observed by Thomas and Hopfield (1962) which they concluded were due to one of the holes on the I_1 complex originating from the B band. The energy difference between the states in which the hole spins are parallel (I_{1B},) and the states in which they are anti-parallel (I_{1B}) accounts for the separation of the two observed lines.

No low energy excited states similar to those reported for I_2 were observed. Possibly they were obscured by the acoustical phonon wing which is much more important on I_1.

It was noted that the precise energy of the excited states of I_1 varied from crystal to crystal. The figures in brackets in Table IV are from a more heavily doped and more accurately compensated crystal. Thomas and Hopfield (1962) noted that

the energy splitting (ΔE) for these two excited states is given by $\Delta E = 0.4\ P(0)$ eV where 0.4 eV is the estimated size of the j-j coupling for holes from the two top valence bands in the same unit cell, and $P(0)$ is the probability that the two holes of the bound state lie in the same unit cell. $P(0)$ is determined by the spatial extent of the wavefunction for the bound exciton.

In this context, the variation in ΔE from crystal to crystal is due to the local environment of a bound exciton varying as a function of doping concentration. The larger ΔE was observed for a crystal with the heavier doping and more complete compensation, suggesting that localized electric fields or doping levels can affect the spatial extent of the bound exciton and therefore increase $P(0)$.

Further investigation of the excited states of the I_1 complex as a function of crystal doping is warranted.

5.3 Neutral Acceptor Transitions

The radiative transitions involving the acceptor in CdS are due to:

a) an exciton bound to a neutral acceptor (I_1)

b) a free electron recombining with the hole bound to the acceptor - the free to bound band.

c) a bound electron recombining with a bound hole - the bound to bound band.

In certain lightly doped crystals it is thought that the free to bound and bound to bound luminescent transitions may both occur at low temperatures. An excitation spectrum (Mode II) of the free to bound band or bound to bound band at large donor-acceptor separations together with a luminescence spectrum enables one to measure the acceptor energy. In Fig. 18a the luminescence from the band at 5130 Å (from Fig. 2) is shown together with a portion of the excitation spectrum. Since the temperature is low, phonon absorption in luminescence and excitation is expected to be small. This agrees with the observation that the 5130 Å band is assymmetric only at low temperatures. The acceptor energy estimated from the cross-over points of the two curves in Fig. 18 is $E_A = 163 \pm 2$ meV which is in agreement with the value 165 meV from Henry et al. (1970), but smaller than the value of 170 meV from the results of Colbow (1966).

The average energy of acoustical phonons emitted in the free to bound transition is 5 meV. In Fig. 18b expression 3.224 for the acoustical phonon interaction with a localized charge is plotted. The position of the maximum in Fig. 18a is, from equation 3.225, consistent with a Bohr radius of 6 Å when a longitudinal sound velocity of 4.4×10^5 cm/sec is used.

The shape calculated for the emission of one acoustical phonon using the deformation potential interaction agrees reasonably well with the observed luminescence of the band at

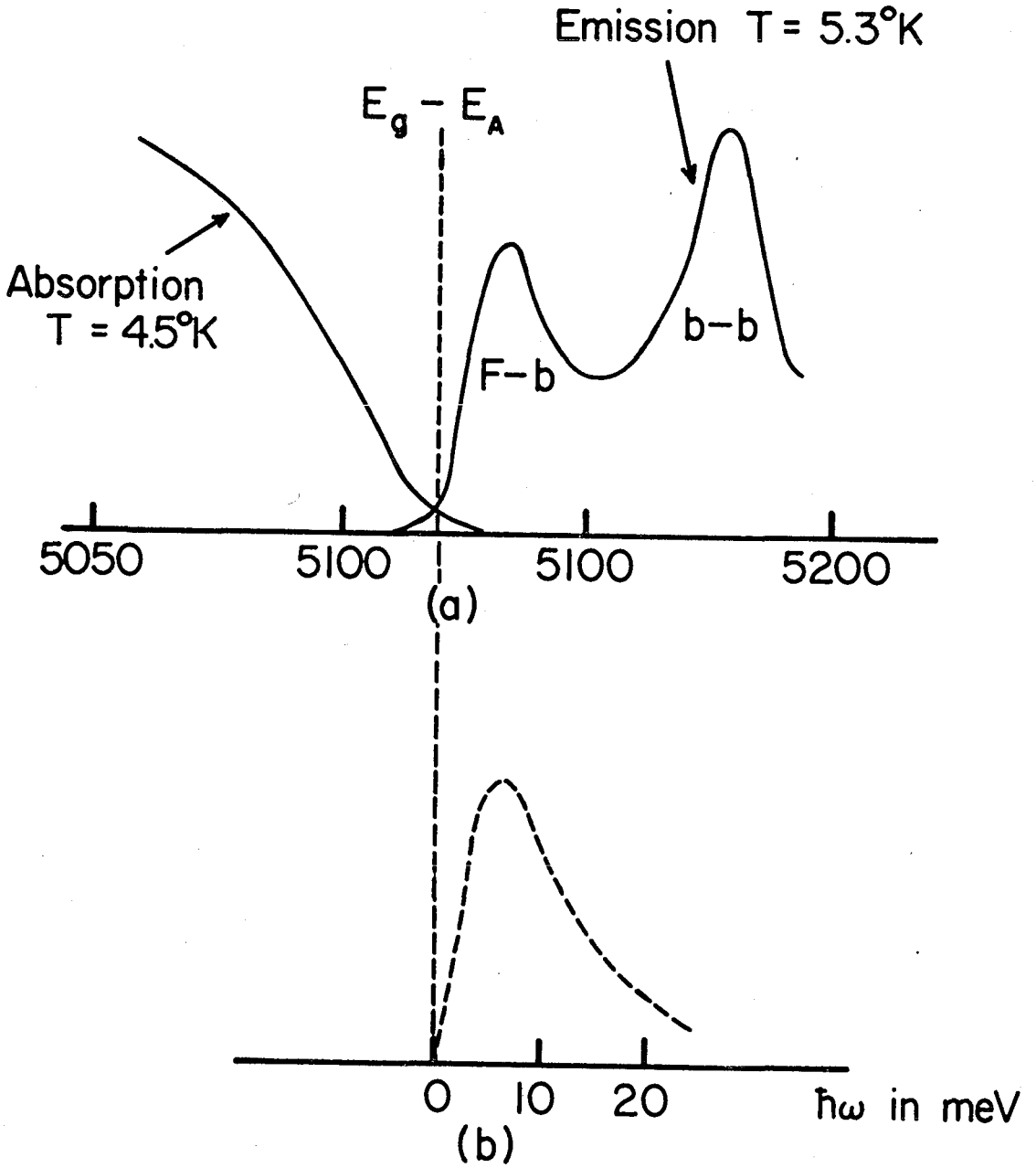

Fig. 18a) A portion of the luminescence together with an excitation spectrum of the luminescence. An estimate of E_A is made.

b) A plot proportional to expression 3.224 for the emission of one acoustical phonon. A Bohr radius of 6 Å was used to match the position of the peak in the luminesence spectrum.

5130 Å. In addition, the low energy portion of the bound to bound band is similar to that given in Fig. 18b.

However, since the electron-phonon coupling due to the piezoelectric effect has not been considered in detail, no definite conclusion can be made on the nature of the interaction of acoustical phonons with localized charges.

5.4 Franck-Condon Effects in Excitation

5.4.1 Crystal Doping

The luminescence of a compensated crystal of CdS (N_A, the number of acceptors $\simeq N_D$, the number of donors) is shown in Fig. 11. There is a weak emission at the energy of free excitons [A(n = 1); B(n = 1); A(n = 2)] and emission from the bound excitons. I_1 (4888.2 Å) is due to an exciton bound to a neutral acceptor (Na) while I_2 (4869.1 Å) is due to an exciton bound to a neutral donor (Cl). Other donor impurities give I_2 transitions in the range 4867-4871 Å according to Henry, Nassau and Shiever (1970) and Henry (1971).

As discussed previously, the intensity of the bound to bound emission relative to the bound exciton emission depends on the doping concentration of the crystal. In a lightly doped crystal the intensity of the bound and free excitons in luminescence increases compared to Fig. 11. Uncompensated crystals that are n type (no acceptors) do not have luminescence at I_1 or in the bound to bound band. Consequently, the

intensity of the I_2 lines and the free excitons is much increased.

Excitation spectra of the luminescence from crystals with a luminescence similar to Fig. 11 or n type crystals which are inefficient in luminescence have the most pronounced LO phonon structure, and will be shown first.

5.4.2 Excitons

In Fig. 19 an excitation spectrum is shown for the free A(n = 1) exciton which emits at 4854.8 Å (Hopfield and Thomas 1961). As expected, the A exciton can be created from a B, an A (n = 2) and a C exciton. For the B and C excitons (so designated because the hole originates from the B or C band) a rapid transition to A excitons is indicated by the widths of these lines (see also Hopfield and Thomas 1961).

The efficiency for creating free A excitons has sharp maxima at incident photon energies of E [A(n = 1)] + pLO where LO is used to designate the LO phonon energy at k = 0. That is, a free A exciton is created with the emission of one to five or more longitudinal optical (LO) phonons. As noted in a previous section, the integrated intensity is required for comparison with theory. This was estimated in a high resolution experiment and the values are recorded in Table VI, normalized to the intensity for the A + 2LO peak and also the incident number of photons from Fig. 10. The intensities for p = 2 to 6 were

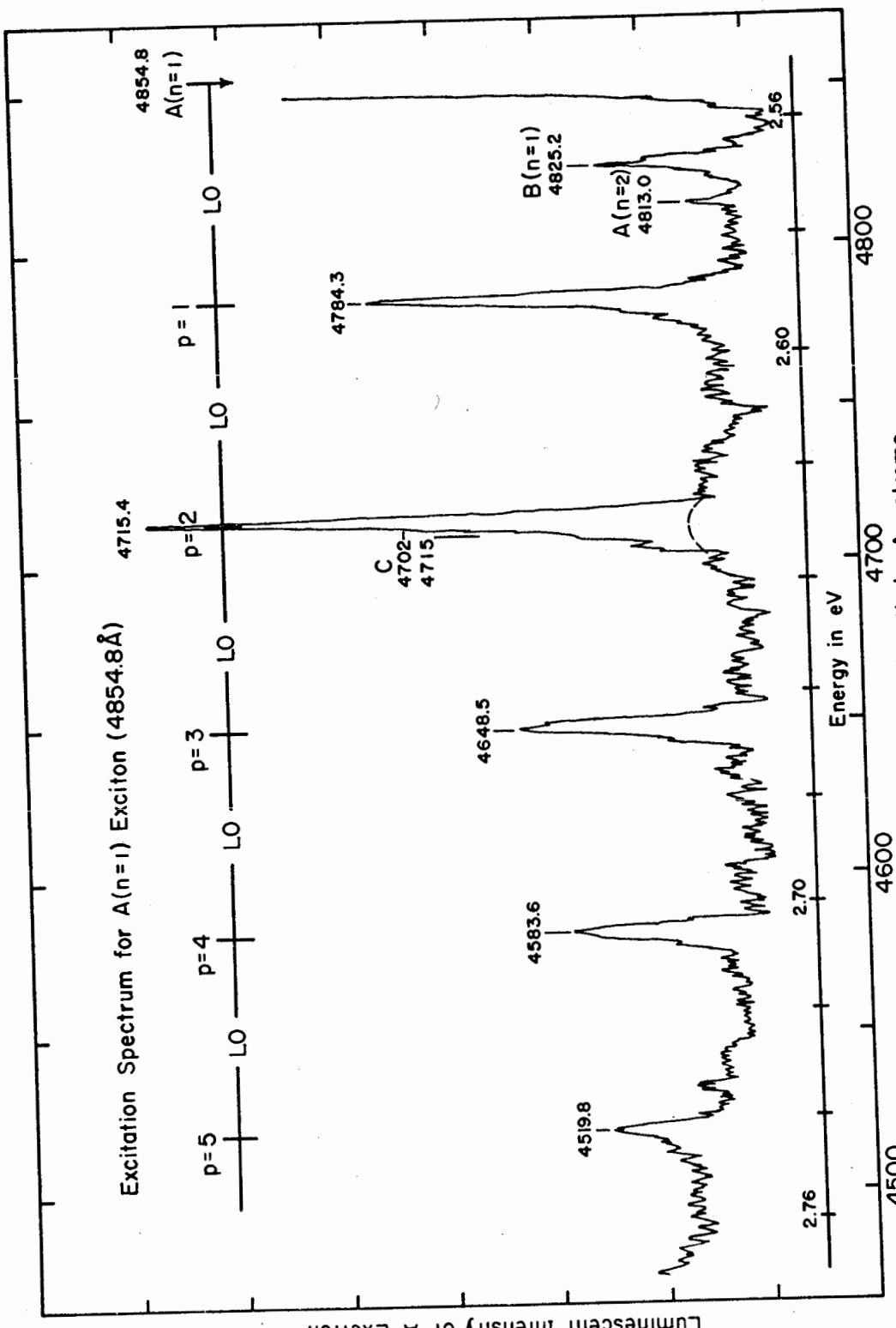

Fig. 19 Excitation spectrum of the luminescence from free A(n = 1) excitons at 8°K. The average spacing of the peaks is 37.8 ± 0.1 meV.

TABLE VI - Energies and Intensities of LO Phonon Replicas in Excitation of the A Exciton

Energy of Peak (eV)	No. of LO Phonons	ΔE Between Peaks (meV)	Integrated Intensities Gross et al. (1970)	Present Results	$\propto \frac{e^{S} S^{p}}{p!}$
			± 10%	± 5%	$\hat{S} = 2.5$
A(n = 1)					
2.55306 ± 0.0001	p = 0		-	-	0.32
		37.6 ± 0.2			
2.5907	1		0.7[a]	0.49(X2)	.80
		37.8			
2.6285	2		1.0	1.0	1.0
		37.9			
2.6664	3		0.6	0.83	.83
		37.7			
2.7041	4		0.3	0.51	.52
		38.1			
2.7422 ± .0002	5			0.17	.26
		37.5 ± 0.4			
2.7797	6			.07	.11
A(n = 2)					$\hat{S} = 0.6$
2.5758 ± .0005	0		-	-	1.67
		39.1 ± 1.0			
2.6149	1		1.0	1.0	1.0
		38.1			
2.6530	2		.36	.28	0.33
		36.5			
2.6895	3		.19	50	0.07
		38.8			
2.7283	4			.45	0.009
		38.7			
2.7670	5			.48	0.001

a) Incident intensity spectrum and polarization unknown.

found to be about equal for both incident polarizations while the p = 1 line was most active only for E⊥c. The A exciton state consists of a hole from the A valence band and is active mainly for E⊥c. However, the A + pLO exciton states for 0 ≥ 2 consist of an admixture of B valence band states and A valence band states, and so are active for both incident polarizations. The A + 1 LO state falls just above the A band edge and so is active mainly for E⊥c. Therefore, for comparison with theory it is suggested that the integrated intensity of the A + 1 LO line be multiplied by a factor between 1 and 2 depending on the incident polarization.

Unfortunately, the broad C(n = 1) exciton line comes under the A + 2 LO line. An estimate of the C exciton line was made from another experiment and is shown as the dashed line in Fig. 19.

The value of S was estimated from the data and values of the integrated intensity calculated from $e^{-S}\frac{S^p}{p!}$ and normalized to p = 2 are shown. Agreement between calculation with $\hat{S} = 2.5$ and experiment is satisfactory. The sharp, nearly symmetric LO phonon replicas of the A exciton in Fig. 19 are in agreement with the observations of Gross et al. (1970) and suggest that the effects of the exciton kinetic energy are small in these experiments (Toyozawa 1970).

The results of an excitation spectrum for the much weaker A(n = 2) luminescence are shown in Table VI together with an estimated value for $\hat{S} = 0.6$. Agreement is reasonable for

$p = 1$ and $p = 2$ but is poor for $p \geq 3$ in our data[†]. The data of Gross et al. (1970) are in better agreement with the calculations. An excitation spectrum for the B(n = 1) exciton luminescence gave a value for $\hat{S}$ of 2.8.

From the high resolution experiments the spacing of successive peaks in the excitation spectra for A(n = 1) could be evaluated with precision. The average value for the longitudinal optical phonon associated with the A(n = 1) exciton is 37.8 ± 0.1 meV.

5.4.3 Bound Excitons

The excitation spectrum for the I_2 luminescent transition is shown in Fig. 20. The outstanding feature is again the appearance of LO phonon replicas based on the I_2 line. As noted by Conradi and Haering (1968, 1969) these replicas correspond to the creation of an exciton bound to a neutral donor. High resolution inserts (bandwidth = 0.50 A) indicate that in addition to a series of lines at $E(I_2)$ + pLO, there is a series of lines at $E(I_2)$ + pLO + ΔE_2. In Table VII, values for LO and ΔE_2 have been calculated from wavelengths of peaks in the excitation spectrum of I_2. From Table VII the average value for the longitudinal optical phonon associated with an exciton on a

[†]The small intensity of the A(n = 2) exciton in luminescence results in experimental difficulties in selecting only the A(n = 2) line for excitation experiments.

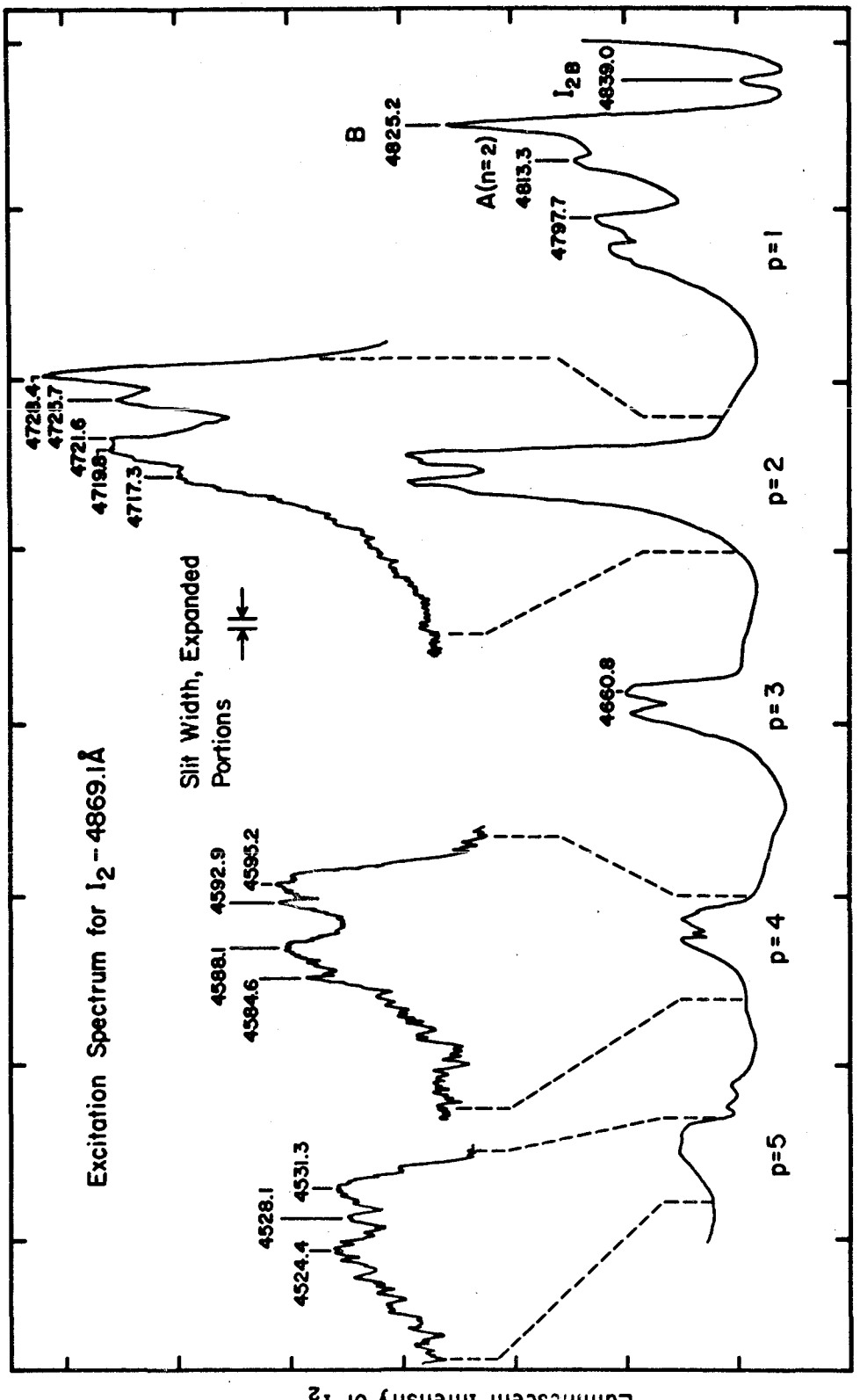

Fig. 20 Excitation spectrum of the luminescence from the I_2 complex (an exciton bound to a neutral donor). Expanded portions of the spectrum at an improved resolution are shown to demonstrate excited states in the LO phonon replicas. A compensated crystal was used. $T < 7°K$.

TABLE VII - Energies of LO Phonon Replicas for I_2 Excitation

$$E_{ex} = E(I_2) + pLO + \Delta E_2$$

Wavelength in Excitation Spectrum Å	Energy (eV) E_{ex}	Assignment	p	Energy Differences LO (meV)	ΔE_2 (meV)
	2.54556 ± 0.00005	I_2	0		
4839.0 ± 0.2	2.5614 ± 0.0001	I_{2B}			15.8
4825.2	2.5687	B(n=1)			
4813.3	2.5751	A(n=2)			
4797.7 ± 0.2	2.5834	I_2 + LO	1	37.9 ± 0.15	
4795.2	2.5848				1.4 ± 0.2
4790.2	2.5875				4.1
4788.7	2.5883				4.9
4785.6	2.5900				6.6
4728.4	2.6213	I_2 + 2LO	2	37.9 ± 0.2	
4725.7	2.6228				1.5
4721.6	2.6251				3.8
4719.8	2.6261				4.8
4717.3	2.6275				6.3
4660.8	2.6593	I_2 + 3LO	3	38.0	
4658.1	2.6609				1.6
4654.1	2.6632				3.9
4652.4	2.6641				4.8
4650	2.6655				6.2
4595.2	2.6973	I_2 + 4LO	4	38.0	
4531.3	2.7353	I_2 + 5LO	5	38.0	

neutral donor is LO = 38.0 ± 0.1 meV.

In section 5.2 the excited state energies of an exciton bound to a neutral Cl donor were measured. In Table VIII the values of ΔE_2 obtained from the p = 1, 2 and 3 phonon replicas of I_2 are shown to agree within experimental error with the excited state energies of an exciton bound to a neutral Cl donor from Table V. Replicas of the sharp $A(\Gamma_6)$ exciton appear in the excitation spectrum of I_2 while replicas of the broader $A(\Gamma_5)_T$ exciton are not distinguishable as peaks.

The excitation spectrum also shows that the I_2 complex (exciton bound to a neutral donor) can be created by free A(n = 2) and B excitons migrating to a neutral donor. The peak denoted by I_{2B} ,first identified by Thomas and Hopfield (1962), is due to a B exciton being created at a neutral donor site.

The high resolution inserts for p = 4 and p = 5 in Fig. 20 show a broadening of the many lines. As noted earlier, each LO phonon replica consists of a convolution integral involving $D(\omega)$. For the approximation $\omega(k) = \omega_o$ all the phonon replicas are of equal width. When a dispersion for optical phonons is taken into account the peaks will widen for $p \geq 1$ according to the convolution integral for the line-shape. For the monochromator resolution used the widening first becomes apparent at p = 4. Also, since each phonon replica consists of a p-1 fold convolution integral, the spacing

TABLE VIII - Energies of Excited States of the I_2 Complex

Energies of Excited States of I_2 Complex		ΔE_2		
Malm & Haering (1971b) meV	Henry & Nassau (1970) meV	p = 1 meV	p = 2 meV	p = 3 meV
0	0			
0.47				
0.89 ± 0.05				
1.25				
1.67	1.66 ± 0.02	1.4 ± 0.2	1.5	1.6
3.77	3.77	4.1	3.8	3.8
4.56	4.49			
4.98		4.9	4.8	4.8
6.3[(a)]		6.6	6.3	6.2
7.5[(b)]				

(a) Energy difference between I_2 and $A(\Gamma_6)$ exciton

(b) Energy difference between I_2 and $A(\Gamma_5)_T$ exciton

between successive peaks would be expected to change as p increases, a consequence of LO phonons with k > 0 participating in the relaxation to the lowest vibrational state. The resolution of our experiments is insufficient to detect such small changes in the spacing of successive LO replicas; however, this has been observed by Collins et al. (1969) in the photoconductivity of semiconducting diamond. No exciton kinetic energy effects are expected since the donor impurity takes up the recoil momentum of the LO phonons.

The intensities of the LO phonon replicas of I_2 are similar to that for the A(n = 1) exciton. With an adjustment in the intensity of the p = 1 peak since it is active for only $E \perp c$, a value of $\hat{S} = 2.3 \pm 0.2$ gives a reasonable fit.

The luminescence in the range 4859 Å to 4867 Å is due to excitons bound to ionized donors (I_3) and excited states of excitons on neutral donors (Henry and Nassau 1970a). Excitation spectra for these luminescent transitions also show resonant LO phonon structure similar to Fig. 20.

In Fig. 21 an excitation spectrum for the luminescence from the I_1 complex (exciton bound to a neutral acceptor) is shown. There is a series of peaks corresponding to I_1 + pLO. There is also a series of peaks which correspond to A + pLO, B + pLO and I_{1B} + pLO. Again I_{1B} and $I_{1B'}$ correspond to the B exciton created on a neutral acceptor according to Thomas

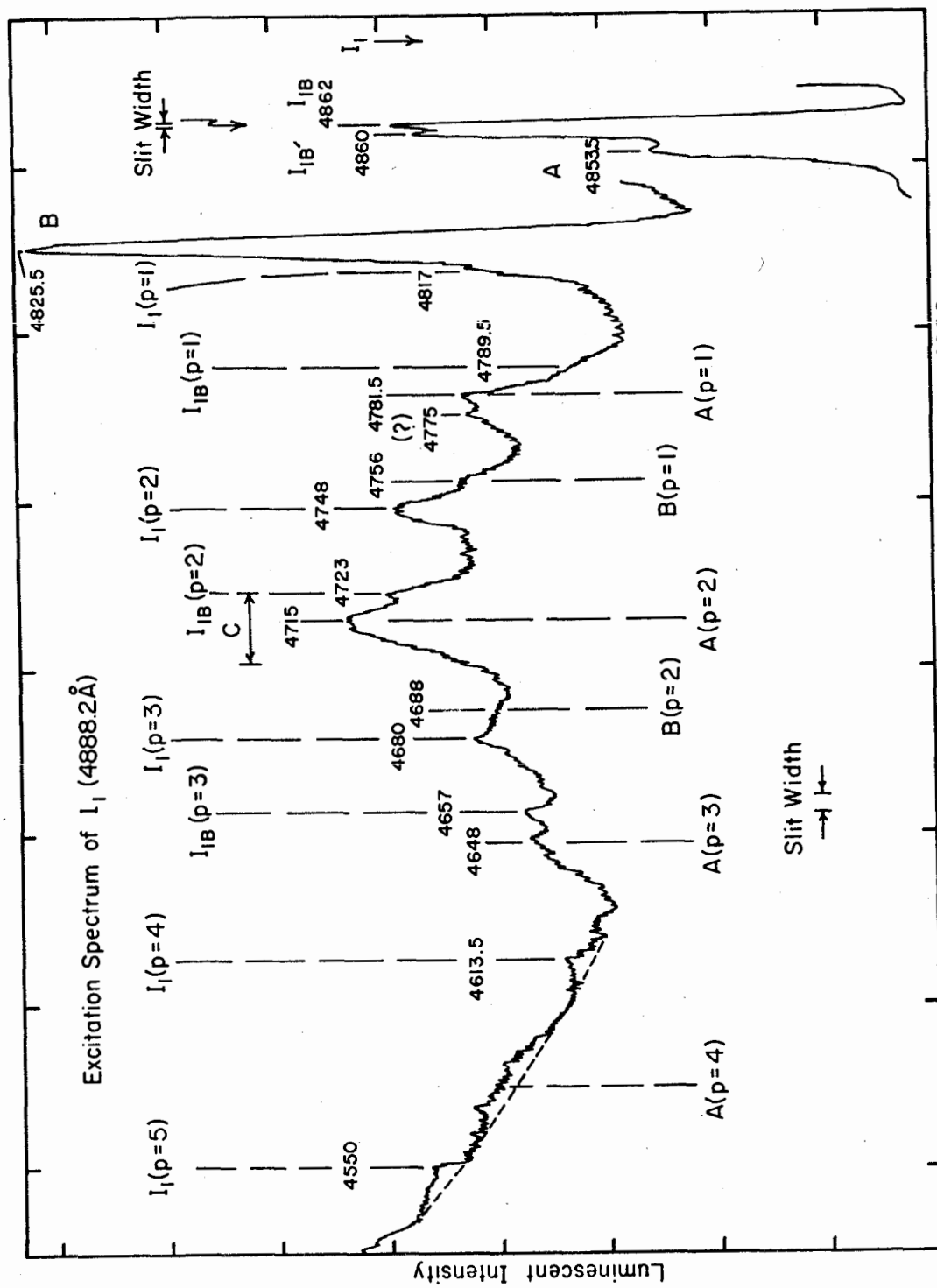

Fig. 21 Excitation spectrum of the luminescence from the I_1 complex (an exciton bound to a neutral acceptor). The number of LO phonons is given by p.

and Hopfield (1962). In each series of LO phonon replicas the p = 2 peak is the largest, suggesting that S $\sim$ 2 for each of the excitations. Unfortunately, a line that would correspond to a bound LO phonon suggested by Toyozawa and Hermanson (1968) and observed in emission by Reynolds et al. (1971) coincides with the strong free B(n = 1) exciton line. It is noted that free excitons make a much larger contribution to the I_1 luminescence than to the I_2 luminescence. This suggests that the trapping cross-section for excitons is much larger for the neutral acceptor than the neutral donor.

For a crystal in which the I_1 + pLO peaks were more prominent than in Fig. 21 a value of S was estimated from the integrated intensities again with the adjustment for the p = 1 peak to allow for polarization effects. It was found that S = 2.5, similar to the value for the A exciton and I_2 bound exciton complexes.

5.4.4 Bound to Bound Transitions

As is well known, the broad band of luminescence which has a maximum at about 5175 Å is due to a bound electron radiatively recombining with a bound hole. A series of excitation spectra of portions of the bound to bound luminescence selected by the spectrometer are shown in Fig. 22. Broad lines corresponding to LO phonon replicas may be distinguished. The lowest curve is an excitation spectrum for luminescence at

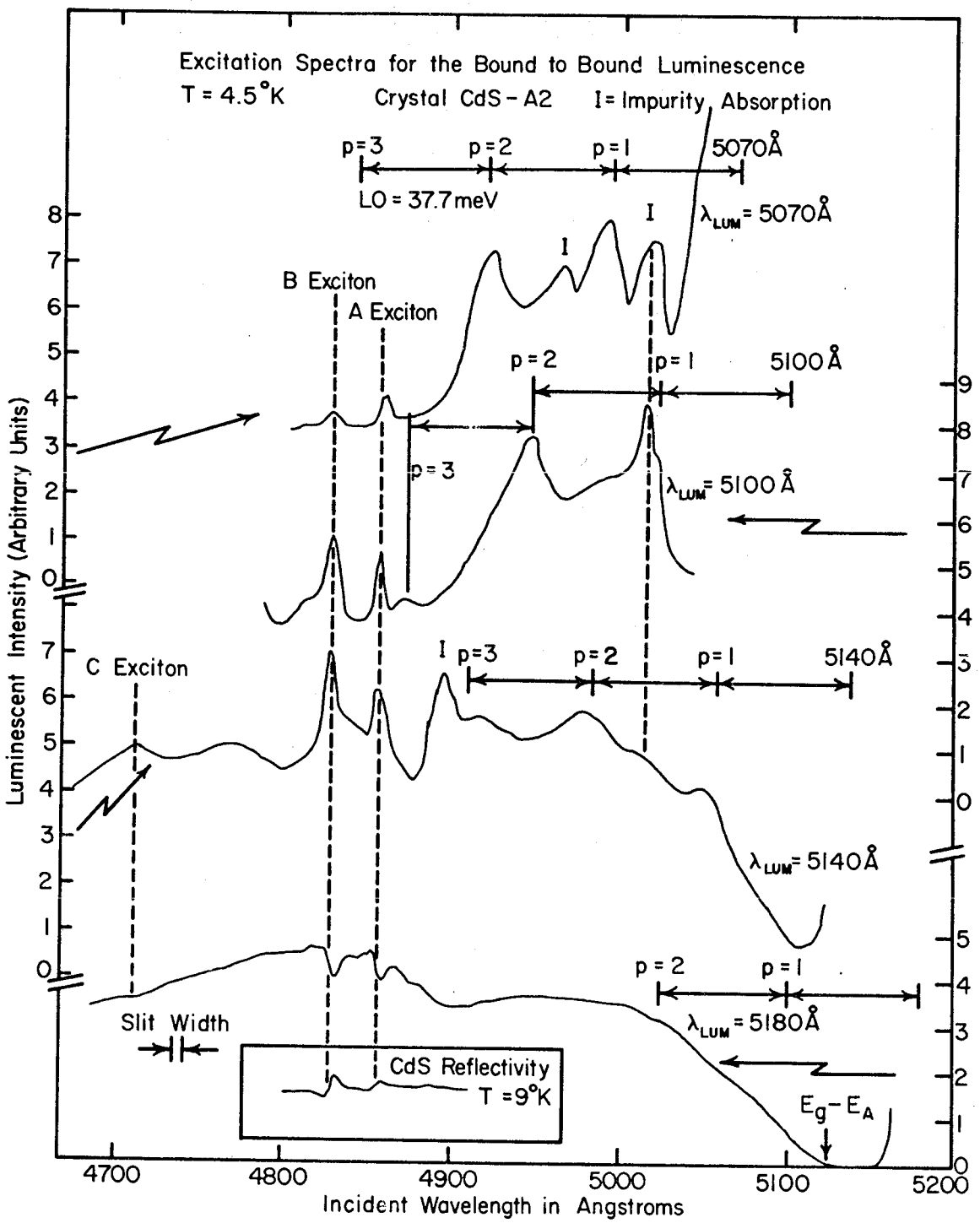

Fig. 22 Excitation spectra for the bound to bound luminescence at 5180 Å, 5140 Å, 5100 Å, and 5070 Å. Donor-acceptor separations for these wavelengths are 150 Å, 55 Å, 33 Å, and 26 Å, respectively. Peaks marked I are thought to be due to other deep impurity states. The Hg lamp was replaced by a tungsten filament for this experiment.

5180 Å, corresponding to distant donor-acceptor pairs. The luminescence is excited by creating a bound hole and a free electron; this is denoted by $E_g - E_A$. The spacing of the donor-acceptor pair is obtained from

$$E = E_g - E_A - E_D + \frac{e^2}{\kappa_s R} . \qquad 5.401$$

A donor energy of 33 meV is used. The energy shift due to acoustical phonons, estimated in section 5.3 as about 5 meV, is added to 163 meV to give an effective value $E_A = 168$ meV.

Excitation spectra of the luminescence from pairs of smaller separations (shorter wavelengths) show the presence of up to 3 LO phonon replicas. Higher order LO replicas are suppressed at energies above the A(n = 1) exciton where the absorption coefficient increases by some three orders of magnitude. The value of S for luminescence at 5140 Å(R = 60 Å) is estimated as $\overline{S} < 3$ since the p = 2 and p = 3 peaks are about equal. The excitation spectrum for the luminescence at 5070 Å which is from pairs separated by R = 25 Å shows that $\overline{S} \approx 1.8$. Thus $\overline{S}$ increases with donor-acceptor separation. This is in qualitative agreement with the curves shown in Fig. 9. However, the data shown in Fig. 22 is not sufficiently good to allow a quantitative fit.

The bound to bound luminescence is also excited by free

excitons. This is a consequence of an electron-hole correlation effect and will be discussed in section 5.6.

5.4.5 Temperature Dependence

Excitation spectra of the luminescence from free and bound excitons were recorded up to the temperature at which the exciton or exciton complex thermally dissociated. The change in energy of the luminescence as a function of temperature was measured and found to agree with the results of Colbow (1966) and Thomas, Hopfield and Power (1960). When the spectrometer was adjusted to allow for the change in wavelength of the luminescence with a change in temperature, it was found that the excitation spectra for the A exciton and the I_1 luminescence were unchanged except for an overall reduction in the intensities of the peaks in the excitation spectra with an increase in temperature. This reduction was a result of the thermal dissociation of the exciton or exciton complex as the temperature T was increased. LO phonon replicas in the excitation spectra of the A(n = 1) exciton were observed up to 100°K.

The excitation spectra of the I_2 luminescence in compensated crystals changed with temperature only with respect to the relative intensities of the LO phonon replicas of unexcited I_2 complex compared with the intensities of the LO phonon replicas of excited states of the I_2 complex. The ratio of $R' = \frac{E(I_2) + 2LO + \Delta E_2}{E(I_2) + 2LO}$ where $\Delta E_2 \simeq 5$ meV was given

by $R' = \exp\left(+\frac{\Delta E}{kT}\right)$ with $\Delta E \simeq 0.6$ meV between 5°K to 45°K. This behaviour is plausible when one considers that at low temperatures the excited states will tend to decay to the unexcited I_2 complex before radiative decay, while at higher temperatures the I_2 complex is more likely to decay radiatively from one of its excited states. In an excitation spectrum of the I_2 luminescence, the relative magnitude of the $E(I_2)$ + pLO + ΔE_2 peak therefore decreases as the temperature increases.

In contrast to the results of Conradi (1968), ultraviolet irradiation of the crystals during the period of cooling in the dark made no observable difference in the excitation spectra of the luminescence at low temperatures. Similarly, a temperature cycle from T < 10°K to T > 100°K and back to T < 10°K, with or without irradiation of the crystal by above band gap photons, made no significant changes to the excitation spectra for our crystals.

5.4.6 Longitudinal Optical Phonon Energy

A comparison of the energies found for the LO phonons associated with excitons (37.8 ± 0.1 meV) and for those associated with an exciton bound to a donor (38.0 ± 0.1 meV) shows a small difference. A comparison of the energy difference between the A + pLO and the I_2 + pLO peaks for a given p from Table VI and Table VII shows that the energy difference decreases as p increases. The binding energy for the A exciton

to the neutral donor (p = 0) is 7.50 meV. However, the energy difference for p = 4 is 6.8 ± 0.2 meV. When all energy differences were considered, it was concluded that LO phonons associated with excitons on neutral Cl donors have an energy 0.15 ± 0.1 meV greater than the phonons associated with free excitons.

The energy of the LO phonon associated with the I_1 complex was evaluated from the difference in energy between the I_1 and I_1 - LO emission lines. The LO phonon energy associated with the exciton on a neutral acceptor is 37.7 ± 0.1 meV. This agrees with the Γ_5 LO phonon energy of Reynolds et al. (1970). In both our excitation and emission spectra we have not observed the Γ_1 LO phonon energy of 37.45 ± .05 eV reported by Reynolds et al. (1970).

The energy of the LO phonon associated with the bound to bound transition was reported to be 36.8 meV by Colbow (1966). From these data it is clear that the LO phonon associated with a small center (the neutral acceptor in the bound to bound transition) has a smaller average energy than the LO phonon associated with the largest center (the exciton bound to a neutral donor).

5.4.7 Non-Resonant Processes

The luminescence due to excitons, bound excitons and bound electron-bound hole pairs can be fed by non-resonant processes as well as by the resonant processes described. In the non-

resonant processes the incident photon may create a free electron and free hole, or an exciton, which emits a number of acoustical phonons in losing its energy.

A crystal which is n type ($N_A << N_D$) has only a strong I_2 luminescence and a weaker luminescence from the free excitons. An excitation spectrum of the I_2 luminescence from such a crystal in Fig. 23, shows that the non-resonant processes have a considerable importance. In fact, the excitation spectrum of a less heavily doped n type crystal is almost featureless except for the exciton peaks. The spectrum in Fig. 23, which is similar to one reported by Park and Schneider (1968), has peaks corresponding to A + pLO as well as the I_2 + pLO and I_2 + pLO + ΔE_2 peaks reported earlier. Since the principal luminescent center is I_2, electrons and holes and excitons created nonresonantly contribute to the continuum in Fig. 23, while the resonant processes make only a small contribution. In addition, since no acceptors are present, the neutral donors are more likely to capture free excitons; hence, peaks occur at A + pLO.

In compensated crystals the ionized donors and acceptors are efficient in capturing the free electrons and holes which then radiatively recombine for the bound to bound emission. Consequently, in these crystals the resonant processes show up much more clearly in excitation spectra of free and bound excitons. Non-radiative recombination centers have the same

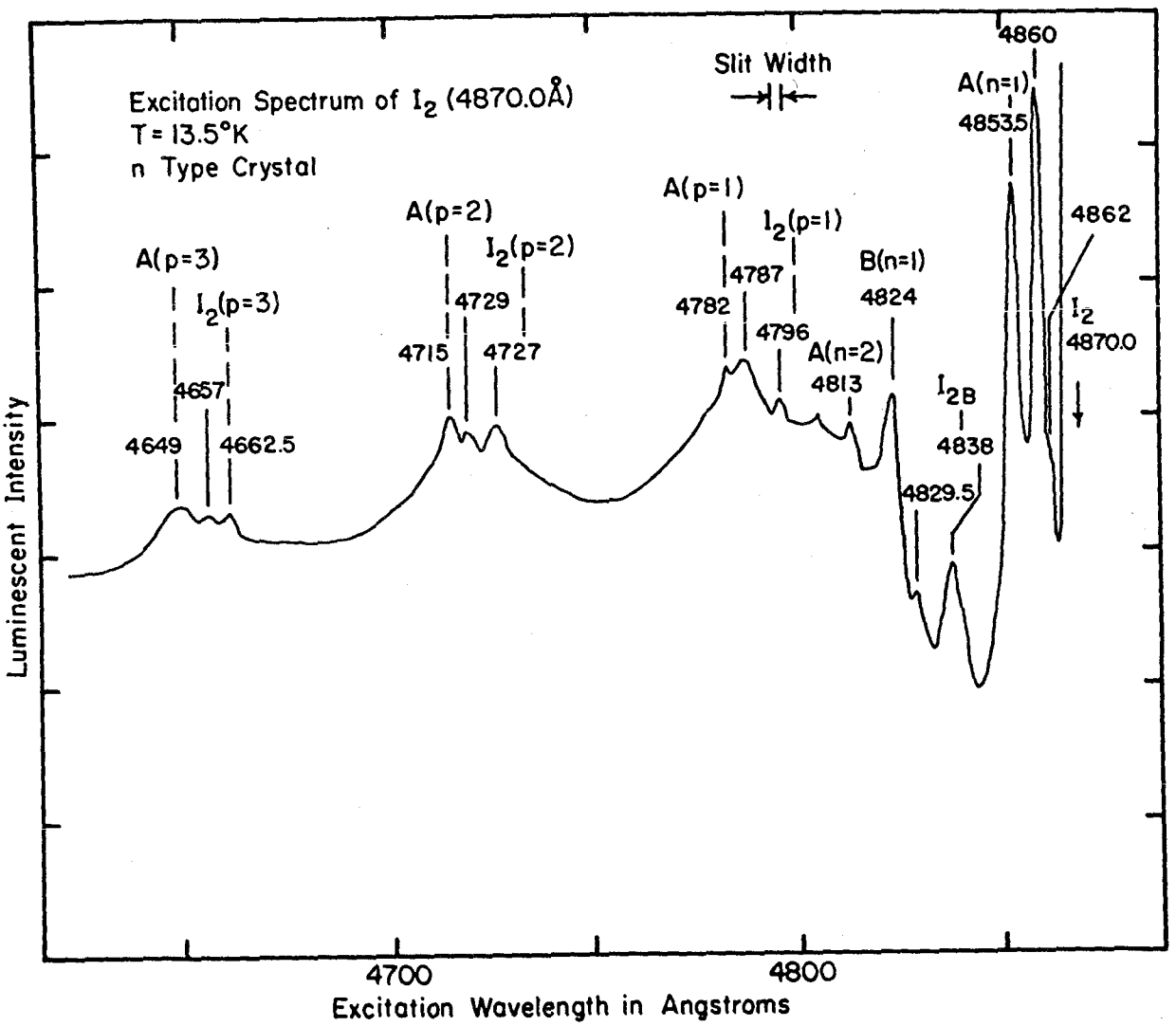

Fig. 23 Excitation spectrum of the I_2 luminescence from an n type CdS crystal. The sharp peaks from resonant processes are superimposed on a continuous background due to non-resonant processes.

effect as the bound to bound recombination processes. As a rule, the weaker the I_2 luminescence in emission, the stronger is the resonant I_2 + pLO and A + pLO structure in the luminescent excitation spectra.

The differences in excitation spectra between crystals with different concentrations and types of impurities are contained in the function P(hν) discussed in section 3.3. Note however, that all excitation spectra show the same relative intensities at the resonant energies associated with the LO phonon emission.

Clearly a myriad of different excitation spectra may be observed, depending on the number and efficiency of trapping centers in the crystal. This qualitatively accounts for the many different excitation spectra for I_2 reported by Conradi and Haering (1968, 1969), Park and Schneider (1968), and Wei et al. (1969).

5.4.8 Discussion of the Franck-Condon Results

The resonant LO phonon processes in absorption associated with the creation of bound electrons and holes, bound excitons, or free excitons in CdS are in qualitative agreement with the theory due to Toyozawa (1970). The experimental value of the coupling parameter for the A(n = 1) exciton was $\hat{S} = 2.5$ while the value for the A(n = 2) exciton was $\hat{S} = 0.6$. These results are in accord with the dependence of $\hat{S}$ as the inverse of the

size. Excitons of higher order should have values of $\hat{S}$ inversely proportional to $n^2 a$ where n is the principal quantum number. As noted earlier, the anisotropic hole makes an accurate comparison with the theoretical curves difficult. The effective Bohr radius of the hole in the A(n = 1) exciton inferred from the above mentioned value of $\hat{S}$ is 3.0 Å using an average electron radius of 26 Å. This value lies between the limits for the hole radii $a_{h\perp}$ = 6.4 Å and $a_{h\parallel}$ = 1 Å calculated earlier from effective mass values.

The excitation spectrum for the I_2 transition is similar to that for the A(n = 1) exciton suggesting that an incident photon at a resonant energy creates an exciton-like excitation at the neutral donor. A similar comment applies to the I_1 + pLO transitions.

Resonant phonon processes may also be observed in emission. In general, the value of the strength parameter S inferred from such studies is different from the value inferred from absorption (excitation) studies, indicating a relaxation of the electronic wavefunctions between absorption and emission events. This is most clearly shown by the LO phonon replicas of the bound exciton lines in emission (Fig. 12). A value of S = 0.10 for the exciton bound to the neutral acceptor and S $\approx$ 0.01 for the exciton bound to the neutral donor is observed. In the model proposed earlier, this suggests the wavefunctions of the individual holes and electrons on the bound exciton

complex are spread over a larger region than in the free exciton.

The bound to bound transition has a value of $\bar{S}$ which varies as the donor-acceptor separation R. The observed variation, in absorption, [$\bar{S}$(25Å)~1.8; $\bar{S}$(55Å) ~ 2 or 3] is in good qualitative agreement with theory.

In emission the value of $\bar{S}$ for the free to bound emission is 0.95 (Gutsche and Goede 1970) giving, according to equation 3.221, an effective Bohr radius of about 10 Å. This is reasonably close to the Bohr radius of 6 Å calculated on the basis of acoustical phonon interaction.

The critical parameter for determining the value of S is the size of the localized charge distribution responsible for the absorption or emission process. In general, deep impurities tend to strongly localize the carrier causing strong electron-phonon coupling.

Our results indicate that the LO phonon energy is slightly dependent on the electronic complex with which the phonon is associated. This is again to be expected from the theory of Toyozawa if the dispersion of the LO phonon band is taken into account. The various k values in this branch are weighted differently for systems of different spatial extent. In general, one may expect a lower mean LO phonon energy for the more localized systems. The k = 0 value of the LO phonon

energy should be observed for very large systems. Slight variations in mean LO phonon energy have been observed by many workers and are probably associated with this effect derived from phonon dispersion.

A comparison of excitation spectra for the various luminescent complexes as a function of crystal doping gives some information on the relative trapping efficiencies for excitons and free electrons and holes by the various impurity complexes. For instance, a quick comparison of Fig. 20 and Fig. 21 shows that in a compensated crystal where $N_D \simeq N_A$,the neutral acceptor is the more efficient exciton trap. A careful analysis of excitation spectra for various doping concentrations should give a better understanding of the motion of excitons, electrons, and holes in a crystal with impurities.

5.4.9 Evaluation of Results from other Workers

The luminescence excitation spectrum for a bound exciton in ZnSe observed by Wei et al. (1971) is similar to the luminescence excitation spectra for CdS. Using a configuration coordinate model to fit the first three LO phonon replicas in their results gives a value of $S \approx 1.8$. Since the effective masses reported for ZnSe by various authors are inconsistent, we will estimate the effective hole Bohr radius by comparing the acceptor energy $E_A = 120$ meV for ZnSe (Dean and Merz 1969) with the acceptor energy in CdS of 163 meV. Since the static

dielectric constants of ZnSe and CdS are nearly equal, one expects that the hole radius in ZnSe is about 163 meV/120 meV = 1.4 times larger than in CdS. When the values of $\kappa_o = 5.6$ and $\kappa_s = 8.7 \pm 0.1$ at low temperatures (Hite et al. 1967) and $\hbar\omega_o \approx 31$ meV (Wei et al. 1971) are used and when the effective value of a_h determined from our experiments is multiplied by the factor 1.4, one obtains S = 1.8 for the exciton in ZnSe. This is in remarkable agreement with the observations of Wei et al. (1971).

The luminescence in CdS doped with the isoelectronic impurity Te observed by Aten et al. (1965) corresponds to the emission of an average of 8 LO phonons. Even though the estimated binding energy of the hole (0.20 eV) is not much larger than for the singly charged acceptor, the bound hole must be smaller in extent to produce such strong electron-phonon coupling.

In the broad band emission, Gutsche and Goede (1970) note that the value of $\overline{S}$ for the bound to bound band (LES or low energy series) varies with excitation intensity while for the free to bound band (HES or high energy series) no such variation is observed. As has been pointed out by numerous workers, the maximum of the bound to bound band goes to higher energies (shorter donor-acceptor separations) as the incident intensity increases. From Fig. 7 in Gutsche and Goede (1970) and using equation 3.401 to evaluate R with $E_A = 163$ meV, and $E_D = 33$ meV

for binding energies and an average value for $m'E_p$ = 5 meV, one finds that $\bar{S}$ (R = 77 Å) = 0.95 while $\bar{S}$ (R = 125 Å) = 1.02.

Gutsche and Goede (1970) observed that S = 0.95 for the free to bound (HES) series. Using an average donor radius of 26 Å gives a value of $\gamma = \frac{2R}{a_e}$ = 5.9 for R = 77 Å and γ = 9.6 for R = 125 Å. Referring to our Fig. 9 and using a ratio for the Bohr radii of α = 6 shows that $\frac{\bar{S}}{S}$ (R = 77 Å) = 0.99, in agreement with observations. From Fig. 9, $\frac{\bar{S}}{S}$ (R = 125 Å) = 1.07 which is again in agreement with $\bar{S}$ (R = 125 Å) = 1.02 observed by Gutsche and Goede (1970) at low excitation intensities where the LES has a maximum at 2.395 eV.

In resonant Raman scattering work Scott et al. (1969) have observed up to nine LO phonon replicas from the 4880 Å laser line incident on a CdS crystal. Using a configurational coordinate model to understand their results gives S $\sim$ 2. This is the same as the value obtained from our excitation spectrum for the A(n = 1) exciton.

5.5 Non-radiative and Radiative Relaxation Rates

As mentioned in section 3.3 the observation of photons of energy $\varepsilon_o + p\hbar\omega_o$ gives an estimate of radiative and non-radiative decay rates. Measurements at these energies have shown no detectable luminescence. This implies that the rate of emission of LO phonons by an exciton or bound exciton complex with p > 1 is at least an order of magnitude less than the radiative decay

rates and confirms the inequality $t << \Gamma_q$ used in section 3.3. This agrees with the measured radiative decay time for a bound exciton, 10^{-9} sec (Henry and Nassau 1970b), and the rate of LO phonon emission, 10^{-13} sec, calculated for $k > 0$ from the expression derived by Stocker and Kaplan (1966).

5.6 Electron-Hole Correlation Effects

5.6.1 Experimental Observations

The bound to bound luminescence is observed in compensated crystals at low temperatures and has been shown in Fig. 3 and Fig. 11. It was found that the shape and position of the bound to bound band depended somewhat on the wavelength of the exciting photons. The shape of the free to bound band on the other hand was independent of the exciting wavelength.

Gross et al. (1962) originally reported that excitons contributed in some way to exciting the luminescence at 77°K. We have observed that excitons contribute to the broad band luminescence both above and below 30°K. By selecting portions of the bound to bound luminescence our experiments show the nature of the exciton contribution.

The influence of excitons is demonstrated in Fig. 24 by a series of excitation spectra taken with $\lambda_{LUM} = 5150$ Å at several different temperatures. At the lowest temperature strong lines show for the (n = 1) A and B excitons. The n = 2 lines come at 4813 Å (A, n = 2) and 4785 Å (B, n = 2) while

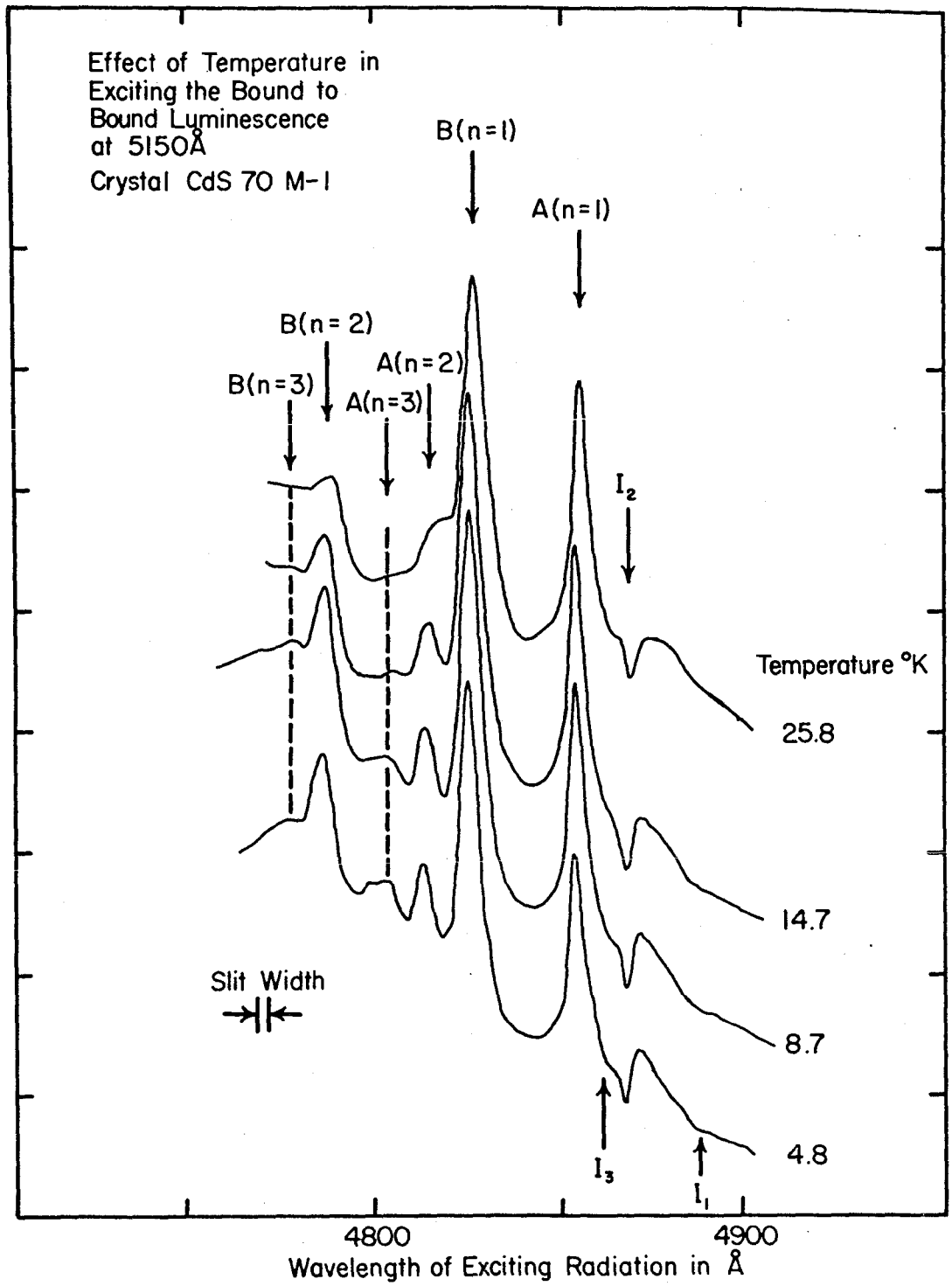

Fig. 24 Effect of temperature on the excitation spectrum of luminescence at 5150 Å. The contribution of excitons with principal quantum number n > 1 is largest at the low temperatures.

an A(n = 3) line shows at 4805 Å. The dip at 4869 Å is due to absorption by the I_2 complex. A small minimum at 4888 Å is from the I_1 complex.

As the temperature is raised the peaks from excitons with principal quantum numbers n > 1 disappear. The n = 3 excitons thermalize at about 10°K while the n = 2 excitons thermalize at 20 to 25°K.

Excitation spectra at all wavelengths of the bound to bound luminescence show structure at energies corresponding to the A(4854 Å), the B(4825 Å), and the C(4710 Å) excitons (see Fig. 22). At the shorter luminescent wavelengths (λ_{LUM}) a maximum appears in the excitation spectra at all three excitons while larger λ_{LUM} (corresponding to large donor-acceptor separations) the anomaly changes to a minimum but now at different wavelengths - 4858 Å and 4829 Å for A and B excitons respectively.

At λ_{LUM} corresponding to large pair separations where most of the donors and acceptors are neutral, excitons are not very effective in exciting the luminescence. In this case the observed luminescent intensity follows 1 - R(hν) where R(hν) is the reflection spectrum shown in the inset of Fig. 22. Only at λ_{LUM} corresponding to short pair separations, where the donors and acceptors are ionized, are excitons effective in exciting the luminescence.

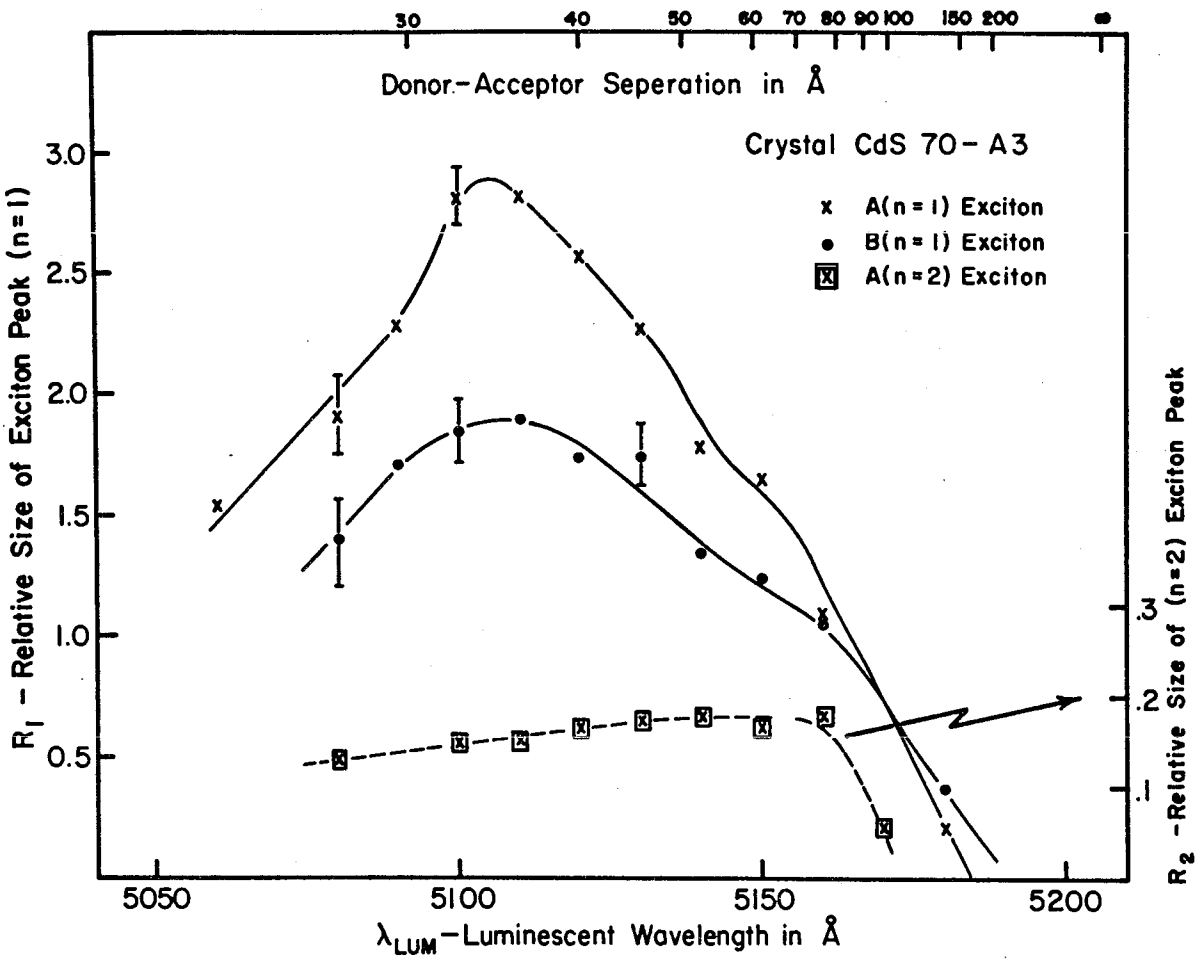

Fig. 25 Relative efficiencies of excitons in exciting the bound to bound luminescence. The excitons with principal quantum number n = 1 are most efficient for a donor-acceptor pair separation of 30-35 Å.

To measure the effectiveness of excitons in exciting the bound to bound luminescence, excitation spectra were taken at a series of positions on the bound to bound luminescence spectrum. From each spectrum ratios R_1 and R_2 were evaluated for exciton states with principal quantum numbers n = 1 and n = 2 respectively. For both A and B excitons R_1 and R_2 give the ratio of the height of the exciton line to the background.

This is a measure of the expression $\frac{AN_2(E)}{N_1(E)}$ derived earlier in equation 3.502. These results are plotted as a function of luminescent wavelength in Fig. 25. The results were substantially the same for the A and B excitons.

For convenience the wavelength has been scaled to the donor-acceptor separation using the expression

$$E = E_g - (E_A + E_D) + \frac{e^2}{\kappa_s R} - mLO - m'E_p \ . \qquad 3.401$$

From the results in section 5.3 the average shift due to acoustical phonons, $\langle m'E_p \rangle_{ave}$,was taken as 5 meV while the acceptor energy, E_A = 163 meV,and the donor energy, E_D = 33 meV. For the highest energy peak m = 0. An average value of $\kappa_s = \sqrt{\kappa_{11}\kappa_{33}}$ was evaluated from the values listed in Table III.

The data shows that excitons in the n = 1 state were most efficient in populating donor-acceptor pairs separated by 30 to 35 Å. From estimates in section 3.2 the Bohr radius,

$a_o = a_e + a_h$, of the A exciton is about 30 Å. Excitons in the n = 2 state with a_o = 120 Å are most effective in populating donor-acceptor pairs separated up to 80 Å. The cut-off at large R results from these donor-acceptor pairs being mostly neutral and therefore insensitive to population by excitons.

Since excitons in the n = 1 state preferentially populate donors and acceptors of separations ~ 30 Å, the net effect on the bound to bound luminescence is to shift the position of maximum intensity to shorter wavelengths (i.e. higher energies). To indicate the effect of excitons in shifting the maximum of the bound to bound luminescence, λ_{max} results from a number of different crystals are shown in Table IX. From excitation spectra of the luminescence a value of R_1 for the B exciton was evaluated for each crystal at the luminescent wavelength of 5150 Å. The B exciton was chosen since it is formed with both incident polarizations. The values of λ_{max} given are for illumination with photons of energy > E_g at intensities in the range 10^{15} to 10^{16} photons/cm^{2}sec. Variations in R_1 from differences in crystal surface conditions, and precise alignment of crystal axis of 20 to 30% are estimated. As has been reported by Gutsche and Goede (1970) a change of incident intensity by 10 times changes λ_{max} by no more than 6 Å.

Examination of the data in Table IX shows that λ_{max} in crystals showing small effects from electron-hole correlation (small R_1) corresponds to large pair separations, while

TABLE IX

Correlation effect observed for luminescence at 5150 Å

Crystal	λ_{max}	R_1 for B (n = 1) Exciton	Notes
CdS70 Cl-1	5186	0	Strong I_2 line which is efficient in exciton capture
A-0	5177	0.16	
Na-1	5184	0.30	Low efficiency for luminescence
A-2	5176	0.34	
M-3	5148[a]	0.75	High purity crystals
	5170		Est $N_D = 5 \times 10^{15}$ cm^{-3}
M-1	5135[a]	1.2	
	5160		
A-3	5155	1.3	
A-4	5157	1.9	

a) This peak is thought to result from the electron-hole correlation.

crystals with a large value of R_1 show a shift of some 35 Å to shorter wavelengths. Undoped crystals such as CdS 70 M3 and CdS 70 A3 show a larger effect from excitons than doped crystals such as CdS 70 Cl-1 and CdS 70 Na-1.

As a final note it is observed that the luminescence spectrum from Fig. 2 is from a crystal displaying a considerable correlation effect. The shape of the spectrum for the leading edge (i.e. small r) is more closely represented by a curve proportional to $r^6 \exp(-\frac{2r}{a_o})$ than by r^4 or $r^4 \exp(-\frac{2r}{a_D})$; that is, by a curve taking into account exciton population of donors and acceptors.

5.6.2 Discussion of Electron-Hole Correlation Results

The experiments have shown clearly that the correlation of electrons and holes in excitons has an effect on the bound to bound emission band. In most crystals the n = 1 excitons contribute the principal effect.

On the assumption that the principal impurities are the donors and acceptors which participate in the green emission one can consider five possibilities for excitons interacting with impurities.

a) attraction to an ionized acceptor

b) attraction to a neutral acceptor

c) attraction to an ionized donor

d) attraction to a neutral donor

e) attraction to an ionized donor-ionized acceptor pair.

Processes b) and d) result in bound excitons which radiate in times of about 1 n sec (Henry and Nassau 1970b). Process c) is not significant in populating a donor-acceptor pair as evidenced by the absence of a peak in the excitation spectra at the energy of an exciton bound to an ionized donor (I_3 = 4866 Å). In CdS where $\frac{m_h}{m_e} \approx 4$, Hopfield (1964) has shown that the exciton is not bound to an ionized acceptor. In process a) it is therefore possible for the hole of the exciton to become trapped at the acceptor, producing a free electron which is then trapped at a nearby donor, thereby enhancing the b-b emission at donor-acceptor separations of a_o. Process a) has been considered by Lashkarev et al. (1971) who deduced that process a) was partly responsible for the dissociation of excitons to give free photocarriers.

The last possibility e) is included since the electric field from an ionized donor-acceptor pair of separation a_o is large enough to field ionize the exciton, resulting in a neutral donor-acceptor pair.

There have been many reports in the literature of luminescent CdS crystals which have spectra different from that shown in Fig. 11. Examples are the low temperature spectra of Gross et al. (1965), Kingston et al. (1968), Maeda (1965) and Handelman and Thomas (1965) to mention a few. Variations

of λ_{max} between different CdS crystals have usually been explained invoking a new defect level with the appropriate energy.

Excitons preferentially populate the closely spaced donor-acceptor pairs and consequently cause a shift in λ_{max}. In high purity crystals this electron-hole correlation effect can in principle result in a luminescent band of the same energy as the free to bound emission. While the possibility of free to bound emission at low temperatures cannot be precluded, existing data should be re-examined in the light of this new model.

In agreement with Gross (1962) we have observed that excitons can also excite the luminescence at T > 30°K. In the free to bound model excitons probably interact with ionized acceptors to give a bound hole and a free electron.

The photoconductivity of CdS at low temperatures has also been a subject of considerable discussion. In particular one point involves the reason for minima or maxima at exciton energies in the photoconductivity spectra. Certain effects have resulted from crystal surface conditions (Schubert and Böer 1970). However, the data shows that excitons are involved in both the bound to bound luminescence and the bound to bound exciton luminescence.

These interactions suggest important effects on photo-

conductivity spectra. Consequently, the role of excitons in photoconductivity spectra should not be interpreted without knowledge of the role of excitons in the luminescence.

6. CONCLUSIONS AND SUMMARY

Our work on the luminescence of CdS gives an improved understanding of the luminescent processes in the II-VI semiconductors in three areas

(i) It was shown that the interaction of a localized electronic excitation with a polar lattice could be understood in terms of a strength parameter S in a model based on the Franck-Condon principle with the magnitude of S calculated from first principles.

(ii) A method for accurately measuring ionization energies of donors and acceptors from the luminescence was demonstrated.

(iii) An electron-hole correlation effect was shown to affect the energy of the bound to bound luminescence.

Investigation of the luminescence in CdS using a monochromator and a spectrometer has resulted in the simplification of a complicated luminescence spectrum. The technique has enabled the accurate measurement of the ionization energies and some of the energy levels of donor and acceptor impurities. The binding energy for a Cl donor was found to be 33.0 ± 0.2

meV and the Na acceptor was 163 ± 2 meV. A radiative Auger process was discovered in CdS and its importance in explaining many aspects of the photodonductivity spectra was recognized. In addition, the energies of the excited states of the exciton bound to a neutral donor were measured. However, there is not yet any theory for the energy levels of this hydrogen molecule-like complex.

Excitation spectra of the luminescence revealed an electron-LO phonon interaction. This interaction is best explained, not by a perturbation calculation, but by a configuration coordinate model based on the Franck-Condon principle. This model gives an intensity profile for the pLO replicas proportional to $e^{-s} \frac{S^p}{p!}$, where the strength parameter S is a function of the lattice adjustment to the electronic transition.

Calculations for the value of the electron-LO phonon interaction parameter S done by Toyozawa (1967) for a bound carrier were extended to include the free exciton, the bound exciton and the bound to bound transition. Experiments showed that $\hat{S}$ for excitons varied inversely with exciton size, in agreement with theory. Calculations which showed that $\overline{S}$ for the bound to bound transitions varied with the donor-acceptor separation were verified by experiment.

The LO phonon energy was accurately measured for several

electronic transitions. The LO energy depends on the spatial extent of the absorbing or emitting center because of the dispersion of the LO phonon branch.

Experiments and calculations showed that excitons can contribute to the bound to bound luminescence. The excitons favor ionized donor-acceptor pairs separated by a distance given by the exciton radius. As a result the bound to bound luminescence in certain crystals can be shifted to energies higher than without any electron-hole correlation. It is concluded that at low temperatures there can be up to three luminescent bands superimposed on each other depending on crystal doping, excitation intensity, temperature, etc. The bands are due to radiative recombination of a free electron and a bound hole, radiative recombination of a bound hole and a bound electron (random capture) and radiative recombination of a bound hole and a bound electron (correlated electron and hole capture).

7. FUTURE STUDIES

Study of the luminescence from a semiconductor using monochromatic tunable incident radiation has given an improved understanding of the physical processes involved in luminescence. CdS is the first semiconductor to be studied in detail this way and it is clear that similar studies on other semiconductors can certainly be done. The techniques discussed

open a rich field for experimental investigation.

Specific to CdS there are several avenues open for study:

(i) a precise measurement of ionization energies of other chemical species of donors and acceptors

(ii) a measurement of excited state energies of excitons bound to donors other than Cl. This may assist in evaluating the central cell correction and so may assist in constructing wavefunctions to describe the bound exciton complexes.

(iii) a more complete study of the nature of the interaction between localized charges and acoustical phonons

(iv) exciton kinetics; that is, a consideration of the motion of excitons in a crystal with impurities and imperfections.

One major problem has been the lack of sufficient incident intensity. While this may be partly overcome by using photon counting techniques in the detection equipment and improving the light gathering power, the most promising development is the tunable laser. Two tunable sources which have been developed to date are the dye laser and the tunable parametric oscillator. As one might expect, multiplying the incident intensity by 10^6 or even by 10^3 will enable a whole new series of experiments. For instance, intense tunable light sources would permit the study of saturation conditions and observation of excitons at high concentrations (Blatt et al. 1962).

References

Aten, A.C., Haanstra, J.H., and de Vries, H. 1965
Philips Res. Rept. 20, 395.

Aven, M. and Prener, J.S. 1967. Physics and Chemistry of II-VI Compounds, ed. M. Aven and J.S. Prener (North-Holland, Amsterdam).

Baer, W.S. and Dexter, R.N. 1964. Phys. Rev. 135, A 1388.

Berlincourt, D., Jaffe, H., and Shiozawa, L.R. 1963. Phys. Rev. 129, 1009.

Birman, J.L. 1959a. J. Phys. Chem. Solids 8, 35.
1959b. Phys. Rev. 114, 1490.

Blatt, J.M., Boer, K.W., and Brandt, W. 1962.
Phys. Rev. 126, 1691.

Bleil, C.E. 1966. J. Phys. Chem. Solids 27, 1631.

Bube, R.H. 1960. Photoconductivity of Solids (Wiley, New York).

Colbow, K. 1966. Phys. Rev. 141, 742.

Collins, A.T., Lightowlers, A.C., and Dean, P.J. 1969.
Phys. Rev. 183, 725.

Conradi, J. 1968. Ph.D. Thesis, Simon Fraser University.

Conradi, J. and Haering, R.R. 1968. Phys. Rev. Lett. 20, 1344.

Conradi, J. and Haering, R.R. 1969. Phys. Rev. 185, 1088.

Cuthbert, J.D., and Thomas, D.G. 1968. J. Appl. Phys. 39, 1573.

Czyzak, S.J., Baker, W.M., Crane, R.C., and Howe, J.B. 1957.
J. Op. Soc. Am. 47, 240.

Dean, P.J., and Merz, J.L. 1969. Phys. Rev. 178, 1310.

Deitz, R.E., Thomas, D.G., and Hopfield, J.J. 1962.
Phys. Rev. Lett. 8, 391.

Fischer, R., Heim, U., Stern, F., and Weiser, K. 1971.
Phys. Rev. Lett. 26, 1182.

Fitchen, D.B. 1966. Proc. Int. Conf. Luminescence, Budapest.

Fitchen, D.B. 1968. Physics of Color Centers, ed. W.B. Fowler (Academic Press, New York) p. 294.

Frankel, J. 1931. Phys. Rev. 37, 17.

Frohlich, H. 1954. Advan. Phys. 3, 325.

Gross, E.F., Razbirin, B.S., and Iakobson, M.A. 1957. Soviet Physics (Technical Physics) 2, 1043.

Gross, E.F., and Razbirin, B.S. 1957. Soviet Physics (Technical Physics) 2, 2014.

Gross, E.F., and Shekhmamet'ev, R.I. 1962. Soviet Physics (Solid State) 3, 2297.

Gross, E.F., Razbirin, B.S., and Shekhmamet'ev, R.I. 1962. Soviet Physics (Solid State) 4, 150.

Gross, E.F., and Shekhmamet'ev, R.I. 1963. Soviet Physics (Solid State) 5, 366.

Gross, E.F., Razbirin, B.S., and Permogorov, S.A. 1965. Soviet Physics (Solid State) 7, 444.

Gross, E., Permogorov, S., and Razbirin, B. 1966a) J. Phys. Chem. Solids 24, 1647; 1966b) Soviet Physics (Solid State) 8, 1180.

Gross, E.F., Permogorov, S., Travnikov, V., and Selkin, A. 1970. J. Phys. Chem. Solids 31, 2595.

Gutsche, E. and Goede, O. 1970. J. of Luminescence 1, 200.

Hagston, W.E. 1971. J. of Luminescence 3, 253.

Handelman, E.T. and Thomas, D.G. 1965. J. Phys. Chem. Solids 26, 1261.

Henry, C.H., Faulkner, R.A., and Nassau, K. 1969. Phys. Rev. 183, 798.

Henry, C.H. and Nassau, K. 1970a). Phys. Rev. B2, 997.

Henry, C.H. and Nassau, K. 1970b). Phys. Rev. B 1, 1628.

Henry, C.H., Nassau, K., and Shiever, J.W. 1970. Phys. Rev. Lett. 24, 820.

Henry, C.H. 1971. Private Communication.

Herzberg, G. 1965. Spectra of Diatomic Molecules (Van Nostrand, Princeton, New Jersey, U.S.A.), 2nd Edition, p. 340.

Hite, G.E., Marple, D.T.F., Aven, M. and Segall, B. 1967. Phys. Rev. 156, 850.

Hopfield, J.J. 1959. J. Phys. Chem. Solids 10, 110.

Hopfield, J.J. and Thomas, D.G. 1960. J. Phys. Chem. Solids 12, 276.

Hopfield, J.J. 1960. J. Phys. Chem. Solids 15, 97.

Hopfield, J.J. and Thomas, D.G. 1961. Phys. Rev. 122, 35.

Hopfield, J.J. 1964. Proceedings of the 7th International Conference on the Physics of Semiconductors in Paris, ed. M. Hulin (Dunod, Paris) p. 725.

Huang, K. and Rhys, A. 1950. Proc. Roy. Soc. (London) A204, 406.

Keil, T.H. 1965. Phys. Rev. 140, A601.

Kingston, D.L., Greene, L.C., and Croft, L.W. 1968. J. Appl. Phys. 39, 5949.

Klein, M.V. and Porto, S.P.S. 1969. Phys. Rev. Lett. 22, 782.

Klick, C.C. 1951. J. Opt. Soc. Am. 41, 816.

Kröger, F.A. 1940. Physica 7, 1.

Kröger, F.A. and Meyer, H.J.G. 1954. Physica 20, 1149.

Lashkarev, V.E., Sal'kov, E.A., and Khvostov, V.A. 1971. Proceedings of the Third International Conference on Photoconductivity, Stanford 1969, ed. E.M. Pell (Pergaman Press, Oxford) p. 111.

Lax, M. 1952. J. Phys. Chem. 20, 1752.

Leite, R.C.C. and Porto, S.P.S. 1966. Phys. Rev. Lett. 17, 10.

Leite, R.C.C., Scott, J.F. and Damen, T.C. 1969. Phys. Rev. Lett. 22, 780.

Lorenz, M.R. 1967. Physics and Chemistry of II-VI Compounds, ed. M. Aven and J.S. Prener (North-Holland, Amsterdam), p. 75.

Maeda, K. 1965. J. Phys. Chem. Solids 26, 1419.

Malm, H.L. and Haering, R.R. 1971a. Can. J. Phys. to be published. 1971b. Can. J. Phys. to be published.

Morgan, T.N., Plaskett, T.S., and Pettit, G.D. 1969. Phys. Rev. 180, 845.

Nassau, K., Henry, C.H., and Shiever, J.W. 1970. Proceedings of the Tenth International Conference on the Physics of Semiconductors, ed. S.P. Keller, J.C. Hansel, F. Stern (U.S. Atomic Energy Commission) p. 629.

Neuberger, M. 1969. II-VI Semiconducting Compounds Data Tables (Clearinghouse for Federal Scientific and Technical Information, Springfield, Va., U.S.A.)

O'Rourke, R.C. 1953. Phys. Rev. 91, 265.

Park, Y.S. and Reynolds, D.C. 1963. Phys. Rev. 132, 2450.

Park, Y.S. and Langer, D.L. 1964. Phys. Rev. Lett. 13, 392.

Park, Y.S. and Schneider, H. 1968. Phys. Rev. Lett. 21, 798.

Pedrotti, L.S. and Reynolds, D.C. 1960. Phys. Rev. 119, 1897.

Pell, E.M. 1971. Proc. of the Third Int. Conf. on Photoconductivity (Pergaman Press, Oxford).

Piper, W.W. and Halsted, R.E. 1961. Proc. of the Int. Conf. on Semiconductor Physics, Prague 1960. (Academic, New York 1961) p. 1046.

Ray, B. 1969. II-VI Compounds (Pergaman Press, Oxford).

Reynolds, D.C. and Litton, C.W. 1963. Phys. Rev. 132, 1023.

Reynolds, D.C., Litton, C.W., and Collins, T.C. 1965a, Phys. Stat. Solidi 9, 645; 1965b. Phys. Stat. Solidi 12, 3.

Reynolds, D.C. and Collins, T.C. 1969. Phys. Rev. 188, 1267.

Reynolds, D.C., Litton, C.W., Collins, T.C., and Frank, E.N. 1970. Proc. of Tenth Int. Conf. on Physics of Semiconductors, Cambridge 1970 (U.S. Atomic Energy Commission) p. 519.

Reynolds, D.C., Litton, C.W., and Collins, T.C. 1971. Bull. Am. Phys. Soc. 16, 374.

Rowe, J.E., Cardona, M., and Pollack, F.H. 1967. Int. Conf. on II-VI Semiconducting Compounds, ed. D.G. Thomas (Benjamin, New York) p. 112.

Schubert, R. and Böer, K.W. 1971. J. Phys. Chem. Solids 32, 77.

Scott, J.F., Leite, R.C.C., and Damen, T.C. 1969. Phys. Rev. 188, 1285.

Scott, J.F., Damen, T.C., Silfvast, W.T., Leite, R.C.C., and Cheesman, L.E. 1970. Optics Comm. 1, 397.

Shionoya, S. 1970. J. of Luminescence 1, 17.

Stiles, L.F. and Fitchen, D.B. 1966. Phys. Rev. Lett. 17, 689.

Stocker, H.J. and Kaplan, H. 1966. Phys. Rev. 150, 619.

Tell, B., Damen, T.C., and Porto, S.P.S. 1966. Phys. Rev. 144, 771.

Thomas, D.G. and Hopfield, J.J. 1959. Phys. Rev. 116, 573.

Thomas, D.G., Hopfield, J.J., and Power, M. 1960. Phys. Rev. 119, 570.

Thomas, D.G. and Hopfield, J.J. 1962. Phys. Rev. 128, 2135.

Thomas, D.G., Hopfield, J.J., and Colbow, K. 1964. Proc. Seventh Int. Conf. on Physics of Semiconductors, Radiative Recombination in Semiconductors, Paris ed. M. Hulin. (Dunod, Paris) p. 67.

Thomas, D.G., Gershenzon, M., and Trumbore, F.A. 1964. Phys. Rev. 133, a 269.

Thomas, D.G., Dingle, R., and Cuthbert, J.D. 1967. II-VI Semiconducting Compounds 1967. Int. Conf. ed. D.G. Thomas, (Benjamin, New York) p. 863.

Toyozawa, Y. 1967. Dynamical Processes in Solid State Optics, ed. R. Kubo and H. Kamimura (Syokabo, Tokyo and W.A. Benjamin, New York) p. 90.

Toyozawa, Y. and Hermanson, J. 1968. Phys. Rev. Lett. 21, 1637.

Toyozawa, Y. 1970. J. Luminescence 1, 732.

Wannier, G.H. 1937. Phys. Rev. 52, 191.

Wei, D.T.Y., Pechina, C.M., and Park, Y.S. 1971. Proc. of the Third Int. Conf. on Photoconductivity, Stanford 1969, ed. E.M. Pell (Pergaman Press, Oxford) p. 343.

Wheeler, R.G. and Dimmock, J.O. 1962. Phys. Rev. 125, 1805.

Woodbury, H.H. and Hall, R.B. 1967. Phys. Rev. 157, 641.